Trade-offs in a 1 Tbps Multiple-Input and Multiple-Output (MIMO) Communication System Between an Airship and Ground Receive Antennas

THESIS

Adam Brueggen, Captain, USAF

AFIT/GE/ENG/12-04

DEPARTMENT OF THE AIR FORCE
AIR UNIVERSITY

AIR FORCE INSTITUTE OF TECHNOLOGY

Wright-Patterson Air Force Base, Ohio

AFIT/GE/ENG/12-04

Trade-offs in a 1 Tbps Multiple-Input and Multiple-Output (MIMO) Communication System Between an Airship and Ground Receive Antennas

THESIS

Presented to the Faculty

Department of Electrical and Computer Engineering

Graduate School of Engineering and Management

Air Force Institute of Technology

Air University

Air Education and Training Command

In Partial Fulfillment of the Requirements for the

Degree of Master of Science in Electrical Engineering

Adam Brueggen, B.S.E.E.

Captain, USAF

March 2012

AFIT/GE/ENG/12-04

Trade-offs in a 1 Tbps Multiple-Input and Multiple-Output (MIMO) Communication System Between an Airship and Ground Receive Antennas

Adam Brueggen, B.S.E.E.
Captain, USAF

Approved:

/signed/	2 Mar 2012
Dr. Richard K. Martin, PhD (Chairman)	date
/signed/	2 Mar 2012
Maj. Mark D. Silvius, PhD (Member)	date
/signed/	2 Mar 2012
Capt. Patrick S. Chapin, PhD (Member)	date

Abstract

As demand for higher data-rate wireless communications increases, so will the interest in multiple-input and multiple-output (MIMO) systems. In a single transmitter, single receiver communication system, there is a fundamental limit to the data-rate capacity of the system proportional to the system's bandwidth. Since increasing the bandwidth is expensive and limited, another option is increasing the system's capacity by adding multiple antennas at the transmitter and receiver to create a MIMO communication system. With a T transmitter, R receiver MIMO communication system, TR channels are created which allow extremely high data-rates. MIMO systems are attractive because they are extremely robust as they are able to operate when encountering channels with severe attenuation also known as deep fades. MIMO systems are known for their ability to achieve extremely high data-rates created by the multiple channels while improving bit error rate (BER) through diversity.

This thesis examined the trade-offs in a 1 Terabit per second (Tbps) MIMO communication system that used Reed Solomon (RS) forward error correction (FEC) between an airship and an array of ground receivers. An airship, similar to a Zeppelin, and a series of ground receivers were used to simulate a MIMO system. Water filling and beam forming were implemented with different antenna ratios to examine the minimum number of antennas needed to achieve a 1 Tbps capacity. Performance metrics, including throughput and BER, were examined with different antenna ratios, different RS codes, and different types of modulation. The results showed that a higher receiver-to-transmitter ratio required fewer total antennas to achieve the capacity objective than a higher transmitter-to-receiver ratio. This thesis also indicated that a higher receiver-to-transmitter ratio yielded a lower BER.

Acknowledgements

Earning my Masters Degree in Electrical Engineering has always been a dream of mine. Although receiving a masters degree is an individual recognition, there are many people to whom I owe a lot of gratitude. First, I would like to thank my family for supporting my Air Force career. Their love and support is the main driving force behind all of my accomplishments. Second, I would like to thank my fiancée for her support. Thank you for your sacrifices and understanding the time requirement that AFIT required. I am looking forward to finally being together again after a 21 month separation. I could not have completed my thesis without the support from my advisor, Dr. Richard Martin. He spent countless hours looking over my results and offering guidance on my research. I would also like to wish Dr. Martin the best of luck on his upcoming years at AFIT. I know that AFIT couldn't be where it is without his inguinity and dedication to his students. Thank you! Lastly, I would like to thank all the AFIT community especially my dedicated instructors and fellow students for the tremendous amount of support. Thank you all.

Adam Brueggen

Table of Contents

Page

Page

List of Figures

List of Tables

List of Abbreviations

Abbreviation		Page
dB	decibel	22
i.i.d.	Independent, Identically Distributed	22
MPSK	M-ary Phase Shift Keying	26
MQAM	M-ary Quadrature Amplitude Modulation	27
OFDM	Orthogonal Frequency Division Multiplexing	28
IFFT	Inverse Fast Fourier Transform	28
CP	Cyclic Prefix	28
FFT	Fast Fourier Transform	28
BCH	Bose-Chadhuri-Hocquenghem	34
MMSE	Minimum Mean Square Error	37
MED	Minimum Euclidean Distance	49

Trade-offs in a 1 Tbps Multiple-Input and Multiple-Output (MIMO) Communication System Between an Airship and Ground Receive Antennas

I. Introduction

This chapter describes essential background information that is necessary for a basic understanding of this research effort. The background information entails the problem statement, objectives, limitations, equipment needed, as well as motivation as to why this research is relevant to Department of Defense (DoD) missions.

1.1 Background

Multiple-Input and Multiple-Output (MIMO) systems have been a popular choice for wireless communications because they are robust and have the capability to provide high data-rate communications. MIMO communication systems are especially effective in environments that have many physical obstructions such as buildings and rugged terrain, which result in severe attenuation also known as deep fading. Fading, which is the attenuation and degregation of a signal, occurs in all wireless communication systems. MIMO can overcome deep fades that would otherwise cripple single-input and single-output (SISO) communication systems by its use of multiple links to transmit information.

Every communication system has a numerical limitation to the number of bits per second (bps) that can be received without experiencing significant error rates. In a one transmitter and one receiver SISO communication system, the data-rate, or bits that can be transmitted through a wireless channel without significant loss of information, is bounded by the Shannon Capacity theorem. This theorem states that the data-rate is proportional to the bandwidth, which is the range of frequencies within which the wireless system can operate. MIMO technology exploits the diversity

gain acquired by the multiple links between each transmitter and each receiver that results in higher data-rates when compared to using the SISO model.

The United States' Unmanned Aerial Vehicles (UAV) primary missions include remote sensing, reconnaissance, and armed attacks. Future UAV systems look to expand their mission to include communications with ground units [1]. As the amount of information being transmitted across the battle space increases, the size of the MIMO array needs to increase. Because most UAVs lack the size, payload capacity, and loiter time to carry the hardware needed to support a high data-rate MIMO communication system, a larger airship is desired. Due to the assigned frequencies in this research, a large airship is needed to support the large array of antennas.

1.2 Problem Statement

Wireless MIMO communication technology is a promising technology that enables users to communicate at robust, high data-rates. Current research indicates that high data-rates in the Megabits per second (Mbps) are being used; however, super high data-rates, which are hundreds of Mbps and higher, are currently not being studied extensively. The reason there is limited research of super high data-rates is the lack of need for these high data-rates. Most commercial and military applications do not require rates of this magnitude; however, since the airship in this research acts as a relay for numerous lower data-rate systems, it requires a high data-rate to accomodate all the lower data-rate systems. Research on how to design a wireless MIMO communication system between a power limited lighter-than-air airship and an array of ground receivers that can support super high data-rates on the magnitude of 1 Terabit Per Second (Tbps) has been limited. This research investigates the trade-offs associated with different configurations that can be used to achieve the 1 Tbps goal between an array of transmitters on an airship and an array of ground receivers similar to the model shown in Figure 1.1. For purposes of this research, an airship is used to reference a lighter-than-air blimp similar to a Zeppelin.

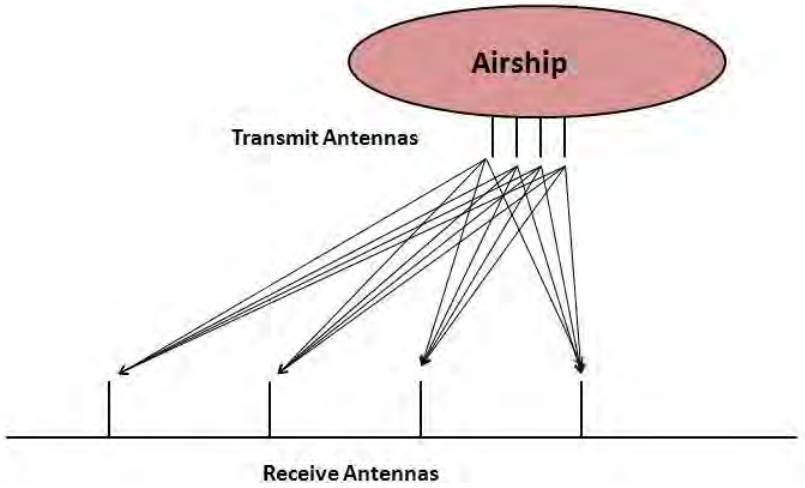

Figure 1.1: Physical System Depiction.

1.3 Scope and Application

This research focuses on the Ku-Band, where the frequency ranges from 10.95-14.5 GigaHertz (GHz). The Ku-Band is used for space-based communications that a MIMO airship system would operate in.

This research uses existing theorems and algorithms in its investigation of trade-offs for a wireless MIMO system.

1.4 Research Objectives

The main objective of this research is to examine different trade-offs, modulations, and forward error correction (FEC) that achieve the desired 1 Tbps with a power constrained airship. The 1 Tbps capacity MIMO system is also to be designed with the lowest cost such as fewest amount of antennas and software needed to support it. This includes looking at ways to increase the MIMO system's capacity including beam forming and water filling. Improvement in error performances using uncoded and FEC signaling schemes are used to investigate which type of signaling scheme best fits this model. There are several ways to use FEC; however, Reed-Solomon (RS), the

most powerful linear FEC code, is tested in this research [2]. Nine different RS FEC codes, which are listed in Chapter III, are studied in this research. Each of the nine different RS FEC codes is capable of correcting a different number of errors based on the coding scheme implemented. The bit-error rate (BER), or the total errors divided by the total number of transmitted bits, and throughput, or the number of bits that can be transmitted through a channel per second, are used to determine the size of array, type of modulation, and RS FEC coding scheme that would be most effective.

This research is used to provide input that helps make a decision on the type of configuration used on the MIMO system. This research does not solve all the unknowns that are needed for this MIMO communication system, but can be used as a starting point for future researchers. The research code will also be made available and can be used for modifications.

1.5 Limitations

There has been extensive research on optimizing a wireless MIMO communication system. Not only are there numerous papers on the design and coding of the system, there are many models for environmental conditions, antenna designs, and channel conditions known at the receiver or transmitter. Due to the length of time needed to investigate and simulate a large MIMO array, several conditions are investigated. These conditions include:

- transmit and receive antenna configurations to achieve 1 Tbps,
- beam forming,
- water filling,
- different types of modulation,
- uncoded signaling scheme,
- RS FEC,
- throughput, and

- multipath effects.

This research is conducted using Matrix Laboratory (MATLAB^{TM}), which is a software program that is commonly used in engineering and other disciplines of science and mathematics. Due to the high cost of building a large MIMO array and recent interest in this topic, hardware implementation of the large arrays is not be used in this research. By contrast, all of this research is based on MATLAB^{TM}simulations. The simulations are created by looping through different antenna arrays as well as different RS(n,k) codes that use different forms of modulation. The channels are modeled using Rician distribution for line-of-sight (LOS) and a Rayleigh distribution for non-line of sight (NLOS).

1.6 Motivation

On today's battlefield, information superiority wins wars and is equally important as air or land superiority. Information superiority has evolved from knowing an enemy's location in a general area to being as precise as describing which room on which floor in a certain building the enemy is located. Information superiority allowed the United States' Armed Forces to kill the world's most wanted terrorist, Osama Bin Laden, in May 2011. Information superiority also allows the United States Armed Forces to operate more efficiently and decreases collateral damage. With the United States armed forces operating in land, air, sea, and space, a tremendous amount of information is being exchanged across these four domains. Since the United States has a world-wide footprint, it is critical that the information can be sent from anywhere in the world to data-collecting centers where it can be analyzed and passed on to military leadership whom can make strategic decisions. A MIMO configured communication system would be the ideal choice to to help the United States obtain information superiority.

MIMO technology is a newer communication system with most technological breakthroughs occurring in the past 15 years and has a promising future communications technology. What makes this thesis unique from other related literature is the

super high data-rates of 1 Tbps. This research investigates a wireless communication system that has a higher capacity than that of other high data-rate literature.

1.7 Organization

This thesis is divided into four additional chapters. Chapter II contains a brief review of important concepts related to MIMO communications and other concepts that are studied in this research. Some of the main topics discussed include review of different antenna configurations, components of diversity gain, multiplexing, fading channels, FEC, and modulation. Chapter III describes and explains the methodology that was used in this research. This chapter includes a basic description of the size and distances for the components of the system as well as the nine different RS coding schemes that are studied in this research. Chapter IV provides the results and includes an explanation of why these results occurred. Chapter V summarizes the contributions of this research and lays the foundation for future work.

II. Background and Theory

This chapter introduces background and theory relevant to MIMO communications and describes the history of how MIMO communications evolved from SISO communications to the high-rate MIMO communication systems used today. Relevant theory and equations are presented in this chapter as well as information that allows the reader to understand basic MIMO theory and related concepts.

2.1 Components of Wireless Communication System

This section discusses a few components of a basic wireless communication system that use FEC. These components are shown in Figure 2.1. For clarify of variables listed in this research, Table 2.1 lists the name, a short description, and size of each variable that are used in this research.

2.1.1 Transmit Antenna. The transmit antenna is an antenna that sends the signal. An ideal transmit antennas can transmit their information omni-directionally or in all directions, sectorally or within a certain set of directions to achieve higher gains. Transmit antennas can also be directive or tuned to one direction.

2.1.2 Receive Antenna. The receive antenna acquires the signal that is sent from the transmit antenna after channel propagation. For high data-rate systems, most receive antennas are dish shaped which allows the receive antenna to aim in the direction of the main lobe of the expected receive signal. By pointing the receive antenna in the direction of the transmitted signal, the communication system maintains a higher probability of receiving a less distorted signal.

2.1.3 Encoder. An (n, k) encoder creates a codeword that is n symbols long where the first k symbols are information symbols and the last $n-k$ symbols are parity symbols. Each symbol contains m bits where $m = \log_2(n+1)$, and each codeword has a total of nm bits. The parity symbols are created using a generator matrix that is unique to each (n, k) coding scheme and are added for verification and correcting

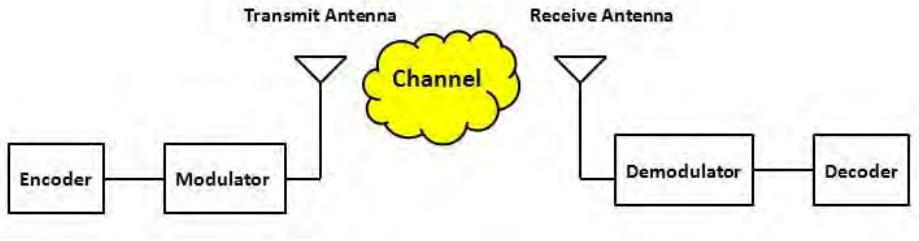

Figure 2.1: FEC communication system.

purposes. The redundancy of bits caused by FEC causes a lower throughput; however, it improves error performance. Once the generated bits are encoded, the nm bits per codeword are sent to the modulator.

2.1.4 Modulator. The modulator maps the received encoded bits at r bits per symbol where $r = \log_2(M)$ for M-ary modulation in the symbols' constellation. There are many types of modulation available. Using Phase Shift Keying (PSK) modulation, the symbols differ based on their phases while using Quadrature Amplitude Modulation (QAM), the symbols differ based on their phases and amplitudes. Once the encoded bits are mapped to the symbols' constellation, they are put on a carrier frequency and are transmitted by a sinusoidal waveform through the channel.

2.1.5 Demodulator. After receiving the estimated transmitted symbols through the channel that is described in Section 2.1.7, the demodulator does the opposite of the modulator. The demodulator takes the distorted received signal waveform and brings it to baseband. From baseband, it maps the distorted received symbol on the constellation map. The demodulator then uses Maximum Likelihood Estimation (MLE) to estimate the received symbol to the closest known symbol. After using MLE, the demodulator converts the estimated symbol to estimated bits. The estimated bits correspond to the same constellation points that were designed in the modulator. Figure 2.2 shows the 4QAM MLE decision boundary for symbols *S1*, *S2*,

Table 2.1: Research Variables.

Variable	Description	Size
T	Number of Transmitters	Scalar
R	Number of Receivers	Scalar
B	Bandwidth	Scalar
n	Total symbols	Scalar
k	Uncoded symbols	Scalar
t	Symbol correcting capability	Scalar
K	Multipath delay	Scalar
SNR	Signal-to-Noise ratio	Scalar
Γ	Coding gain	Scalar
γ_i	SNR in i^{th} channel	Scalar
γ_0	Arbitrary cutoff	Scalar
ρ	SNR per transmit antenna	Scalar
N	IFFT/FFT length	Scalar
v	Cyclic prefix length	Scalar
σ_x^2	Transmit power	Scalar
σ_n^2	Noise power	Scalar
$\|x\|$	Determinant	Scalar
$\mathbf{x}$	Transmitted symbols	T x 1
$\mathbf{n}$	Gaussian noise	R x 1
$\mathbf{y}$	Received symbols	R x 1
$\mathbf{I}$	Identity matrix	R x R
$\mathbf{H}$	Channel matrix	R x T
$\mathbf{H}^\dagger$	MMSE equalizer	T x R
x^H	Hermitian transpose	Varies

S3, *S4*, and the red x markers represent the received distorted symbols. Any red x marker that falls within a symbol's estimation box is estimated as that symbol.

2.1.6 Decoder. The decoder multiplies the received symbols by the inverse of the generator matrix and are compared to a syndrome that is unique to each (n, k) symbol. The syndrome value that is obtained locates the position of the errors and the decoder corrects the identified errors. Each (n, k) code has a limit to the number of correctable errors, so (n, k) codes have different error correcting capability. After the errors are corrected, the last $n - k$ symbols in each codeword are removed leaving the k estimated information symbols. These estimated information symbols are converted

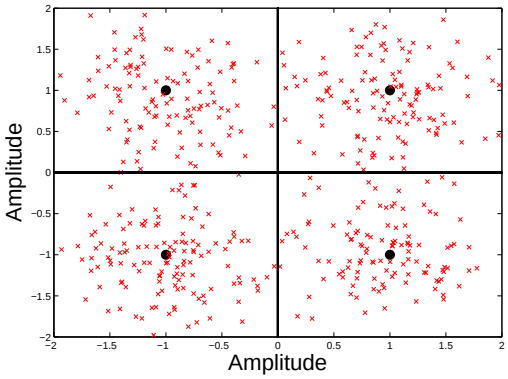

Figure 2.2: 4QAM decision boundaries.

to km bits and are compared to the transmitted bits. An error occurs when the value of an estimated bit differs from a transmitted bit.

2.1.7 Channel. The channel is the medium or space that the signal propagates between the transmitter and the receiver and is the most difficult component of wireless communications to model. The channel is the most difficult part to model because of the unknown changing environmental conditions. Most communications systems are able to estimate the channel conditions, but estimation takes time and utilizes signal processing techniques. Fading, which is the attenuation of a signal as it travels through a medium, creates signal distortion. Because fading varies with time and location, it is modeled as a random process. Terrestrial systems have NLOS which creates a phenomenon of scattering where the signal gets sent in all directions. The effect of scattering creates an effect called multipath and can be seen in Figure 2.3. The challenge with channels is that no two channels are the same. Channel effects are typically modeled as a Rayleigh or Rician distribution.

2.1.7.1 Rayleigh Fading Model Channel. Rayleigh fading channels are terrestrial channels that are modeled when no dominant LOS is present between the transmitter and receiver. In a Rayleigh fading channel, the signals' amplitude fade and phase varies with a Rayleigh distribution. In a Rayleigh fading channel, multipath is severe due the numerous obstructions that exist in the environment. Terrestrial

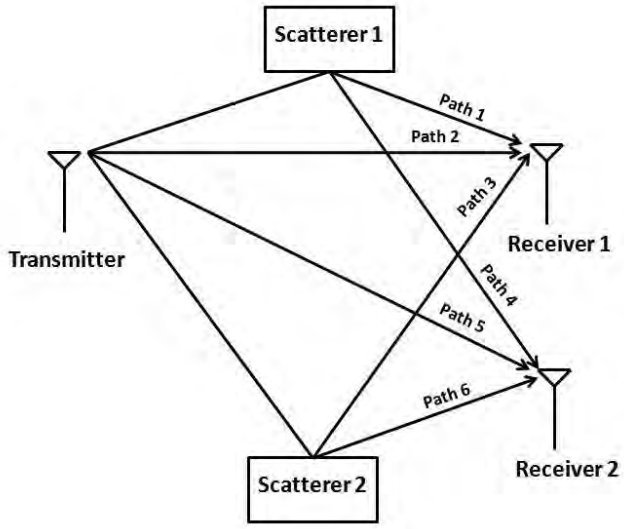

Figure 2.3: Multipath in SIMO system.

environments are modeled as a Rayleigh fading channel because trees and buildings hinder the signal's propagation.

2.1.7.2 Rician Fading Model Channel. Rician fading channels are used when there is a dominant LOS present between the transmitter and the receiver. In Rician fading channels, fading effects are small due to the strong LOS communication link and most space-based communications are modeled as such.

2.1.7.3 Flat Fading. Flat fading, the simplest type of fading, has constant gain and linear phase response over a bandwidth, and its radio channel is greater than the bandwidth of the transmitted signal [3]. Flat fading affects all frequencies across the channel equally. A flat fading channel occurs when the signal bandwidth is narrow enough so that all of the spectrum experience the same fading coefficient [4]. Flat fading channels are referred to as narrowband channels since the bandwidth of the signal is narrow compared to channel flat fading bandwidth. This type of fading is known as "amplitude fading channels since the bandwidth of the

applied signal is narrow compared to the channel flat fading bandwidth" [3]. A signal undergoes flat fading if

$$B_s < B_c, \tag{2.1}$$

and

$$T_s > \sigma_\tau, \tag{2.2}$$

where T_s is the symbol period, B_s is the bandwidth of the transmitted modulation, and σ_τ and B_c are the Root Mean Square (RMS) used to measure varying quantity, delay spread and coherence bandwidth of the channel [3].

2.1.7.4 Frequency Selective Fading. Frequency selective fading occurs when the channel has a constant-gain and linear phase response over a bandwidth that is smaller than the bandwidth of the transmitted signal [5]. Frequency selective fading is different from flat fading in that it affects different frequencies across the channel to different degrees, which causes the phases and amplitudes to vary. Different frequency components of the signal experience decorrelated fading. Under frequency selective fading, the delay spread of the impulse response is greater than the reciprocal of the bandwidth of the transmitted message waveform. The channel induces intersymbol interference due to the receiving signal containing multiple versions of the transmitted waveform that are attenuated and faded in time. These channels are known as wideband channels due to the bandwidth of the received signal being wider than the bandwidth of the channel impulse response. A signal undergoes frequency selecting fading if [3]

$$B_s > B_c, \tag{2.3}$$

and

$$T_s < \sigma_\tau. \tag{2.4}$$

OFDM signaling or antenna displacement diversity is used to help counter the effects of frequency selective fading.

2.1.8 Bandwidth. The bandwidth is the range of frequencies in which a system can operate and is the component that is most widely studied for wireless communication efficiency. In calculating the data-rate of a system, increasing the bandwidth is the most direct way to increase the rate; however, bandwidth is expensive and limited. Increasing the bandwidth should be one of the last options to consider.

2.1.9 Capacity. Capacity is the maximum rate (bps) that information can be reliably transmitted through a communication channel. The capacity is the absolute best that a communication system can operate and is rarely obtained due to noise, interference, and other hardware deficiencies. The Shannon-Hartley theorem states that the maximum rate that can be transmitted through a communication channel is directly related to the bandwidth. For a SISO system, the signal-to-noise ratio (SNR) is modeled as

$$SNR = \frac{\sigma_x^2}{\sigma_n^2}, \tag{2.5}$$

where σ_x^2 is total signal power and σ_n^2 is total noise power. For a one transmitter and one receiver model, the Shannon-Hartley Theorem is

$$C_{SISO} = B \times \log_2(1 + SNR). \tag{2.6}$$

Capacity can be increased by either increasing the bandwidth, which is normally expensive and limited, or by increasing the SNR by increasing signal power.

Figure 2.4: SISO antenna model.

2.1.10 Noise and Interference. Noise and interference, which distort the transmitted signal, are used in models to simulate randomness. In MIMO communication systems, noise and interference are present in the channel, transmitter, and receiver.

2.2 Antenna Configuration Models

This section briefly describes the main points of different antenna configuration models that are used in various communication systems. Each model discusses the advantages and disadvantages as well as state the capacity limit for each configuration. For this thesis, T is used to represent the number of transmitters and R is used to represent the number of receivers.

$Single-Input\,and\,Single-Output$. The simplest wireless model consists of a single transmitter antenna, channel, and a receive antenna, which is seen in Figure 2.4. This configuration, also known as SISO, is used when low data-rates are required or space limited. The transmit antenna transmits a signal at a certain level of power, P, which experiences interference and noise from the channel, and a distorted version of the signal is received at the receive antenna. The capacity for a SISO model was given in (2.6).

$Single-Input\,and\,Multiple-Output$. The single-input and multiple-output (SIMO) antenna model is an extension of the SISO model except it has more receivers

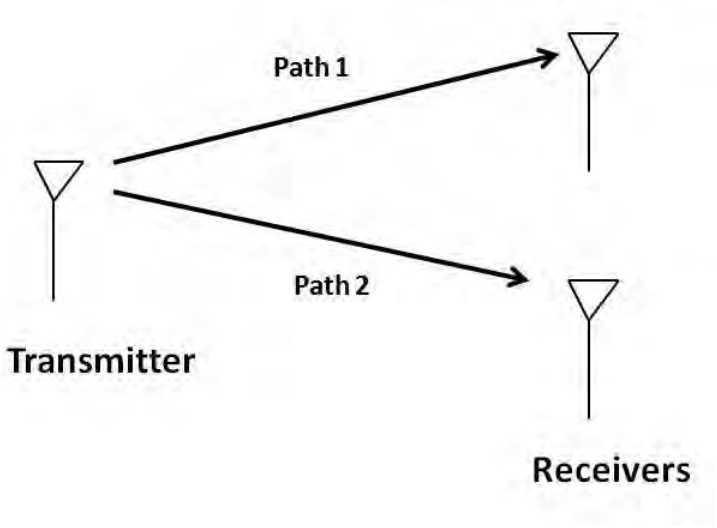

Figure 2.5: SIMO antenna model.

as seen in Figure 2.5. The addition of multiple channels increases the reliability of the system as well as the capacity. If one channel's link becomes unreliable due to severe fading, the other paths can still transmit the signal. The SIMO diversity increases the capacity because it creates R independent paths. The R independent paths' capacities linearly add up for a total capacity that equates to the sum of each independent path. The resulting capacity in a SIMO system is [6]

$$C_{SIMO} \approx B \log_2 (1 + R \times SNR), \tag{2.7}$$

where R is the number of receivers and a overall increase in the SNR of $R \times SNR$ occurs. From (2.7), it can be seen that the capacity increases as the number of receivers increases. A SIMO is desired when space at the transmitter is limited and a medium data rate is required. An example of a useful SIMO system would be a small UAV communicating with a ground station.

$Multiple - Input\,and\,Single - Output$. The multiple-input and single-output (MISO) antenna is similar to the SIMO antenna model except it has one receiver and

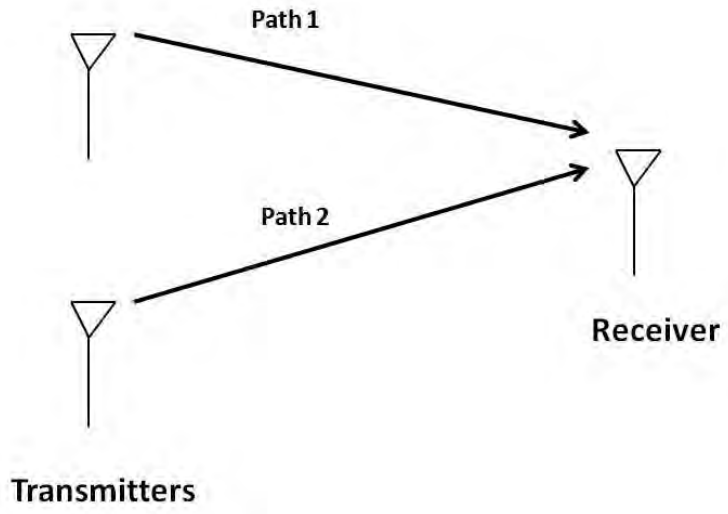

Figure 2.6: MISO antenna model.

T transmitters, where $T > 1$ is seen in Figure 2.6. Like the SIMO antenna model, the MISO antenna model is beneficial because it creates T additional independent paths that increase the reliability of the link. The T additional independent paths causes the SNR to increase by T, which increases the capacity of the system.

$$C_{MISO} = B \times \log_2 |1 + SNR \|\mathbf{h}\||, \tag{2.8}$$

where $\mathbf{h}$ is the unit magnitude vector of size T x 1. A MISO antenna model is desirable if significant physical space is available at the transmitter, and the system requires a medium data-rate. An example of a good MISO system would be an array of ground transmitters transmitting to a satellite.

Multiple − Input and Multiple − Output. The MIMO antenna model is a combination of the SIMO and MISO antenna configurations with T transmitters and R receivers where R and T are > 1. MIMO takes advantage of the TR channels that are created which allows for the high data-rate. A two receiver, two transmitter model is shown in Figure 2.7 that shows the four independent paths between the transmit-

ters and receivers. MIMO configurations are used in environments that require high data-rates or when severe fading is an issue. A MIMO configuration system creates TR independent channels which causes the amount of data being sent to drastically increase. These independent channels allow multiple streams of data across the same channel, which increases the data capacity of the MIMO system. Figure 2.8 shows the capacity between a SISO antenna configuration and a 2x2, 4x4, and 8x8 MIMO models as a function of SNR. It can be seen that as the size of the MIMO array increases, the capacity significantly increases. An important advantage of MIMO technology is that it allows the system to make more efficient use of the available bandwidth. In a SISO model, a single transmitter uses the entire allotted bandwidth. A MIMO system allows all of its transmitters to use the allotted bandwidth. For example, having 50 SISO systems with each system having a bandwidth of 1 MHz would require 50 MHz of bandwidth. Meanwhile, a 50 transmitter MIMO system with a bandwidth of 1 MHz would require a total bandwidth of only 1 MHz. A MIMO system has the same data-rate as multiple SISO channels with the use of a fraction of bandwidth. Since bandwidth is limited and expensive, making the most use of this limited resource is important. A disadvantage of MIMO technology is the size, spacing, and weight needed for multiple antennas. As new technologies continue to decrease in size, it is becoming more difficult to properly space transmit antennas without causing interference. The capacity of a MIMO system is endless; however, physical size is a limiting factor for MIMO systems. If a large MIMO system is desired, it is crucial that the transmitting and receiving areas are large enough to allow the amount of spacing required for the large number of transmitters.

In 1996, Gerard Foschini designed a coding algorithm that used the increased capacity added by a MIMO communications system. This algorithm, later called Bell Labs Layered Space-Time (BLAST), became the one of the first space-time algorithms to encode data across time and across all transmit antennas [7]. Foschini found that the capacity for a MIMO system using his BLAST algorithm was

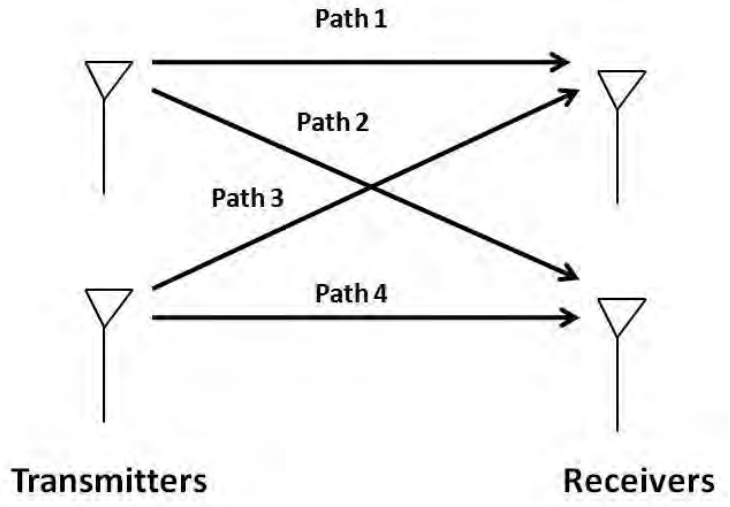

Figure 2.7: 2x2 MIMO antenna model.

$$C_{MIMO} = B \times \log_2 \left| \mathbf{I_R} + \frac{1}{\sigma_n^2} \mathbf{H} \mathbf{R_x} \mathbf{H}^H \right| \ (bps), \tag{2.9}$$

where B was the Bandwidth, $|x|$ was the determinant, $\mathbf{R_x}$ was the covariance matrix, $\mathbf{H}$ was the channel gain matrix, and $\mathbf{I_R}$ was the identity matrix that is the size of R.

Consider a MIMO configuration with T transmitters and R receivers similar to Figure 2.9. The received information in a MIMO system can be modeled as

$$\mathbf{y} = \mathbf{H}\mathbf{x} + \mathbf{n}, \tag{2.10}$$

where $\mathbf{H}$ is a R x T matrix of channel gains, $\mathbf{x}$ represents the T x 1 vector of transmitted symbols, $\mathbf{n}$ is the R x 1 noise vector, and $\mathbf{y}$ is the R x 1 vector of the received symbols.

Following Telatar's [8] derivation, any matrix $\mathbf{H} \in \mathbb{C}^{r \times t}$ can be written by applying singular value decomposition (SVD) theory as

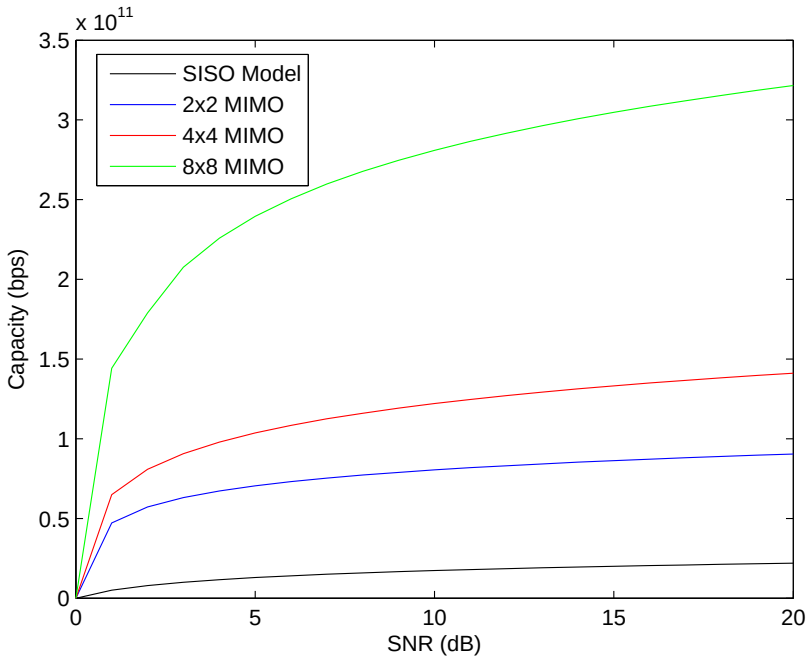

Figure 2.8: SISO vs MIMO capacity comparison.

$$\mathbf{H} = \mathbf{U}\mathbf{D}\mathbf{V}^H, \tag{2.11}$$

where $\mathbf{U} \in \mathbb{C}^{r\times r}$ and $\mathbf{V} \in \mathbb{C}^{t\times t}$ are unitary, and $\mathbf{D} \in \mathbb{R}^{r\times t}$ is non-negative, diagonal matrix of singular values σ_i of $\mathbf{H}$. Each singular value (σ_i) represents the channel gains for channel i [9]. Applying (2.11) to (2.10), (2.10) can be re-written as

$$\mathbf{y} = \mathbf{U}\mathbf{D}\mathbf{V}^H\mathbf{x} + \mathbf{n}. \tag{2.12}$$

Foschini's BLAST equation or (2.9) was the first equation used to calculate the capacity of a MIMO communication system. Telatar investigated Foschini's BLAST equation and found a way to make the most use of the power in a MIMO system. Telatar [8] stated the following theorem:

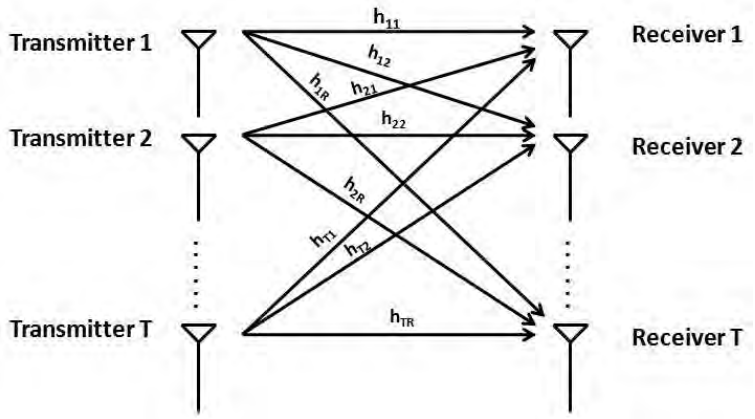

Figure 2.9: MIMO model diagram.

THEOREM 1. The capacity of the channel is achieved when x is a circularly symmetric complex Gaussian with zero-mean and covariance $\frac{P_T}{T}\mathbf{I_r}$, where R is the number of receive antennas. The capacity is given by $B \times \log_2 \left|\mathbf{I_r} + \frac{P_T}{T}\mathbf{H}\mathbf{H}^H\right|$.

From his theorem, Telatar stated that the maximum way to allocate power without considering water-filling is to evenly distribute the power amongst the number of transmit antennas. Applying Telatar's theorem to 2.9, the capacity for a MIMO system can be rewritten as

$$C = B \log_2 \left|\mathbf{I} + \frac{P_T}{T}\mathbf{H}\mathbf{H}^H\right|, \tag{2.13}$$

where $\mathbf{I}$ is the identity matrix of size R and x^H denotes the Hermitian transpose.

2.3 MIMO Gain

In this section, a quick overview is provided of gains that are obtained in MIMO communications.

2.3.1 Multiplexing Gain. Multiplexing gain is obtained by decomposing T transmit antennas and R receive antennas into R parallel independent channels.

Table 2.2: Alamouti's Transmit Diversity Scheme.

	Antenna 0	**Antenna 1**
time t	s_0	s_1
time $t + T$	$-s_1^*$	s_0^*

By sending data across these independent channels, a R-fold increase in data-rate is obtained compared to using a single transmit and receive antenna [9]. This is better known as multiplexing gain.

2.3.2 Diversity Gain. Another gain that is receiving attention is diversity gain or space diversity. Using space diversity, no increase in bandwidth or transmit power is needed for independent fading paths [9]. Alamouti was the first to come up with an optional method on the performance of antenna diversity trade-offs for wireless communications. Diversity gains help a MIMO system, because deep fades occurring on all independent signal paths have a low probability of occurring at the same time. He suggested that an effective technique to mitigate multipath fading in a wireless channel is done by controlling the transmitted power [10]. One of the most challenging principles of wireless transmission is overcoming time-varying multipath fading [11]. Alamouti demonstrated that antenna diversity is an effective technique for overcoming the effect of multipath fading. A problem with antenna diversity is the cost, size, and power of the remote units [10]. In wireless communication systems, transmit antenna real estate is usually limited due to the size of the transmitting system. Alamouti found that it is more economical to add antennas at the receiving or base stations than it is to add antennas at the transmitting station.

Alamouti investigated the Maximal-Ratio Receive Combing (MRRC) Scheme as well as a new two-branch transmit diversity with M receivers. Each transmit antenna transmitted signals through independent Rayleigh fading channels. The encoding and transmission sequences that were used in Alamouti's transmit diversity scheme is seen in Table 2.2.

Using Binary Phase Shift Keying (BPSK) modulation, the MRRC and new scheme's total transmit power were the same. From these results, it can be concluded that the new scheme provided results that were similar to the MRRC, regardless of the employed modulation schemes [10].

Alamouti was able to demonstrate that his proposed new scheme had the same diversity order as MRRC. He also showed that a diversity order of $2M$ can be obtained using two transmit antennas and M receive antennas. His new scheme had a 3-decibel (dB) disadvantage because of the simultaneous transmission of two distinct symbols from two antennas which resulted from a fixed total transmit power [10]. If the new scheme had transmitted twice the total power, the performance would have had similar results to the MRRC.

One important advantage to spatial diversity is more efficient use of bandwidth. It is important to note that all transmit and receive antennas require a minimal separation of one half-wavelength distance to achieve independent fading [9].

2.3.3 Beam Forming. Beam forming is another form of gain that is used in MIMO systems and provides diversity and array gain via coherent combining of multiple signal paths [9]. Using beam forming, the transmitted signal is weighted by a complex scale factor and is transmitted by each transmit antenna where the resulting received signal is

$$y = \mathbf{u}^H \mathbf{H} \mathbf{v} \mathbf{x} + \mathbf{u}^H \mathbf{n}, \tag{2.14}$$

where $\mathbf{n} = (n_1, ..., n_R)$ are independent, identically distributed (i.i.d.) noise samples [9] and $\mathbf{u}$ and $\mathbf{v}$ are weights placed at the receiver and transmitter to steer the beams. Figure 2.10 shows a graphic description of a 2 transmitter, 2 receiver MIMO system using beam forming.

While using beam forming, the SNR is shown to equal

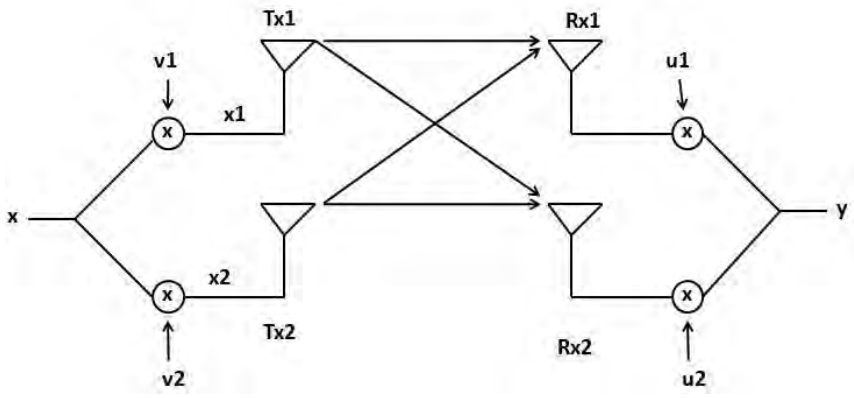

Figure 2.10: 2x2 Beam forming gain.

$$\gamma = \sigma_{max}^2 \rho, \tag{2.15}$$

where σ_{max} is the largest singular value of $\mathbf{H}$ and ρ is the SNR per antenna [9]. Using the largest singular value obtained in (2.15), the resulting capacity obtained when using beam forming is

$$C = B \log_2 \left(1 + \sigma_{max}^2 \rho\right), \tag{2.16}$$

or optimizing (2.16), by substituting $\rho = \frac{SNR}{T}$ into (2.16) results in a beam forming capacity shown in (2.17)

$$C_{Beam\,Forming} = B \log_2 \left(1 + \sigma_{max}^2 \frac{SNR}{T}\right). \tag{2.17}$$

2.4 Water Filling

A popular method of optimizing power allocation is implementing a method known as water filling. Water filling allocates the transmit power to the branches of the MIMO system that gives the system the best chance at successfully transmitting

the signal and does not allocate any signal power on channels that have deep fades. In a MIMO system, there are $min(T, R)$ different eigenmodes. Each eigenmode's contribution to capacity depends on both the average SNR per receiving antenna, ρ, and its singular values [12].

According to [12], water filling techniques give three different kinds of power allocations, which depend on the SNR:

Low SNR: When a receiving antenna is being implemented in a low SNR region, the only eigenmode corresponding to the highest singular value is active. In this case, the optimal power allocation goes to the channel with the highest receiver SNR. In this region, capacity increases at a rate of 1 bps/Hz per each 3 dB increase in transmit power.

Intermediate SNR: In this SNR region, L modes are active, where $1 < L < min(R, T)$. The capacity has an increase of L bps/Hz for every 3 dB increase in transmit power.

High SNR: In a high SNR region, all $min(R, T)$ modes are active. In this region, the capacity increases by $min(R, T)$ bps/Hz for every 3 dB increase in transmit power.

When applying a water filling algorithm to (2.13) and substituting SVDs, the MIMO capacity becomes

$$C = \max_{\rho_i : \sum_i \rho_i \leq \rho} \sum_{i=1}^{R_H} B \log_2 \left(1 + \sigma_i^2 \rho_i\right), \tag{2.18}$$

where B is the bandwidth, σ_i is the nonzero singular value in the i^{th} channel, R_H is the number of nonzero singular values σ^2 of $\mathbf{H}$, and $\rho = \frac{P_T}{\sigma^2}$ [9]. A MIMO channel has R_H degrees of freedom due to the fact that it contains R_H parallel channels [9]. To determine the power allocation to each channel, (2.18) can be written as

$$C = \max_{P_i : \sum_i P_i \leq P} \sum_{i=1}^{R_H} B \log_2(1 + \frac{P_i \gamma_i}{P_T}), \tag{2.19}$$

where P_T is the transmitted power, and $\gamma_i = \frac{\sigma_i^2 P}{\sigma}$ which is the SNR in the i^{th} channel at full power [9].

Using (2.19) for water filling power optimization for any MIMO channel yields

$$\frac{P_i}{P_T} = \frac{1}{\gamma_0} - \frac{1}{\gamma_i},\ \gamma_i \geq \gamma_0, \tag{2.20}$$

where γ_0 is an arbitrary cutoff value [9]. The resulting water filling capacity for the MIMO system is

$$C_{Water\ Filling} = \sum_{i:\gamma_i \geq \gamma_0} B \log_2 \left(\frac{\gamma_i}{\gamma_0} \right). \tag{2.21}$$

To show an example of water filling and its effects on a MIMO channel, consider a 5 transmitter, 5 receiver system whose channel gain is

$$H = \begin{bmatrix} .1 & .3 & .7 & .6 & .3 \\ .1 & .4 & .5 & .4 & .1 \\ .9 & .9 & .2 & .6 & .8 \\ .3 & .5 & .7 & .1 & .1 \\ .4 & .6 & .7 & .8 & .1 \end{bmatrix}$$

With no water filling being implemented, the power would be transmitted evenly among these five transmit antennas; however, when applying water filling, it can be seen in Figure 2.11 that antennas 4 and 5 do not receive any power. Only antennas 1-3 receive power with antenna 1 and antenna 2 receiving nearly 95% of the transmitted power.

2.5 Transmitter Design

2.5.1 Modulation. This section briefly discusses three common forms of modulations used in wireless communications. Modulators transmit a symbol on a

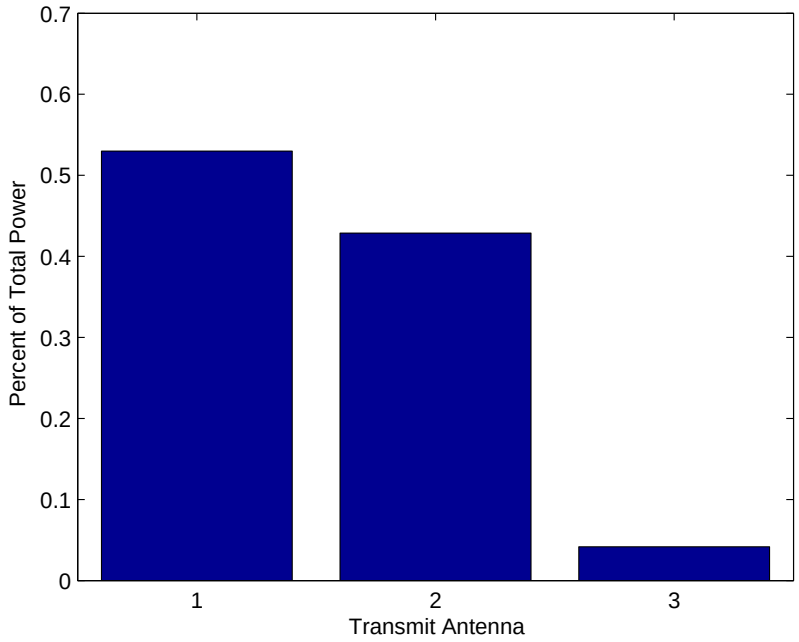

Figure 2.11: Power allocation.

carrier frequency by using a sinusoidal wave to represent the symbol. The symbols are distinguished from each other by either phase, amplitude, or both depending on the type of modulation.

2.5.1.1 M-ary Phase Shift Keying. In (MPSK) modulation, all the information is located in the phase of the transmitted sinusoidal waveform and has one degree of freedom. The following derivation follows the derivation seen in [9]. The transmitted signal over one symbol time T_s is given by

$$s_i(t) = Re\left\{Ag(t)e^{j2\pi(i-1)/M}e^{j2\pi f_c t}\right\}, \tag{2.22}$$

where M is the size of the alphabet, $g(t)$ has orthonormal properties, and A is a function of signal energy. (2.22) simplifies to

$$s_i(t) = Ag(t)\cos\left[\frac{2\pi(i-1)}{M}\right]\cos 2\pi f_c t - Ag(t)\sin\left[\frac{2\pi(i-1)}{M}\right]\sin 2\pi f_c t \qquad (2.23)$$

for $0 \leq t \leq T_s$. Using (2.23) the constellation points or symbols $s_1(t)$ and $s_2(t)$ are given by $s_1(t) = A\cos\left[\frac{2\pi(i-1)}{M}\right]$ and $s_2(t) = A\sin\left[\frac{2\pi(i-1)}{M}\right]$ for i=1,....,M. The different phases in the signal constellation are given by

$$\theta_i = 2\pi\frac{(i-1)}{M}. \qquad (2.24)$$

The minimum distance between constellation points in MPSK signaling is

$$d_{min} = 2A\sin\frac{\pi}{M}. \qquad (2.25)$$

All transmitted signals in MPSK constellation have equal energy and are expressed as

$$E_{s_i} = \int_0^{T_s} s_i^2(t)dt = A^2. \qquad (2.26)$$

Each signal within the constellation is equally spaced by $\frac{2\pi}{M}$. An important feature of MPSK modulation is that all symbols have equal energy and have one degree of freedom where symbols are distinguished based on their phase.

2.5.1.2 M-ary Quadrature Amplitude Modulation. In M-ary Quadrature Amplitude Modulation (MQAM), the symbols are distinguished based on the transmitted sinusoidal signal's phase and amplitude; hence, QAM has two degrees of freedom. Due to the fact that MQAM modulation has an extra degree of freedom over MPSK modulation, it is more spectrally efficient since it can encode the most number of bits per symbol for a given average energy [9]. A transmitted signal using MQAM modulation is represented as

$$s_i(t) = A_i \cos(\theta_i) g(t) \cos(2\pi f_c t) - A_i \sin(\theta_i) g(t) \cos(2\pi f_c t),\ 0 \leq t \leq T_s. \tag{2.27}$$

Similar to MPSK modulation, MQAM modulation signal's energy in symbol $s_i(t)$ is

$$E_{s_i} = \int_0^{T_s} s_i^2(t) dt = A_i^2, \tag{2.28}$$

where A_i is the symbol's amplitude.

2.5.1.3 Orthogonal Frequency Division Multiplexing. When a channel exhibits severe attenuation, Orthogonal Frequency Division Multiplexing (OFDM) modulation is commonly implemented. OFDM modulation is also able to resist deep fades without the use of equalization filters. In order for signals s_i and s_j to be orthogonal, they must have the property

$$\int_0^{T_s} s_i(t) s_j(t)\, dt = 0, for\, i \neq j, \tag{2.29}$$

where T_s is the symbol duration. OFDM modulation implements a guard channel between users that allows multiple users without having interference between them. OFDM signals are obtained by taking the MQAM or MPSK signals and implementing an N-point Inverse Fast Fourier Transform (IFFT) of the data. After implementing the IFFT of the MQAM or MPSK modulated data, a cyclic prefix (CP) is added to the front of each OFDM symbol. The cyclic prefix is created by accessing the last μ IFFT data points of the OFDM symbol and putting them on the front of the OFDM symbol. The cyclic prefix acts as a guard interval that eliminates the intersymbol interference from the previous symbol. The process of creating OFDM signals can be seen in Figure 2.12. At the receiver, the cyclic prefix is removed and a N-point Fast Fourier Transform (FFT) is conducted as seen in Figure 2.13. Figure 2.14 shows one

OFDM symbol with the shaded portion representing the cyclic prefix. Figure 2.15 gives a pictorial description of multiple OFDM signals in series.

Taking the IFFT produces an OFDM symbol consisting of the sequence x[n] = x[0], x[1],....x[N-1] of length N, where

$$x[n] = \sum_{i=0}^{N-1} X[i] e^{j2\pi ni/N},\ 0 \leq n \leq N-1. \tag{2.30}$$

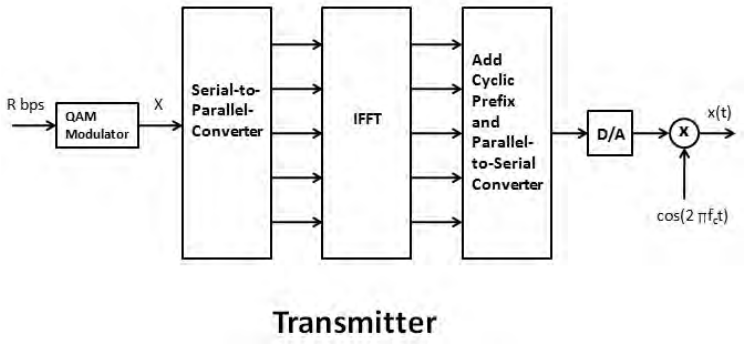

Figure 2.12: OFDM transmitter [9].

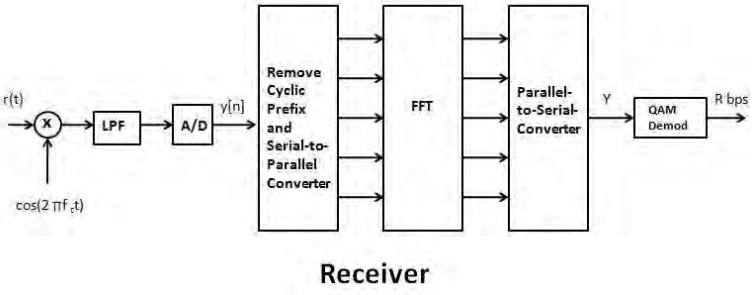

Figure 2.13: OFDM receiver [9].

2.5.2 Gray Coding. Gray coding is a popular way to design the symbol constellation where one of the m bits in a symbol's constellation differs from each

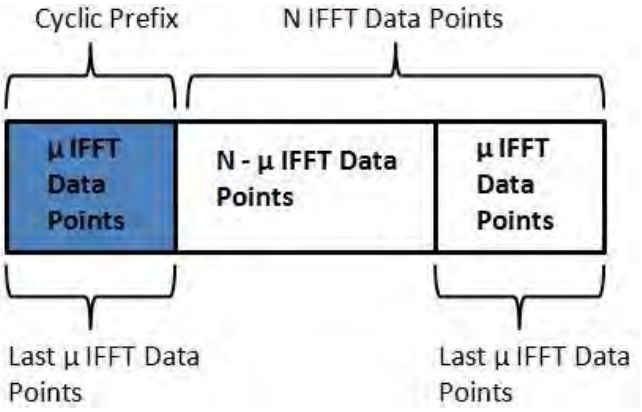

Figure 2.14: OFDM signal with CP.

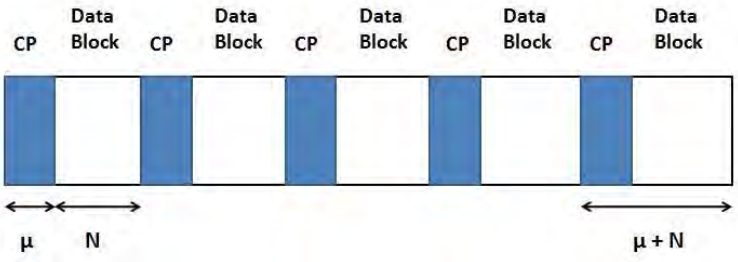

Figure 2.15: OFDM output.

neighboring symbol constellations. Gray coding is commonly used because it decreases the BER. Figure 2.16 shows an 8PSK gray coded symbol constellation.

2.6 Multipath

Multipath is the propagation of radio signals to a receive antenna by two or more separate paths and is the result of reflections off of physical obstructions or atmospheric conditions in the environment. Multipath causes destructive interference as well as phase shifting to the transmitted signal, but it also causes constructive interference which increases the received power. There are many radio propagation

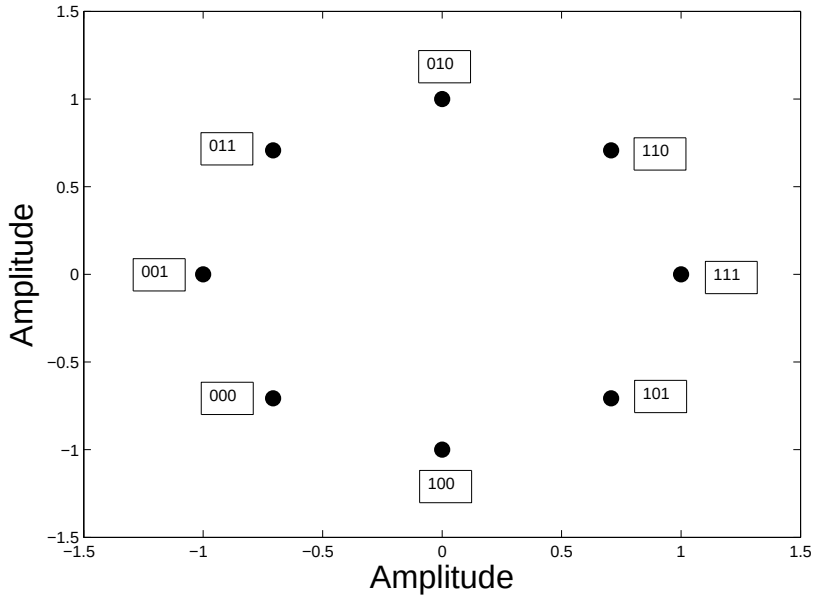

Figure 2.16: 8PSK Gray coded symbol constellation.

models in literature; however, after conducting a literature review, a decision was made that the two-ray model seemed the most appropriate multipath model due to the LOS model requirement.

Two − Ray Model. The two-ray model is used when modeling radio wave propagation over a flat terrain and contains a direct ray from the source and a ray reflected from the surface [13], seen in Figure 2.17 where $h1$ and $h2$ represent the height of the transmitter and receive antennas respectfully. The Rician distributed LOS ray path length is modeled as $r1$, and the reflected path length or multipath is modeled as $r2$. In most multipath model, including the two-ray model, the LOS signal power is higher than the reflected multipath signal power.

SISO Multipath. The received symbols using a SISO model with multipath can be modeled as

$$\mathbf{y}[\mathbf{n}] = \sum_{k=0}^{K} \mathbf{h}(\mathbf{k})\mathbf{x}(\mathbf{n}-\mathbf{k}) + \mathbf{n}(\mathbf{n}), \tag{2.31}$$

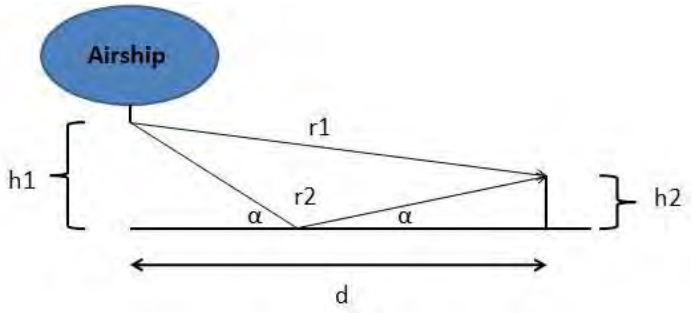

Figure 2.17: Two-ray multipath model.

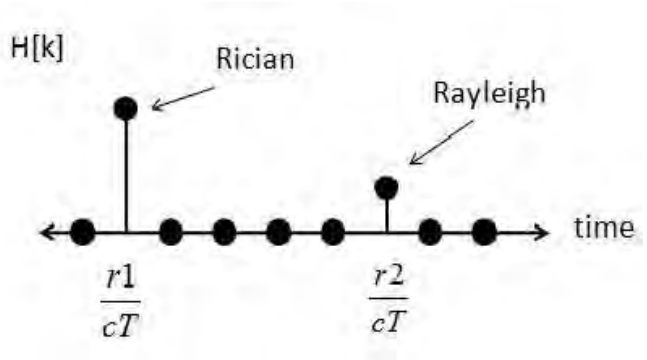

Figure 2.18: Two-ray multipath received signals.

where K is the delay of the multipath array, k is the time delay in terms of T or $\frac{1}{B}$, **h(k)** is the channel gain matrix, **x(n-k)** is the transmitted symbol, and **n(n)** is noise at time n.

The delay caused by the longer multipath, or K, is related to the sampling period, T_{sample}, by

$$K = \frac{R}{c \times T_{sample}}, \tag{2.32}$$

where c is the speed of light in ft/sec and R is the path length distance in ft. Figure 2.18 shows a picture of the LOS and multipath received rays as a function of time.

MIMO Multipath. Similar to the SISO multipath in (2.31), a MIMO system's multipath equation is

$$\mathbf{y[n]} = \sum_{k=0}^{K} \mathbf{H(k)x(n-k)} + \mathbf{n(n)}, \tag{2.33}$$

where **H(k)** is channel gain matrices for the LOS Rician channel as well as all multipath, **x(n-k)** is the transmitted signals, **H(k)** is the channel matrix, and **n(n)** is the noise vector. Using a two-ray model to model a MIMO communication airship with T Transmitters and R Receivers creates $T \times R$ LOS paths or $r1$'s, and $T \times R$ multipaths or $r2$'s. This brings the total number of received arrays in a MIMO two-ray mulitpath model to $2 \times T \times R$.

2.7 Receiver Design

2.7.1 Coding. Coding introduces deliberate redundancy into messages [14], which is commonly written as (n, k) where n is the total symbols, and k is the number of uncoded symbols or information symbols. Each symbol is composed of m bits where $m = log_2(n + 1)$. A drawback of coding is that it creates redundancy which reduces the code rate by a factor of $\frac{k}{n}$. Meanwhile, coding allows the user to increase the rate at which information may be transmitted over a channel while maintaining a fixed error rate [14].

According to the Channel Coding theorem in [15],

All rates below capacity C are achievable. Specifically, for every rate $R < C$, there exists a sequence of (2^{nR}, n) codes with maximum probability of error $\lambda^n \to 0$. Conversely, any sequence of (2^{nR}, n) codes with $\lambda^n \to 0$ must have $R \leq C$.

Following Channel Coding theorem, a code exists for any system that can cause the BER to approach 0. Coding gain, or Γ, is the difference in SNR between the uncoded system and the coded system when error correcting is used or

$$\Gamma = SNR_{Uncoded} - SNR_{Coded}, \tag{2.34}$$

where SNR_{Coded} and $SNR_{Uncoded}$ are expressed in dB.

In coded communication systems, the coding rate is

$$Coding\,Rate = \frac{k}{n}, \tag{2.35}$$

where n and k are the total number of symbols and the number of information symbols.

Popular coding schemes including Hamming and Bose-Chadhuri-Hocquenghem (BCH) codes are discussed in this section for their application to RS codes. Codes are sometimes written as (n, k, d) where d is the Euclidean Distance between the symbols. The error-coding capability, t, of the code is the maximum number of correctable symbols per codeword and is calculated as

$$t = \left\lfloor \frac{d_{min} - 1}{2} \right\rfloor, \tag{2.36}$$

where $\lfloor x \rfloor$ means the largest integer not to exceed x.

2.7.2 Hamming Codes. Hamming codes are a class of block codes which contain the traits of

$$(n, k) = (2^m - 1, 2^m - 1 - m), \tag{2.37}$$

where m = 2,3,.... and have a minimum distance of 3. By using (2.36), Hamming codes are capable of correcting all single errors or detecting all combinations of two or fewer errors within a block [2].

2.7.3 BCH Codes. BCH codes contain a large class of cyclic codes. They are a simpler version of Hamming codes that allow multiple error corrections [2]. They are typically the most important block codes because they exist for a wide range of rates, achieve high coding gains, and can be used at high speeds [3]. BCH codes are constructed with parameters [5]

$$n = 2^m - 1,$$

$$n - k \leq mt,$$

$$d_{min} = 2t + 1, \tag{2.38}$$

where m ($m \geq 3$) and t are positive integers. BCH codes allow a large selection of block lengths and code rates [5]. BCH codes work well with errors that occur randomly rather than in bursts; however, if bursts do occur, RS codes are better designed to fix the errors.

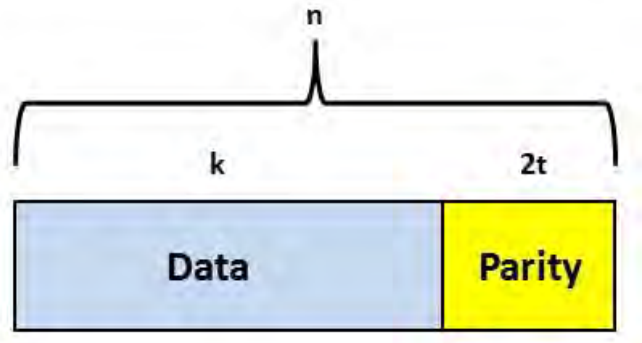

Figure 2.19: Reed Solomon codeword.

2.7.4 Reed-Solomon Codes. RS codes are non-binary, cyclic, linear BCH codes that are a popular correcting code frequently used in satellite communications [2]. They are especially effective at fixing errors that occur in bursts or when a number of bits are close together that may have resulted from impulse-type noise or interference [16]. RS codes are commonly written as RS(n,k) with m-bit symbols where $n = 2^m$ - 1. RS codes are commonly written by accessing k symbols and adding $2t$ parity check symbols where $2t = (n - k)$ at the end of the symbols seen in Figure 2.19. A RS decoder can correct up to t symbols in each RS codeword. RS codes are popular because they achieve the largest possible code minimum distance for any linear code with the same encoder input and output block lengths [2]. RS codes have efficient hard-decision decoding algorithms, which make it possible to implement long codes in applications where coding is desirable [5]. There are m bits per RS symbol where [17]

$$0 < k < n < 2^m + 2,$$

and a RS can be written as

$$(n, k) = (2^m - 1, 2^m - 1 - 2t),$$

$$d_{min} = n - k + 1,$$

RS codes are guaranteed to correct up to

$$t = \left\lfloor \frac{d_{min} - 1}{2} \right\rfloor = \left\lfloor \frac{n - k}{2} \right\rfloor$$

symbol errors.

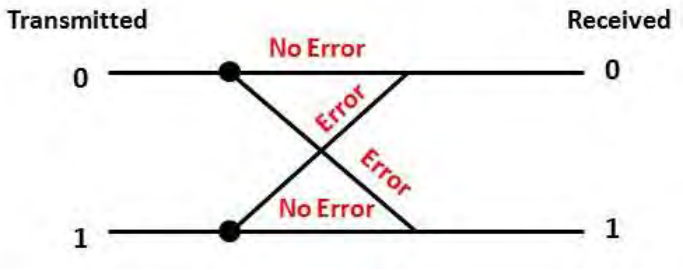

Figure 2.20: Binary error diagram.

2.7.5 Minimum Mean Square Error Equalizer. Crosstalk, or the effect of transmitted signals causing undesired effects on other receivers and channels, exists in MIMO systems. Using a Minimum Mean Square Error (MMSE) equalizer, which acts like a linear filter, is needed to eliminate the crosstalk. Another benefit of the MMSE equalizer is that it inverts the channel, which causes the number of received and transmitted signals to be the same and is useful when $T \neq R$. $\mathbf{H}^{\dagger}$, which is the pseudo inverse of the channel $\mathbf{H}$ with noise taken into effect, acts as a MMSE equalizer and is modeled as

$$\mathbf{H}^{\dagger} = (\mathbf{H}^{\mathbf{H}}\mathbf{H} + \sigma_{\mathbf{n}}^{\mathbf{2}}\mathbf{I})^{-1}\mathbf{H}^{\mathbf{H}}, \tag{2.39}$$

where $\mathbf{H}$ is the channel gain matrix, σ_n^2 is the SNR per transmit antenna, x^H denotes the Hermitian transpose, and $\mathbf{I}$ the identity matrix of size T. Applying $\mathbf{H}^{\dagger}$ eliminates crosstalk and gives an approximation to the transmitted signals.

2.8 Performance Metrics

2.8.1 Bit Error Rate. BER is a common metric used in communications that shows how efficiently a communication system is able to exchange information. An error occurs when the received signal and the transmitted signal are different as seen in Figure 2.20. BER is the percentage of errors or

$$BER = \frac{Errors}{Total\,Bits}, \tag{2.40}$$

where "Errors" is the total number of errors at the receiver and "Total Bits" is the sum of bits transmitted. A low BER, on the order of 10^{-5} and lower, is a highly desirable trait in any communications system.

If an uncoded system has an unacceptable BER, the system can be improved by increasing the transmit power and FEC. Increasing the transmit power increases the performance of the system by decreasing the effect of noise, causing less distortion in the received symbols. If the system is power limited, another technique for BER improvement is using FEC. Coding gain is the power saving that is avoided by not having to transmit more power. A disadvantage to FEC is lower throughput due to extra parity bits.

2.8.2 Throughput. Throughput is the average rate of successful receipts over a communication channel and is measured in bps. Similar to BER, throughput is an important metric when determining the effectiveness of a communication system. Throughput, per transmit antenna, for OFDM modulation is calculated as

$$Rate\,(bps) = \underbrace{\left(\frac{Bits}{TransmitSample}\right)}_{log_2(M)} \times \underbrace{\left(\frac{Samples}{Sec}\right)}_{B} \times \underbrace{(CodingLoss)}_{\frac{k}{n}} \times \underbrace{(CPLoss)}_{\frac{N}{N+v}} \tag{2.41}$$

where M is the size of the constellation, B is the bandwidth, k is the number of uncoded symbols, n is the number of total symbols, N is the length of the IFFT, and v is the length of the cyclic prefix. MPSK and MQAM throughput are calculated as in (2.41) except "CP Loss"' is removed. A MIMO system's total throughput is calculated by multiplying T and (2.41).

2.9 Conclusion

Chapter II introduced background which included throughput, modulation, multipath, and FEC. It also introduced theory relevant to MIMO communications. Relevant theory and equations were presented that allowed the reader understand basic MIMO theory and related concepts. Table 2.1 listed the important variables that are used throughout this research. Chapter III presents the methodology used in this research. In Chapter III, the reader becomes familiar with how theory presented in Chapter II is applied to this research.

III. Methodology

This research evaluates several trade-offs of a MIMO communications system between an airship and a ground station that has a capacity of 1 Tbps. There was much flexibility in the design of the system; however, there were some design requirements that had to be met. These basic requirements are discussed in this chapter. This chapter also discusses all methodology and procedures that are used in this research.

3.1 MIMO Model and Requirements

Table 3.1 lists all the physical constraints that were used in this research based on requirements from the sponsor. Using reverse engineering and applying the given constants with a fixed bandwidth of 5 GHz and a capacity of 1 Tbps with fixed transmit power into (2.6), it was determined that the SISO SNR listed in Table 3.1 was 4.77 dB. The Ku-Band (10.95-14.5 GHz) was the designated operating band. An operating center frequency of 12 GHz was selected because it fell near the center of the Ku-Band. This research did not investigate antenna designs and assumed that all antennas were isotropic. "Max separation" was the maximum horizontal separation between the airship and the array of ground receivers. "Receiver area" was is the total distance between the first and last ground receiver. This research also used the entire alloted bandwidth of 5 GHz.

Table 3.1: MIMO System Requirements.

Desired Capacity	$>$ 1 Tbps
Bandwidth	5 GHz
Operating Frequency	12 GHz
Max Separation	100 miles
Receiver Area	3 miles
Airship Altitude	60000 ft
Airship Length	600 ft
SNR	4.77 dB
Transmit Signal Power	1 W
Channel Fading	Frequency Selective
Sampling Rate	5 Gs/sec

Due to complexity issues, the MIMO system assumed that the airship was stationary. This research focused on different combinations of transmit and receive antenna arrays between 2-160 antennas.

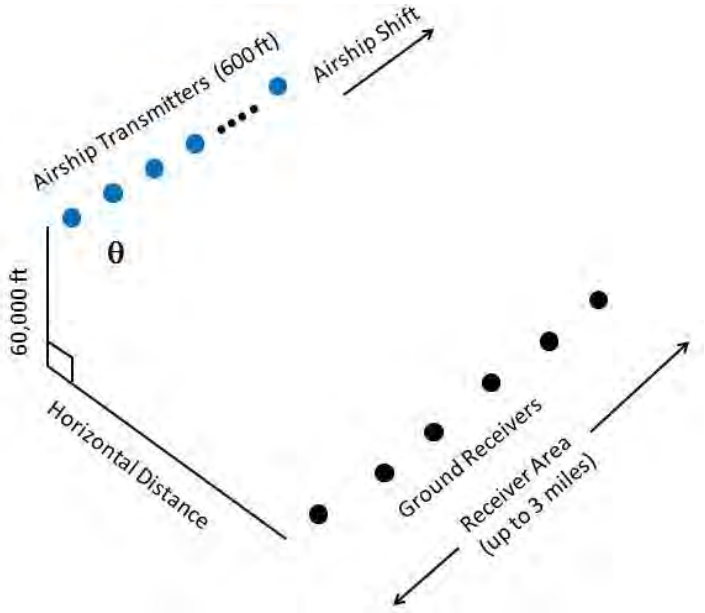

Figure 3.1: MIMO Communication System Model.

The sampling rate, T_{sample}, which was a function of the bandwidth, that was listed in Table 3.1 was calculated as

$$T_{sample} = \frac{1}{B} = \frac{1}{5.0E9\,Hz} = 2E-10\,Hz \tag{3.1}$$

and was used in this research. For all symbols shown throughput this chapter, all values listed with their abbreviation in Table 3.1 were used unless otherwise stated.

3.2 Channel Simulation

This section discusses the three channel models that were used in this research and applicable constants to their distribution.

3.2.1 Unit Magnitude, Phase Varying Channel. The first channel that was investigated was the unit magnitude, phase varying channel. This type of channel was selected to acquire an accurate estimate on how a channel would distort the transmitted symbols. In this model, the phase of the received signal changed while the amplitude remained fixed. A phase varying channel was a model used to simulate atmospheric effects. Although there was no change in the amplitude of the signal, phase effects were still important to see what impact they had had on the capacity. The unit magnitude, phase varying channel was modeled as

$$H_{ij} = e^{\frac{-j2\Pi F_c}{c} \cdot Length_{ij}}, \tag{3.2}$$

where c was the speed of light in ft/sec and $Length_{ij}$ was the distance between receive antenna i and transmit antenna j. Figure 3.2 shows the 2500 channel phases caused by a unit magnitude, phase varying channel distribution for 50 transmitters and 50 receivers.

3.2.2 Rician Distributed Channel. Since it was assumed that the airship transmit antennas has LOS with the ground receivers, a Rician distributed model was the most realistic channel used. In a Rician distributed model, the LOS factor from the transmitting antenna to receiving antenna was the dominating factor of the distribution.

The amplitudes and phases of the transmitted symbols had i.i.d. Rician distribution attenuation of

$$f(x) = \frac{x}{\sigma^2} e^{\frac{-(x^2+v^2)}{2\sigma^2}} I_0\left(\frac{xv}{\sigma^2}\right), \tag{3.3}$$

where I_0 was the modified Bessel function of the first kind and $\sigma = 0.1$ was used for all Rician distributions. Figure 3.3 shows a Rician distribution for a 50 transmitter and 50 receiver MIMO model.

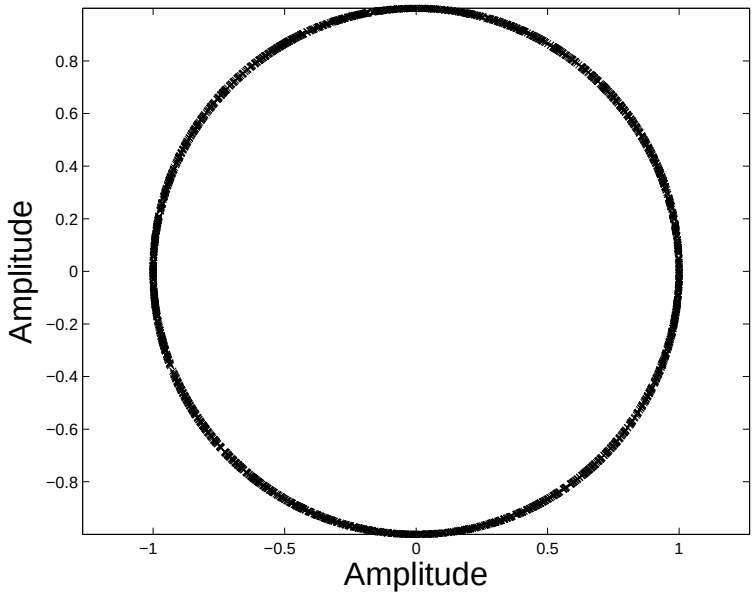

Figure 3.2: Unit magnitude, phase varying channel for 50 receivers and 50 transmitters model.

3.2.3 Rayleigh Distributed Channel. Rayleigh fading was used when modeling the multipath portion and followed the Rayleigh distribution of

$$f(x) = \frac{x}{\sigma^2} exp\left(-\frac{1}{2}\frac{x^2}{\sigma^2}\right), \tag{3.4}$$

where $x \geq 0$ and $\sigma = 0.01$ was used for multipath.

3.3 Water filling

Water filling as well as beam forming were examined to investigate whether an increase in capacity could be achieved without increasing T or R. Using (2.21), an algorithm was written that investigated the effects of water filling on capacity.

3.4 Beam forming

Beam forming was tested using (2.17) to investigate effects that beam forming had on the capacity of the large MIMO system. An algorithm was written that

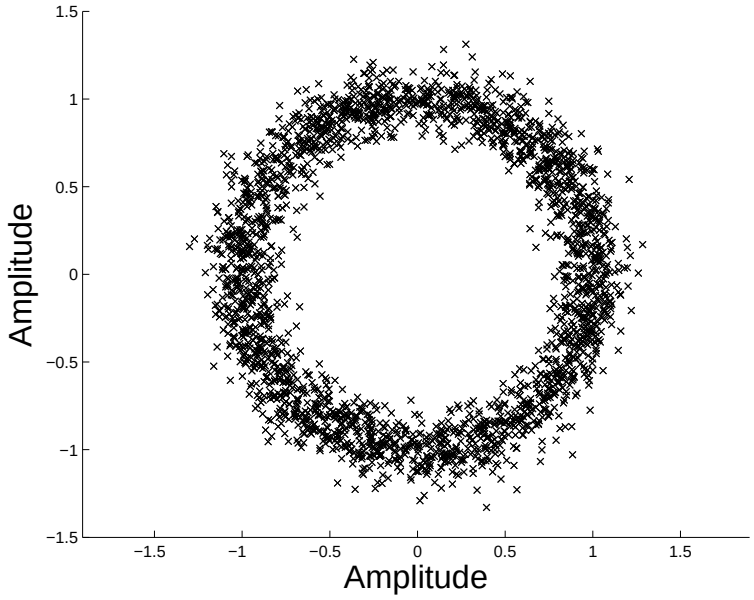

Figure 3.3: Rician distribution with phase channel for 50 receivers and 50 transmitters model.

calculated the capacity using beam forming for two 100-antenna arrays using the ratios that were listed in Table 3.2.

3.5 Performance Metrics

3.5.1 Capacity. This research examined the number of transmitters and receivers needed to achieve the super high data-rate of 1 Tbps. Table 3.2 shows 14 different cases of transmitter to receiver ratio and channel conditions that this research investigated. The numbers listed in Table 3.2 show the ratio of receivers to transmitters and not the actual number of antennas. Using Telatar's Optimal Power Allocation theorem and (2.13), an algorithm was written that examined antenna combinations with the ratios listed in Table 3.2 from 2-100 with an SNR of 3 and $\rho = \frac{3}{T}$.

3.5.2 Throughput. Throughput was calculated to investigate which antenna configuration and type of modulation transmitted the most bits through a channel. After viewing the results from beam forming and water filling and their affects on

Table 3.2: Ratio of Receivers to Transmitters and Channel Conditions.

Case	**T : R**	**Channel**
1	1:1	Unit Mag
2	1:2	Unit Mag
3	1:4	Unit Mag
4	1:8	Unit Mag
5	2:1	Unit Mag
6	4:1	Unit Mag
7	8:1	Unit Mag
8	1:1	Rician
9	1:2	Rician
10	1:4	Rician
11	1:8	Rician
12	2:1	Rician
13	4:1	Rician
14	8:1	Rician

capacity, throughput calculations were going to be made on the closest antenna configuration that exceeds the 1 Tbps requirement. The throughput results were plotted against the BER to assist in decision making on which coding scheme was the best. As mentioned in Chapter II, the best system had a low BER while maintaining a high throughput rate. M-ary modulation throughputs, such as MPSK and MQAM, were calculated as

$$Throughput = R\frac{Bits}{Symbol} \times B \times \frac{k}{n}, \tag{3.5}$$

where $R = log_2(M)$ of the M-ary modulation type while the throughput for 4QAM OFDM signaling was calculated as

$$Throughput = 2\frac{Bits}{Symbol} \times B \times \frac{k}{n} \times \frac{N}{N+v}, \tag{3.6}$$

where $N = 64$ for a 64-point IFFT and $v = 16$ was the length of the cyclic prefix.

3.5.3 BER. The last performance metric investigated was the BER and was used to determine a system's efficiency. For the no multipath, two-ray, and five-ray

multipath models, an algorithm was written that calculated the BER for each RS(n,k) code and different forms of modulation.

3.6 Transmitter Methods

3.6.1 BPSK, 4QAM, and 4QAM OFDM Modulation. For uncoded and coded signaling, this research began by studying the effectiveness of BPSK, 4QAM, and 4QAM OFDM modulation. Due to the small size of these constellations, the BER for these modulations may yield inconclusive results. Inconclusive results would be results that are all the same. For example, all RS BPSK modulation FEC, which has the largest spacing between the two symbol constellation points of the three listed, may all have results of BER of zero. If this research encounters inconclusive results, this research was going to investigate higher MPSK and MQAM modulation. Based on previous experience in digital communications, BPSK and 4QAM modulation should yield the lowest BER while yielding the lowest throughput compared to higher M-ary PSK or QAM modulation. One of the objectives of this research was to determine the best FEC and modulation type. If BER for smaller M-ary modulation is extremely low, it is advantageous to explore higher M-ary modulation to increase the throughput. If needed, this research will continue to increase the size of the M-ary modulation until a BER saturation has been reached for all RS codes that are being tested. BER saturation occurred when all RS codes for a given type of antenna configuration and modulation all yielded similar BER results. BPSK was modeled by taking one bit at a time and mapped to a constellation while 4QAM took two bits at a time and mapped the bits to the appropriate constellation. The 4QAM OFDM was modeled by taking 64 4QAM constellation points and taking a 64-point IFFT. A cyclic prefix of the last 16 IFFT points was inserted before the front of the other 64-point IFFT values in each RS codeword and sent through the channel. At the receiver, the cyclic prefix was removed and a 64-point FFT was done to each received RS codeword. The decoder then conducted MED decoding and mapped each of the 64-point FFT outputs to the closest constellation point.

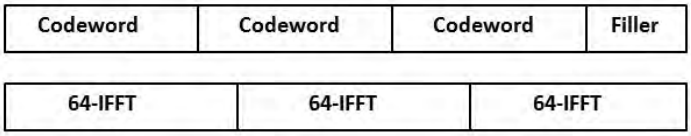

Figure 3.4: OFDM filler.

When generating OFDM symbols, it was important to take into consideration MATLAB^{TM}'s implementation of its IFFT and FFT functions. By implementing the N-point FFT of the signal, MATLAB^{TM}increased the received signal's power by a factor N. At the same time when implementing the N-point IFFT of the transmitted signal, MATLAB^{TM}'s IFFT function decreased the transmitted signal power by a factor of N. To overcome the reduction or increase in power while implementing a 64-point IFFT and FFT, a scaling factor of $\sqrt{64}$ was used. Table 3.3 shows the proper scaling factors that were used where X represents the 64 constellation points that were selected at the time.

Table 3.3: OFDM Scaling Factors.

Function	**Scaling Factor**
64-Point IFFT	$X \times \sqrt{64}$
64-Point FFT	$\frac{X}{\sqrt{64}}$

To ensure that all data were divisible by 64, extra constellation points were added to ensure that the number of constellation points after the modulator were exactly divisible by 64. Figure 3.4 shows three RS codewords whose lengths are less than three 64-point IFFT blocks. A filler of random constellation points was added to the end of the last RS codeword to make the RS codewords' and filler's length to be the same length as three 64-point IFFTs. At the demodulator, the same filler positions were removed to eliminate extra bits. Adding these random constellation points did not cause extra errors and did not affect the performance of the system.

Table 3.4: RS Signaling Table.

n	k	m	t	RS Codewords
7	3	3	1	5556
15	7	4	2	1786
15	5	4	3	2500
31	11	5	5	910
63	7	6	15	1190
127	29	7	21	246
255	223	8	4	28
255	71	8	29	88
127	99	7	4	72

3.7 Multipath

3.7.1 No Multipath Model. When performance with no multipath was modeled, each transmitter transmitted approximately 50 K bits per transmit antenna though a Rician fading channel. After initial capacity performance, the unit magnitude, phase varying channel were no longer investigated. The unit magnitude, phase varying channel model was used as a starting point. The bits were i.i.d. and generated using MATLAB$^{\text{TM}}$'s "rand" function. This research began by investigating the uncoded as well as RS encoded performance for four different transmitter to receiver combinations that favored a higher ratio of receivers to transmitters. Since each (n, k) FEC code had different bits per symbol and a different number of uncoded symbols, an algorithm was used to calculate the 50 K bits per transmit antenna. The 50 K bits transmitted per transmit antenna were calculated by

$$RS\,codewords = \left\lfloor \frac{50K\,bits}{m\frac{bits}{symbol} \times k\,uncoded\,symbols} \right\rfloor, \tag{3.7}$$

where $\lfloor x \rfloor$ was the floor operation. Table 3.4 lists the nine RS FEC schemes as well as the number of RS codewords that were transmitted per transmit antenna. The algorithm indexed from 2 to 100 transmit antennas and the number of RS codewords in Table 3.4 were transmitted per transmit antenna.

Using a signaling schematic similar to that seen in Figure 2.1 with physical parameters listed in Table 3.1 and RS codewords in Table 3.4, a MIMO communication algorithm was written that examined this communication scheme from 2-100 transmit and receive antennas. Bits were generated using MATLAB^{TM}'s "rand" function and were encoded using MATLAB^{TM}'s "rsenc" function. After encoding, the modulator mapped the bits to corresponding constellation points. These constellation points, which corresponded to symbols, were distorted by the channel and i.i.d. Gaussian noise was added to the constellation points. The distorted received symbols were mapped to constellation points using Minimum Euclidean Distance (MED) which mapped the receive symbol to the closest constellation symbol. The estimated symbols were sent to the decoder where symbol corrections were made. After corrections were made, the parity symbols were removed and the information symbols were converted to estimated bits. The estimated bits were then compared to the transmitted bits to determine the number of errors.

3.7.2 Multipath Model. Any terrestrial communication is effected by multipath and any model should represent those effects. Although it was known that multipath should be implemented in any model, multipath was difficult to accurately model. This thesis chose the two-ray model and five-ray model to simulate multipath. These models were chosen due to the LOS link. In these models, the most significant multipath were the reflections from the earth.

When calculating the BER with multipath added to the model, approximately 1 M bits were generated from each transmit antenna for each of the following RS signaling schemes. Due to memory constraints in MATLAB^{TM}, the 1 M bits were sent in 50 iterations with 20 K bits in each iteration. Sending the bits through 50 iterations also helped average channel effects and decreased the chance of generating multiple deep fading channels. The two performance metrics used in determining signaling performance were throughput and BER, which are typical performance met-

rics in communications system. Table 3.5 lists the number of RS codewords that was generated for each (n, k) FEC two-ray and five-ray multipath model.

Table 3.5: Multipath Signaling Table.

n	**k**	**m**	**t**	**RS Codewords**
7	3	3	1	222
15	7	4	2	72
15	5	4	3	100
31	11	5	5	36
63	7	6	15	48
127	29	7	21	10
127	99	7	4	2
255	223	8	4	2
255	71	8	29	4

3.7.2.1 Two-Ray Model. As previously discussed in Chapter II, the two-ray model had two paths, a LOS and a reflected path that simulated multipath. When modeling the two-ray model multipath, a delay in terms of T between the LOS factor and the reflected factor needed to be calculated. Since the airship was at most 100 miles away and the maximum distance that separated any set of receivers was three miles, it was determined that the rounded delay (K) to the nearest integer was five sampling periods. K remained the same for all transmitter and receiver combinations that operated within the constraint of this research. Using the two-ray model, it can be shown that the received signal was

$$\mathbf{y_k} = \underbrace{[\mathbf{H_k}, \mathbf{H_{k-5}}]}_{\mathbf{H}} \underbrace{\begin{bmatrix} \mathbf{x_k} \\ \mathbf{x_{k-5}} \end{bmatrix}}_{\mathbf{x}} + \mathbf{n_k}, \tag{3.8}$$

where k was the current time element, $\mathbf{H_k}$ was the current time Rician channel matrix and $\mathbf{H_{k-5}}$ was the time delayed Rayleigh distributed multipath matrix, $\mathbf{x_k}$ was the current time and time delayed transmitted symbols, $\mathbf{n_k}$ was the noise vector, and $\mathbf{y_k}$ was the received symbol vector. $\mathbf{H_{k-5}}$ and $\mathbf{H_k}$ as well as $\mathbf{x}$ and $\mathbf{x_{k-5}}$ were placed next

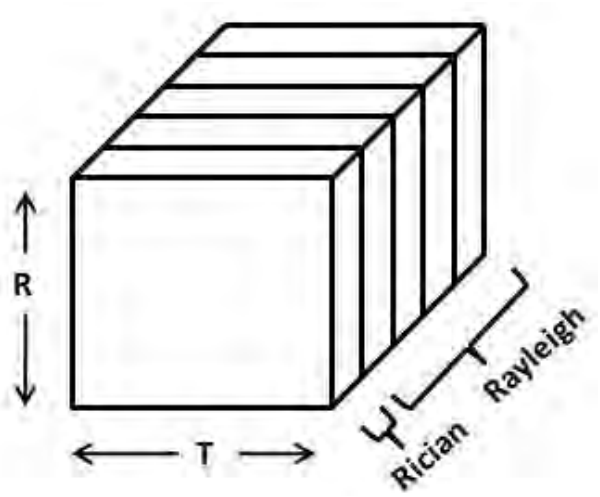

Figure 3.5: Multipath channel diagram.

to each other in (3.8). A LOS signal power of 0.01 W and reflected multipath power of 100 μW were used.

The multipath channel effects were stored as a cube of dimensions R x T x K as seen in Figure 3.5. The face of the block was the Rician distributed channel or LOS and the non-face depths of the cube were modeled as Rayleigh fading to represent multipath.

3.7.2.2 Five-Ray Model. The five-ray model was an extension of the two-ray model except there were four multipath links instead of one. Although the two-ray model conceptually was used for multipath, a five-ray model was a more realistic model due to the extra multipath. In terrestrial ground receivers, there were numerous multipaths due to reflected signals. The five-ray model was modeled as

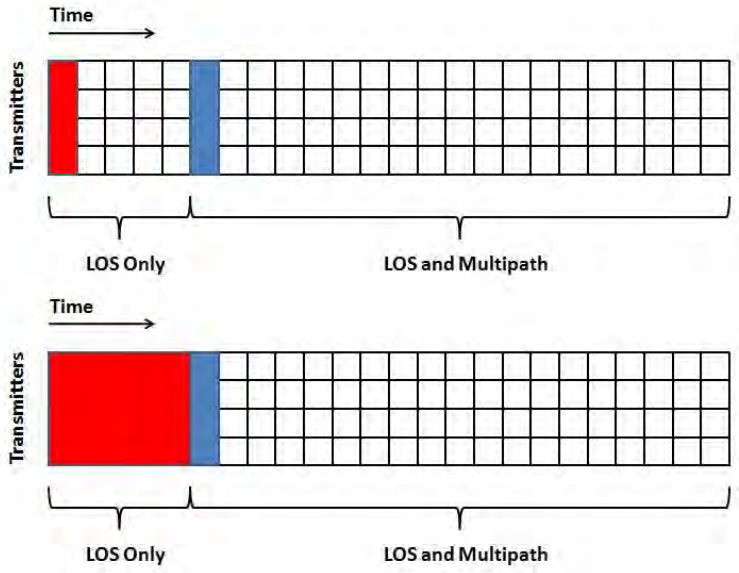

Figure 3.6: Multipath signaling models for two-ray (top) and five-ray (bottom).

$$\mathbf{y_k} = \underbrace{[\mathbf{H_k}, \mathbf{H_{k-1}}, \mathbf{H_{k-2}}, \mathbf{H_{k-3}}, \mathbf{H_{k-4}}]}_{\mathbf{H}} \underbrace{\begin{bmatrix} \mathbf{x_k} \\ \mathbf{x_{k-1}} \\ \mathbf{x_{k-2}} \\ \mathbf{x_{k-3}} \\ \mathbf{x_{k-4}} \end{bmatrix}}_{\mathbf{x}} + \mathbf{n_k}, \tag{3.9}$$

where the $\mathbf{H_k}$ was the Rician LOS channel and $\mathbf{H_{k-1}}$, $\mathbf{H_{k-2}}$, $\mathbf{H_{k-3}}$, and $\mathbf{H_{k-4}}$ were the reflected Rayleigh distributed multipath channel matrices, $\mathbf{x_k}$ contained the current time through the t - 4 delayed transmitted symbols, and $\mathbf{n_k}$ was the noise vector. $\mathbf{H}$ and $\mathbf{x}$ had the channel matrices and transmitted delayed symbol vectors placed next to each other. A LOS signal power of 10 mW and reflected multipath power of 100 μW were used.

The signaling constellation for the two-ray (top graph) and five-ray model (bottom graph) can be seen in Figure 3.6 where red represents the received time delayed

multipath symbols and blue represents the LOS symbols. In the two-ray model for $t < 6$ sampling periods, only the LOS ray was received; however, after 5 sampling periods, a LOS ray was received at time τ and a multipath ray was received at time tau - 5. Similarly the five-ray model begins receiving multipath at $t = 2$ sampling periods. Starting at $t = 6$ sampling periods, five multipaths from t - 5, t - 4, t - 3, t - 2, and t - 1 are received.

3.7.3 Noise Scaling Factor. It was mentioned in Chapter II that all noise introduced into a communication system must be properly scaled. The SNR for a SISO system was shown in (2.5). In a MIMO communication system, the total SNR was

$$SNR_{Total} = \frac{\sigma_x^2 \times T}{\sigma_n^2}, \tag{3.10}$$

which increased by a factor T compared to a SISO SNR. Solving (3.10) for the noise power yielded

$$\sigma_n^2 = \frac{\sigma_x^2 \times T}{SNR}. \tag{3.11}$$

Solving for σ_n yielded a scaling noise factor of

$$noise = \sqrt{\sigma_n^2} = \sqrt{\frac{\sigma_x^2 \times T}{SNR}}. \tag{3.12}$$

Fixing the transmit signal power to 1 W in (3.12), resulted in a MIMO noise scaling factor of

$$MIMO\, noise\, scaling\, factor = \frac{\sigma_x^2 \times T}{\sqrt{2} \times SNR} \tag{3.13}$$

that was used to scale the noise for any symbol constellation.

Coding gains are implemented to give an increase to the signal power without adding power to the system. There exists research that contains the Γ listed for different FEC. If a table with a specific coding gain is obtained, Γ can be placed into (3.14) and the SNR improvement is obtained.

$$SNR = \frac{\sigma_x^2}{\sigma_n^2} \times \Gamma = \frac{\sigma_x^2 \times T \times \Gamma}{\sigma_n^2}, \tag{3.14}$$

which would result in a MIMO scaling factor of

$$MIMO\,noise\,scaling\,factor\,with\,FEC = \frac{\sigma_x^2 \times T \times \Gamma}{\sqrt{2} \times SNR}, \tag{3.15}$$

where Γ is the signal power gain (in dB) caused by coding gain.

3.8 MMSE Equalizer

The MMSE equalizer was used to decouple the crosstalk between receivers. It was represented as $\mathbf{H}^{\dagger}$ and was modeled as

$$\mathbf{H}^{\dagger} = \left(\mathbf{H}^H\mathbf{H} + \frac{T}{SNR} \times \mathbf{I}\right)^{-1} \mathbf{H}^H, \tag{3.16}$$

where $\mathbf{H}$ was the channel gain matrix, x^H denoted the Hermitian transpose, and $\mathbf{I}$ was the identity matrix with the size of the number of columns in $\mathbf{H}$.

3.9 MATLAB Implementation

MATLAB was used for all results in this research. The code began by modeling the physical parameters seen in Table 3.1. The transmit and receive antennas were evenly spaced over the "Air Ship Length" and "Receiver Area" distances that were provided. The code then calculated the distance between each transmitter and receiver and was used for calculating the channel matrix. The code iterated through the antenna array with different $T : R$ for each RS(n,k) for all different modulation

types. When multipath was not incorporated into the model, a new **H** was generated for each $T : R$ and a total of 50,000 bits per T were transmitted. When multipath was incorporated, 50 **H** were generated for each $T : R$ for channel averaging and 1 M bits per transmit antenna were transmitted. MATLAB's "rsenc" and "rsdec" were used to simulate the RS encoder and decoder.

3.10 Conclusion

Chapter III represented the methodology that was used in this research, and a summary of the MATLAB implementation is summarized in Table 3.6. Table 3.1 showed the physical system requirements that were used. The unit magnitude, phase varying channel and Rician distributed channel models were discussed, and Table 3.2 listed the interested antenna configurations. This chapter also took relevant equations listed in Chapter II and changed them to reflect this research. The next chapter presents and describes the results that were obtained by implementing information from this chapter.

Table 3.6: MATLAB Model Implementation.

Topic	**Implementation**	**Iterations**
>1 Tbps capacity higher $T : R$	Loop Increments	8
>1 Tbps capacity higher $R : T$	Loop Increments	8
Water Filling Capacity	Loop Increments	4
Beam Forming Capacity	Loop Increments	4
Throughput	Loop Increments	1
No Multipath Model	50K Bits per Transmitter	1
Multipath Model	1M Bits per Transmitter	50
RS Encoder	rsenc	As Required
RS Decoder	rsdec	As Required

IV. Results

This chapter reveals the results that were obtained using the methodology described in Chapter III. These results include capacity using the unit magnitude, phase varying channel and Rician distributed channel for different transmitter and receiver ratios, beamforming and water filling capacities, throughput calculations for various forms of modulation, and BER performance with no multipath and two-ray and five-ray simulated multipath.

4.1 Capacity

4.1.1 Unit-Magnitude, Phase Varying Channel Capacity. Figures 4.1 and 4.2 show the capacity for the unit-magnitude, phase varying channel without using water filling techniques. Technical specifications required a 1 Tbps threshold, which is represented by the solid red line seen in Figures 4.1 - 4.5. Figure 4.1 shows the capacity for a higher ratio of transmitters to receivers configuration while Figure 4.2 shows the capacity for a higher ratio of receivers to transmitters. Since this research began with an unknown antenna array size needed to achieved the desired capacity, an antenna array size within the tested antenna size could reach the 1 Tbps capacity using a unit-magnitude, phase varying channel. From these results, it can be seen that using a higher ratio of receivers to transmitters allows the threshold capacity of 1 Tbps to be achieved with fewer transmit antennas compared to the number of receive antennas needed for the higher transmitter to receiver case. Not only are fewer antennas needed, but the improvement as the ratio increases also dramatically increases.

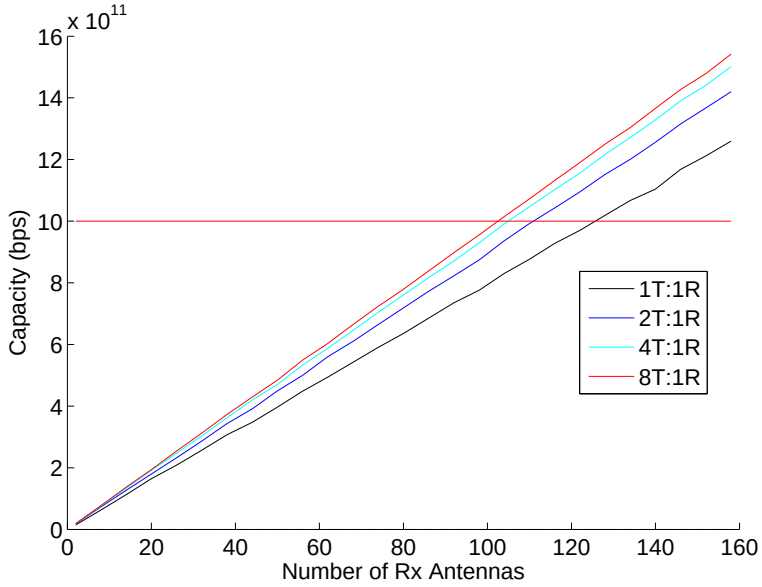

Figure 4.1: System capacity performance with phase varying channel and higher ratio of $T : R$.

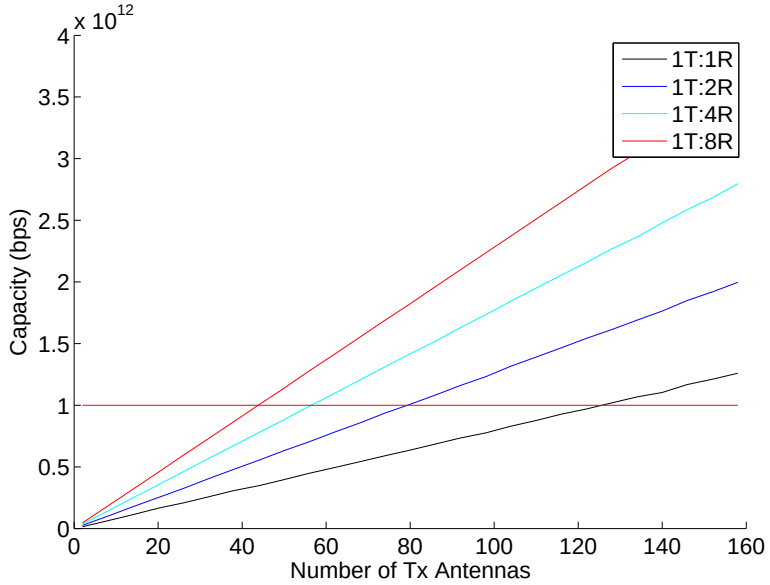

Figure 4.2: System capacity performance with phase varying channel and higher ratio of $R : T$.

4.1.2 Rician Channel Capacity with Water Filling. After discovering that a phase-varying channel allowed the 1 Tbps capacity to be allowed under the antenna arrays, the channel was changed to the Rician distributed channel to simulate a LOS link between the airship and receivers. The capacity results can be seen in Figures 4.3 and 4.4. The figures show that the capacity results are similar to the results seen with the unit magnitude, phase varying channel. The capacities were plotted without using the water filling method (solid line) and with using water filling (dashed lines). As seen from the plots, water filling does not add any benefit to the capacity. The capacities that resulted from water filling are shown in Table 4.2 and Table 4.3. The results show that water filling does not increase the capacity for any number or ratio of transmitters to receivers. This can be explained because $\Gamma_i = \sigma_i^2 \rho$, which is the SNR at the i^{th} channel at full power decreases as the size of the antenna array increases. In some research models where water filling was implemented, the SNR per channel was fixed regardless of the size of the array. With a power fixed airship, the SNR per channel decreases as the array increases which limits the capacity of water filling. It can be seen that as the ratio of transmitters to receivers increases, so does the water filling capacity.

The systems that did not implement water filling shows some important information. Table 4.1 shows the minimum number of transmitters and receivers for different antenna ratios that are needed to reach the desired 1 Tbps which were obtained from Figure 4.3. It can be seen that eight different ratios listed were able to obtain the desired 1 Tbps capacity. The improvement seen in the ratio of more transmitters to receivers is not as significant as when there are more receivers than transmitters. Another factor to consider is the weight and cost associated with each transmitter. Due to the fact that the airship has limited resources, it is best to have as few antennas on the airship as possible. This theory also coincides with what Alamouti discovered in his paper cited in Chapter II [10] that it is best to have more antennas at the receiver. From this point forward, only higher receiver to transmitter antenna configuration ratios are considered.

The results presented for the rest of the chapter represent antenna configurations that have the capacity to achieve a 1 Tbps throughput. Due to losses and other mitigated factors, this throughput is not always achieved. In order to account for these losses, a simple scaling factor could be performed on the configuration of the system in order to achieve the desired 1 Tbps throughput.

Table 4.1: Number of Antennas Needed to Reach 1 Tbps with Rician Channel and no Water Filling.

T : R Ratio	**T**	**R**	**Total**
8:1	816	102	918
4:1	416	104	520
2:1	220	110	330
1:1	124	124	248
1:8	44	352	396
1:4	62	248	310
1:2	80	160	240
1:1	124	124	248

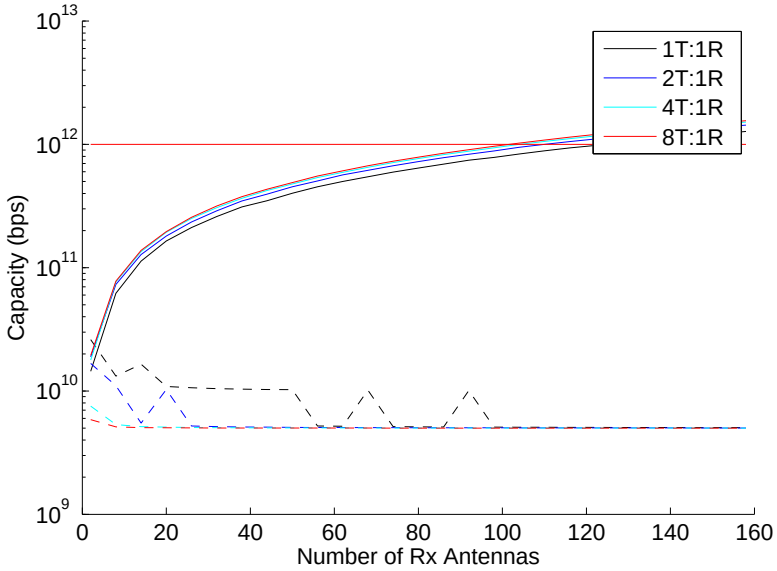

Figure 4.3: System capacity performance with Rician channel and higher ratio of $T : R$.

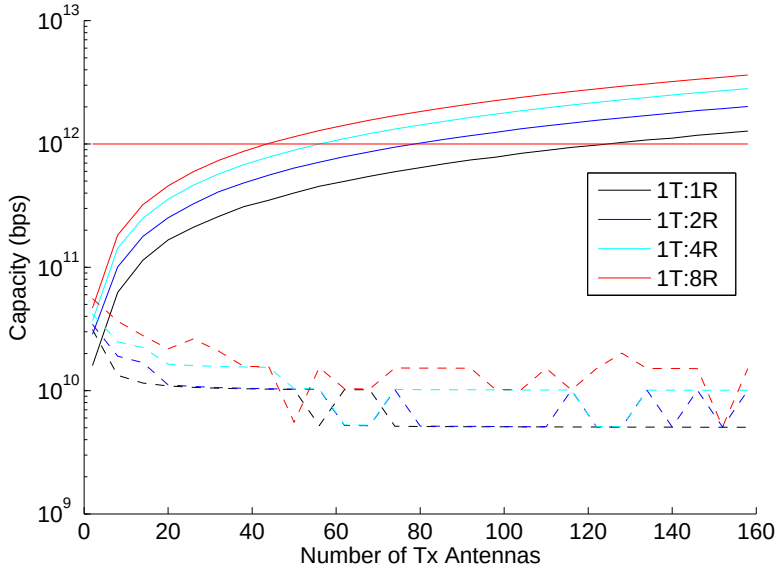

Figure 4.4: System capacity performance with Rician channel and higher ratio of $R : T$.

Table 4.2: Water Filling Capacity (bps) with more Transmitters and Rician Channel.

T	R	C	T	R	C	T	R	C	T	R	C
2	2	3.22e10	4	2	1.64e10	8	2	7.56e9	16	2	5.86e9
8	8	1.33e10	16	8	1.11e10	32	8	5.35e9	64	8	5.11e9
14	14	1.14e10	28	14	1.05e10	56	14	5.15e9	112	14	5.05e9
20	20	1.09e10	40	20	5.29e9	80	20	5.09e9	160	20	5.03e9
26	26	1.06e10	52	26	5.20e9	104	26	5.06e9	208	26	5.02e9
32	32	1.05e10	64	32	5.15e9	128	32	5.05e9	256	32	5.02e9
38	38	1.03e10	76	38	5.11e9	152	38	5.04e9	304	38	5.01e9
44	44	1.02e10	88	44	5.10e9	176	44	5.03e9	352	44	5.00e9
50	50	1.02e10	100	50	5.08e9	200	50	5.0e9	400	50	5.00e9
56	56	5.21e9	112	56	5.06e9	224	56	5.02e9	448	56	5.00e9
62	62	5.18e9	124	62	5.05e9	248	62	5.02e9	496	62	5.00e9
68	68	5.15e9	136	68	5.05e9	272	68	5.02e9	544	68	5.00e9
74	74	5.14e9	148	74	5.04e9	296	74	5.01e9	592	74	5.00e9
80	80	5.12e9	160	80	5.04e9	320	80	5.01e9	640	80	5.00e9
86	86	5.11e9	172	86	5.03e9	344	86	5.01e9	688	86	5.00e9
92	92	5.10e9	184	92	5.03e9	368	92	5.01e9	736	92	5.00e9
98	98	5.09e9	196	98	5.03e9	392	98	5.01e9	784	98	5.00e9

4.1.3 Beam Forming Capacity. The results for a higher ratio of receivers to transmitters beam forming capacity can be seen in Figure 4.5 and are listed in Table 4.4. Comparing the beam forming capacities to the water filling capacities, it can be seen that beam forming does produce a higher capacity than water filling; however, all beam forming capacities fall short of the 1 Tbps threshold. Similar to water filling, beam forming is advantageous to use on a fixed power communication system. The final beam forming capacity or (2.17) says that the capacity is related to σ_{max}^2 of the channel matrix. As the size of the antenna array increases, σ_{max} increases; however, at the same time ρ, which is the SNR per transmitter, decreases. The σ_{max}^2 term increases faster than it can be reduced by the ρ term which causes a slight overall increase in capacity seen in Table 4.4. If the airship could be designed with a fixed power per channel and not a total fixed power, beam forming would be advantageous. If the power were fixed per channel, then the ρ term would remain fixed and σ_{max} grows exponentially, which would result in much higher capacities.

Table 4.3: Water Filling Capacity (bps) with more Receivers and Rician Channel.

T	R	C	T	R	C	T	R	C	T	R	C
2	2	2.59e10	2	4	3.27e10	2	8	4.21e10	2	16	5.43e10
8	8	1.33e10	8	16	1.90e10	8	32	2.50e10	8	64	3.65e10
14	14	1.15e10	14	28	1.69e10	14	56	2.23e10	14	112	2.80e10
20	20	1.09e10	20	40	1.12e10	20	80	1.64e10	20	160	2.68e10
26	26	5.64e9	26	52	1.60e10	26	104	2.09e10	208	208	2.62e10
32	32	1.04e10	32	64	1.06e10	32	128	1.57e10	32	256	1.59e10
38	38	1.53e10	38	76	1.04e10	38	152	1.55e10	38	304	1.57e10
44	44	1.03e10	44	88	1.04e10	44	176	1.54e10	44	352	1.56e10
50	50	1.03e10	50	100	1.03e10	50	200	1.04e10	50	400	5.54e9
56	56	5.20e9	56	112	1.03e10	56	224	1.03e10	56	448	1.54e10
62	62	5.18e9	62	124	5.22e9	62	248	5.28e9	62	496	1.04e10
68	68	1.02e10	68	136	5.20e9	68	272	5.23e9	68	544	1.04e10
74	74	5.14e9	74	148	5.17e9	74	296	1.02e10	74	592	1.52e10
80	80	5.12e9	80	160	1.01e10	80	320	1.02e10	80	640	1.52e10
86	86	5.10e9	86	172	5.13e9	86	344	1.02e10	86	688	1.52e10
92	92	1.00e10	92	184	5.13e9	92	368	5.10e9	92	736	1.52e10
98	98	5.10e10	98	196	5.12e9	98	392	5.09e9	98	784	1.02e10

At this point the results show that in a fixed power MIMO system, water filling and beam forming do not increase the overall system's capacity. This research shows the results for the minimum number of antennas needed to exceed the 1 Tbps threshold for the 1:1, 1:2, 1:4, and 1:8 transmitter to receiver ratio.

4.2 Throughput

Tables 4.5, 4.6, and 4.7 show the throughput (bps) for BPSK, 4QAM, and 4QAM OFDM for 98 transmitters and 98 receivers, 80 transmitters and 160 receivers, 62 transmitters and 248 receivers, and 44 transmitters and 352 receivers using RS FEC. It can be seen that the RS(255,223) had the highest throughput and the RS(127,99) had the second highest throughput. By similar comparison, 4QAM modulation had the highest throughput, followed by 4QAM OFDM, and BPSK modulation had the lowest throughput. If high throughput is desired, a RS code with a high coding gain and modulation with the most transmit antennas is needed. An important conclusion that can be drawn is that none of the RS codes listed in Tables 4.5 - 4.7

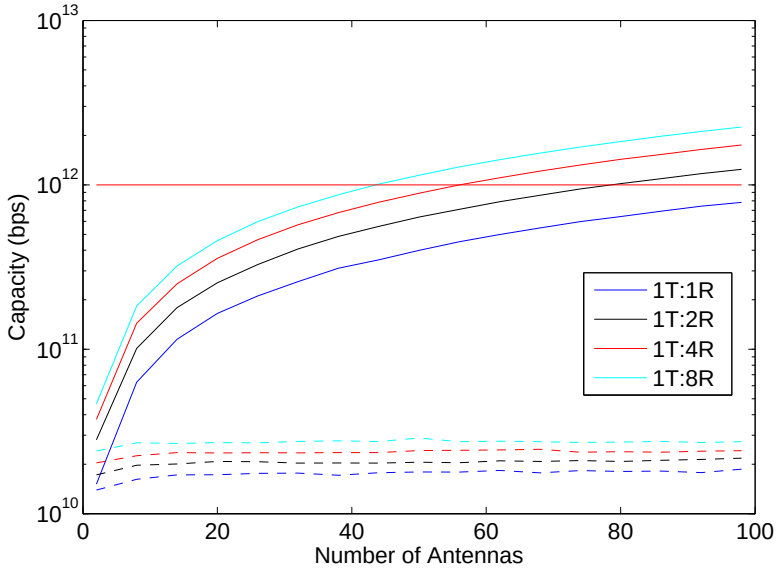

Figure 4.5: Beam forming capacity with Rician channel and higher $R:T$ ratio.

are capable of reaching a 1 Tbps throughput. The Shannon Hartley Capacity theorem is the best capacity that a system can reach and getting a throughput to match the system's capacity is not always achievable. One solution increases T in any $T:R$ (scaling factor) that is above the 1 Tbps seen in Figure 4.4 to meet the throughput requirement. Another solution increases the modulation size, which allows more bits per symbol, to increase the throughput.

4.3 BER Performance

4.3.1 BER with no Multipath. BER is a highly studied and researched part of a communication system's performance. The first signaling model that was tested was BER performance with no multipath. The BER plots for different antenna configurations using FEC can be seen in Appendices A and B. The solid lines represent BER with no FEC and the dashed lines show the BER performance with FEC. By examining the graphs, three important conclusions can be made. The first result is that the BER performance for a fixed transmitter to receiver ratio remains fairly constant, and there is minimal improvement in BER performance for selecting a

Table 4.4: Beamforming Capacity (bps) with Rician Channel.

T	R	C	T	R	C	T	R	C	T	R	C
2	2	1.42e10	2	4	1.68e10	2	8	1.99e10	2	16	2.45e10
8	8	1.64e10	8	16	1.99e10	8	32	2.28e10	8	64	2.69e10
14	14	1.67e10	14	28	2.02e10	14	56	2.34e10	14	112	2.67e10
20	20	1.71e10	20	40	2.06e10	20	80	2.34e10	20	160	2.71e10
26	26	1.75e10	26	52	2.07e10	26	104	2.35e10	208	208	2.71e10
32	32	1.75e10	32	64	2.03e10	32	128	2.35e10	32	256	2.74e10
38	38	1.71e10	38	76	2.04e10	38	152	2.35e10	38	304	2.77e10
44	44	1.79e10	44	88	2.06e10	44	176	2.40e10	44	352	2.74e10
50	50	1.80e10	50	100	2.06e10	50	200	2.41e10	50	400	2.89e10
56	56	1.79e10	56	112	2.05e10	56	224	2.44e10	56	448	2.74e10
62	62	1.79e10	62	124	2.09e10	62	248	2.47e10	62	496	2.75e10
68	68	1.77e10	68	136	2.09e10	68	272	2.37e10	68	544	2.74e10
74	74	1.82e10	74	148	2.10e10	74	296	2.38e10	74	592	2.70e10
80	80	1.82e10	80	160	2.07e10	80	320	2.38e10	80	640	2.73e10
86	86	1.82e10	86	172	2.12e10	86	344	2.37e10	86	688	2.74e10
92	92	1.79e10	92	184	2.14e10	92	368	2.39e10	92	736	2.72e10
98	98	1.87e10	98	196	2.18e10	98	392	2.43e10	98	784	2.75e10

specific set of transmitters to receivers within a fixed transmitter to receiver ratio. The second conclusion that can be made is that FEC for all tested signaling increases BER performance. This is important to note because for all FEC, there does exist a SNR where the coded and uncoded BER performances cross. If the system had a SNR that was lower than the SNR of the cross-over point, FEC decreases performance. Verifying this ensures that a SNR of 4.77 dB is to the right of the cross-over point for all 9 tested codes. If one code had poorer performance while implementing FEC, then it would need to be eliminated as a possible signaling scheme for this system. The third important conclusion that can be made is that the higher the ratio of receivers to transmitters, the better the BER performance of the system. With this conclusion, selecting an antenna configuration that has a high receiver to transmitter antenna configuration is more advantageous for best BER performance.

4.3.2 BER with Two-Ray Multipath Model. Tables 4.8 - 4.10 show the BER results for the two-ray model for 3 antenna configurations: 80 transmitters and 160

Table 4.5: BPSK Throughput (bps) with Rician Channel without Water Filling.

$(\mathbf{n}, \mathbf{k})$	**98 T, 98 R**	**80 T, 160 R**	**62 T, 248 R**	**44 T, 352 R**
(7,3)	2.10e11	1.71e11	1.33e11	9.43e10
(15,5)	1.63e11	1.33e11	1.03e11	7.33e10
(15,7)	2.29e11	1.87e11	1.45e11	1.03e11
(31,11)	1.74e11	1.42e11	1.10e11	7.81e10
(63,7)	5.44e10	4.44e10	3.44e10	2.44e10
(127,29)	1.12e11	9.13e10	7.08e10	5.02e10
(127,99)	3.82e11	3.12e11	2.42e11	1.72e11
(255,71)	1.36e11	1.11e11	8.63e10	6.13e10
(255,223)	4.29e11	3.50e11	2.71e11	1.92e11

Table 4.6: 4QAM Throughput (bps) with Rician Channel without Water Filling.

$(\mathbf{n}, \mathbf{k})$	**98 T, 98 R**	**80 T, 160 R**	**62 T, 248 R**	**44 T, 352 R**
(7,3)	4.20e11	3.43e11	2.66e11	1.89e11
(15,5)	3.27e11	2.67e11	2.07e11	1.47e11
(15,7)	4.57e11	3.73e11	2.89e11	2.06e11
(31,11)	3.48e11	2.84e11	2.20e11	1.56e11
(63,7)	1.09e11	8.89e10	6.89e10	4.89e10
(127,29)	2.24e11	1.83e11	1.42e11	1.00e11
(127,99)	7.64e11	6.24e11	4.83e11	3.43e11
(255,71)	2.73e11	2.23e11	1.73e11	1.23e11
(255,223)	8.57e11	7.00e11	5.42e11	3.85e11

receivers, 62 transmitters and 248 receivers, and 44 transmitters and 352 receivers using 50 generated Rician channels for the LOS component and 50 Rayleigh channels for multipath simulation. Errors listed in all tables that were zero are listed in the tables as $< 10^{-8}$ because of the finite number of samples. From the tables, it can be seen that BPSK modulation had the best BER performance, followed by 4QAM, and 4QAM OFDM had the poorest BER performance. Using BPSK modulation, RS FEC was able to correct all errors for all ratios. For the 1 transmitter to 2 receiver ratio or data seen in Table 4.8, only the RS(31,11), RS(63,7), RS(127,29), and RS(255,71) codes were able to correct all errors for BPSK and 4QAM modulation. What makes this interesting is that all four of these codes have a symbol correction capacity, $t \geq 5$. The other RS codes have $t \leq 4$ and all had errors. When examining the 1 transmitter to 4 receiver and the 1 transmitter to 8 receiver ratio, all BPSK and 4QAM

Table 4.7: 4QAM OFDM Throughput (bps) with Rician Channel without Water Filling.

$(\mathbf{n}, \mathbf{k})$	**98 T, 98 R**	**80 T, 160 R**	**62 T, 248 R**	**44 T, 352 R**
(7,3)	3.36e11	2.74e11	2.13e11	1.51e11
(15,5)	2.61e11	2.13e11	1.65e11	1.17e11
(15,7)	3.66e11	2.98e11	2.31e11	1.64e11
(31,11)	2.78e11	2.27e11	1.76e11	1.24e11
(63,7)	8.71e10	7.11e10	5.51e10	3.91e10
(127,29)	1.79e11	1.46e11	1.13e11	8.03e10
(127,99)	6.11e11	4.98e11	3.86e11	2.74e11
(255,71)	2.18e11	1.78e11	1.38e11	9.80e10
(255,223)	6.85e11	5.59e11	4.33e11	3.07e11

code errors were all corrected which resulted in BER of $< 10^{-8}$. This was mostly due to the fact that the noise scaling factor compared to the spacing of the symbol constellation for these two ratios was lower causing less distortion of the received symbols allowing for more accurate symbol estimation. OFDM modulation had the worst BER performance for all ratios. Although BER performance improved as diversity increased, it underperformed BPSK and 4QAM modulation in terms of BER. The BER performance improved as the ratio of receivers to transmitters increased which was expected. One positive effect caused by multipath is the extra power that is obtained at the receive antenna which caused a decrease in the number of errors causing improvement in the system's performance. Comparing these performances to the performances in Section 4.2, BER performance can be seen to have an improvement for all signaling schemes. Although OFDM modulation has some advantages over BPSK and 4QAM modulation such as synchronization, it is no longer considered a modulation candidate due to its under performing BER performance. Since most BPSK and 4QAM modulated codes resulted in a BER $< 10^{-8}$, it indicates that a transmit power of 1 W may not be optimally used since all errors were corrected. Due to the 1 W transmit power constraint, higher modulation types is needed to be investigated to determine which type of modulation causes a saturation in the transmit power.

Table 4.8: 80 Transmitters, 160 Receivers BER using Two-Ray Model.

(n, k)	BPSK	4QAM	4QAM OFDM
(7,3)	<1.00e-8	8.80e-5	8.48e-3
(15,5)	<1.00e-8	7.07e-6	8.41e-3
(15,7)	<1.00e-8	1.25e-6	8.47e-3
(31,11)	<1.00e-8	<1.00e-8	8.44e-3
(63,7)	<1.00e-8	<1.00e-8	8.41e-3
(127,29)	<1.00e-8	<1.00e-8	8.46e-3
(127,99)	<1.00e-8	1.35e-4	8.51e-3
(255,71)	<1.00e-8	5.05e-3	8.47e-3
(255,223)	<1.00e-8	<1.00e-8	8.43e-3

Table 4.9: 62 Transmitters, 248 Receivers BER using Two-Ray Model.

(n, k)	BPSK	4QAM	4QAM OFDM
(7,3)	<1.00e-8	<1.00e-8	2.82e-4
(15,5)	<1.00e-8	<1.00e-8	2.86e-4
(15,7)	<1.00e-8	<1.00e-8	2.87e-4
(31,11)	<1.00e-8	<1.00e-8	2.82e-4
(63,7)	<1.00e-8	<1.00e-8	2.86e-4
(127,29)	<1.00e-8	<1.00e-8	2.81e-4
(127,99)	<1.00e-8	<1.00e-8	2.79e-4
(255,71)	<1.00e-8	<1.00e-8	2.78e-4
(255,223)	<1.00e-8	<1.00e-8	2.85e-4

4.3.3 BER with Five-Ray Multipath Model. Tables 4.11 - 4.13 list the BER results for BPSK, 4QAM, and 4QAM OFDM modulation using the five-ray model. Each simulation created 50 LOS, Rician channels and 50 multipath, Rayleigh channels. The Rician had a power of $\sigma^2 = 10$ mW and the multipath coefficients had a power of $\sigma^2 = 100$ μW which resulted in a LOS power that was 100 times that of the reflected multipath. The results from the five-ray model are similar to those of the two-ray model. Since the results are comparable, the results are not being elaborated. Also, to investigate more multipath rays using the two-ray model is not practical since the results would be similar. The five-ray multipath model's BER vs. throughput graphs were placed in Appendix C.

Table 4.10: 44 Transmitters, 352 Receivers BER using Two-Ray Model.

(n, k)	BPSK	4QAM	4QAM OFDM
(7,3)	<1.00e-8	<1.00e-8	4.55e-7
(15,5)	<1.00e-8	<1.00e-8	4.51e-7
(15,7)	<1.00e-8	<1.00e-8	2.27e-7
(31,11)	<1.00e-8	<1.00e-8	4.59e-7
(63,7)	<1.00e-8	<1.00e-8	<1.00e-8
(127,29)	<1.00e-8	<1.00e-8	2.24e-7
(127,99)	<1.00e-8	<1.00e-8	3.28e-7
(255,71)	<1.00e-8	<1.00e-8	6.37e-7
(255,223)	<1.00e-8	<1.00e-8	1.4e-6

Table 4.11: 80 Transmitters, 160 Receivers BER using Five-Ray Model.

(n, k)	BPSK	4QAM	4QAM OFDM
(7,3)	<1.00e-8	8.38e-5	8.46e-3
(15,5)	<1.00e-8	7.94e-6	8.40e-3
(15,7)	<1.00e-8	5.00e-7	8.51e-3
(31,11)	<1.00e-8	<1.00e-8	8.50e-3
(63,7)	<1.00e-8	<1.00e-8	8.47e-3
(127,29)	<1.00e-8	<1.00e-8	8.55e-3
(127,99)	<1.00e-8	1.42e-4	8.46e-3
(255,71)	<1.00e-8	5.10e-3	8.45e-3
(255,223)	<1.00e-8	<1.00e-8	8.50e-3

4.4 Throughput vs. BER

4.4.1 Throughput vs. BER with No Multipath. At this point, it is important to begin narrowing down which antenna configurations is being considered for the large MIMO array. Since it was discovered in Section 4.3.1 that the number of transmitters or receivers selected in a given transmitter to receiver ratio does not affect the BER, it is most important to keep costs down by selecting the minimum T and R. At the same time, the throughput depends on which number of antennas were selected. Throughput is a function of the number of transmit antennas as well as the type of modulation. For a fixed type of modulation, a designer could increase T to increase the throughput; however, this would increase the cost by increasing the number of antennas which increases the hardware and software implementation needed to support them. An objective of this thesis was to select the fewest number of antennas

Table 4.12: 62 Transmitters, 248 Receivers BER using Five-Ray Model.

(n, k)	BPSK	4QAM	4QAM OFDM
(7,3)	<1.00e-8	<1.00e-8	2.85e-4
(15,5)	<1.00e-8	<1.00e-8	2.84e-4
(15,7)	<1.00e-8	<1.00e-8	2.90e-4
(31,11)	<1.00e-8	<1.00e-8	2.73e-4
(63,7)	<1.00e-8	<1.00e-8	2.92e-4
(127,29)	<1.00e-8	<1.00e-8	2.78e-4
(127,99)	<1.00e-8	<1.00e-8	2.84e-4
(255,71)	<1.00e-8	<1.00e-8	2.88e-4
(255,223)	<1.00e-8	<1.00e-8	2.82e-4

Table 4.13: 44 Transmitters, 352 Receivers BER using Five-Ray Model.

(n, k)	BPSK	4QAM	4QAM OFDM
(7,3)	<1.00e-8	<1.00e-8	2.28e-7
(15,5)	<1.00e-8	<1.00e-8	9.02e-7
(15,7)	<1.00e-8	<1.00e-8	<1.00e-8
(31,11)	<1.00e-8	<1.00e-8	6.89e-7
(63,7)	<1.00e-8	<1.00e-8	1.35e-6
(127,29)	<1.00e-8	<1.00e-8	2.24e-7
(127,99)	<1.00e-8	<1.00e-8	9.84e-7
(255,71)	<1.00e-8	<1.00e-8	3.82e-7
(255,223)	<1.00e-8	<1.00e-8	4.00e-7

needed to meet the 1 Tbps threshold. By selecting the antenna configurations with a higher receiver to transmitter ratio in Table 4.1, their corresponding throughput and BER were plotted. This section shows plots of the BER and throughput that were obtained from Sections 4.2 and 4.3.1. As mentioned earlier, a communication system that has a low BER and high throughput is desired. Figures 4.6-4.9 plot the BER vs throughput for all nine RS FEC and the three forms of modulation with no multipath. For all BER vs throughput plots, the lower right corner is the most desired area. The BER values for these plots were extracted from the BER plots in Appendix A and B for the minimum number of antennas needed that were obtained in Table 4.1.

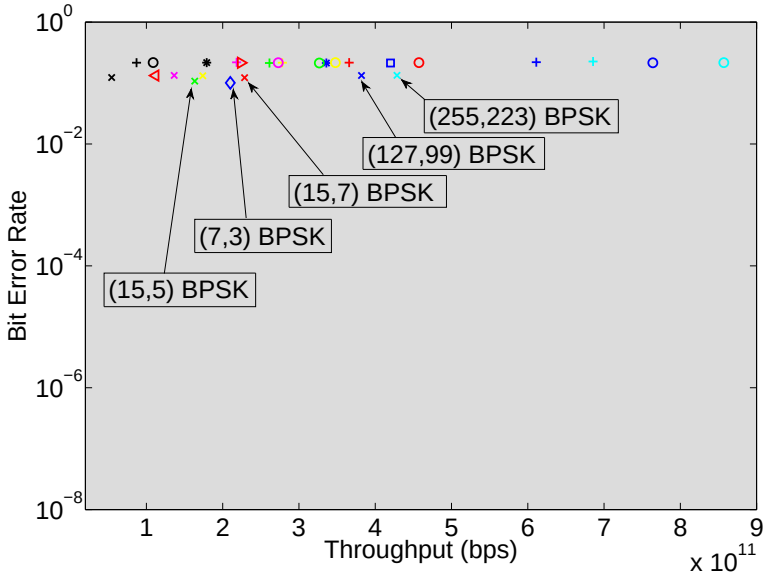

Figure 4.6: Throughput vs. BER, 98 transmitters and 98 receivers, no multipath.

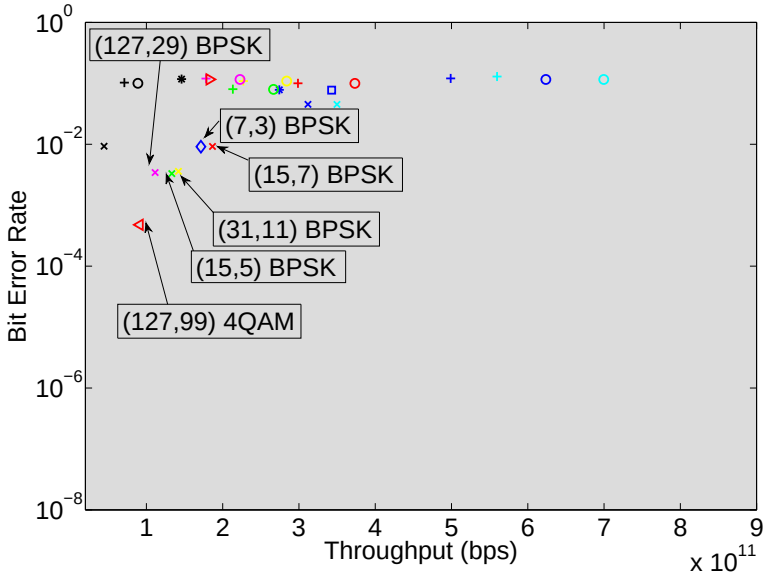

Figure 4.7: Throughput vs. BER, 80 transmitters and 160 receivers, no multipath.

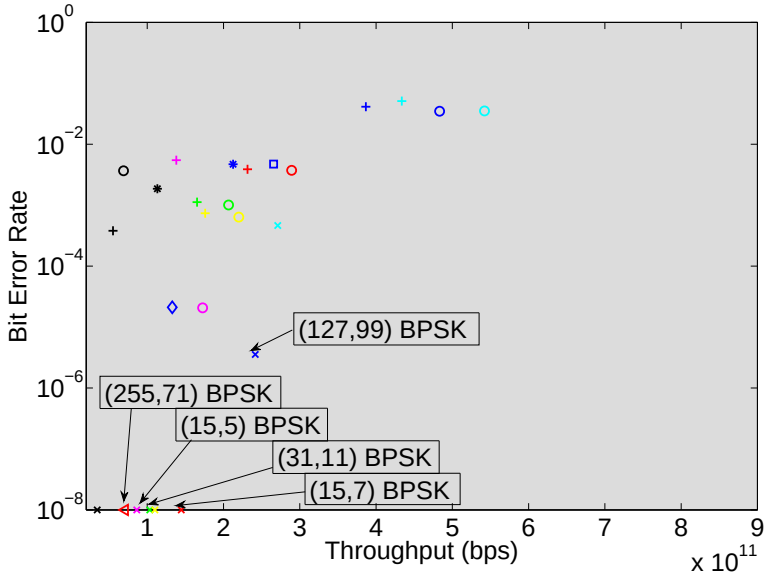

Figure 4.8: Throughput vs. BER, 62 transmitters and 248 receivers, no multipath.

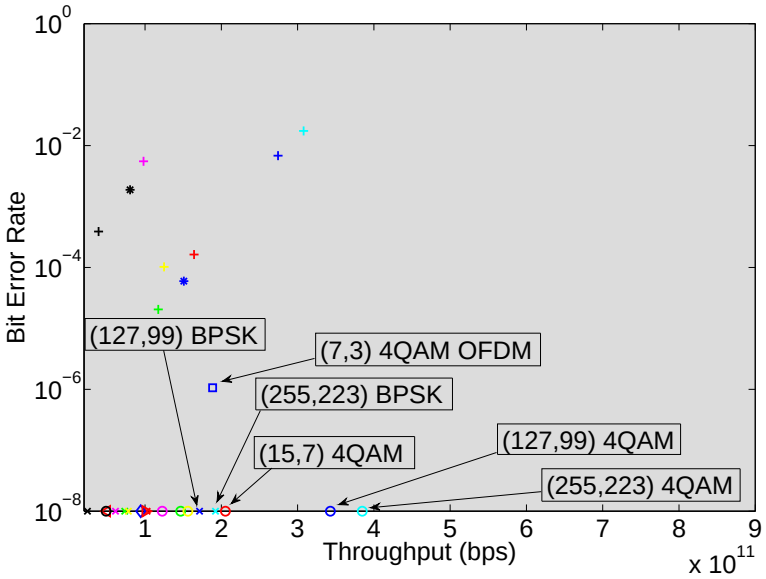

Figure 4.9: Throughput vs. BER, 44 transmitters and 352 receivers, no multipath.

Figures 4.6-4.9 show that as the ratio of transmitters to receivers increases, the throughput decreases while the BER performance increases. Figure 4.9 has the best performance in terms of highest throughput and lowest BER. The blue and cyan markings, which represented the RS(127,99) and RS(255,223) FEC respectively, BPSK, 4QAM, and 4QAM OFDM modulation symbols were consistently the best RS codes in terms of BER and throughput. Since the 98 transmitter and 98 receiver antenna configuration had the worst BER performance, it was no longer considered a viable configuration in this research. This transmitter to receiver ratio has the highest throughput; however, a BER of over 10% is unacceptable and would make the system unreliable.

4.4.2 Throughput vs. BER Results for Two-Ray Multipath Model. Figures 4.10-4.12 show the plots of the BER plotted against the throughput. Since some of the BER exceeded 10^{-8}, these BERs were plotted on the 10^{-8} line. By looking at the graphs, it can be seen that the RS(255,223) and RS(127,99) 4QAM modulation had the best placing on the figures for all ratios even though none of the RS codes were able to achieve a 1 Tbps throughput. This was due to their high coding rates and the codes ability to still be able to correct all the errors with a transmit power of 1 W. The RS(255,223) and RS(127,99) BPSK modulation were consistently the next best pair. The RS(255,71) and RS(127,29) are able to correct 29 and 21 symbols respectfully compared to 4 symbol corrections by RS(255,223) and RS(127,99); however, the RS(255,71) and RS(127,29) have low coding rates which causes their throughputs to be lower. If a communication system with both a low BER and high throughput is desired, RS(255,71) and RS(127,29) would not be the best choice of FEC. It would be best to select a RS code that has a high coding rate and the highest number of bits per symbol for modulation which in turn results in the highest throughput. As with other engineering design concerns, there are trade-offs associated with selecting different RS FEC. The trade-off in coding is that the more powerful or more symbols

that a (n, k) code is able to correct, the worse its coding rate is which causes a low throughput.

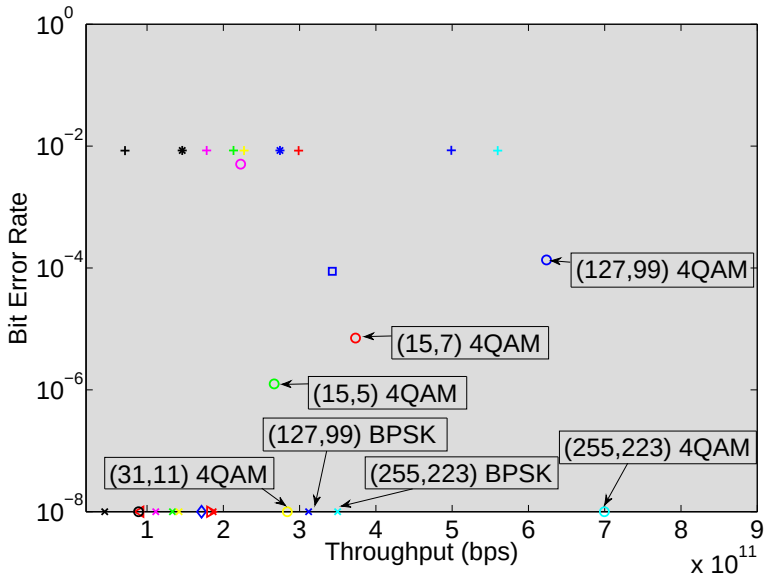

Figure 4.10: Throughput vs. BER, 80 transmitters and 160 receivers using two-ray model.

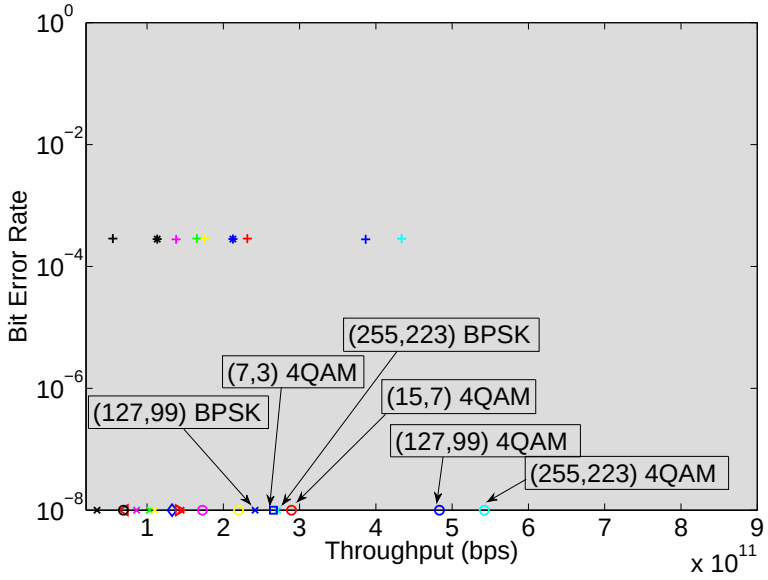

Figure 4.11: Throughput vs. BER, 62 transmitters and 248 receivers using two-ray model.

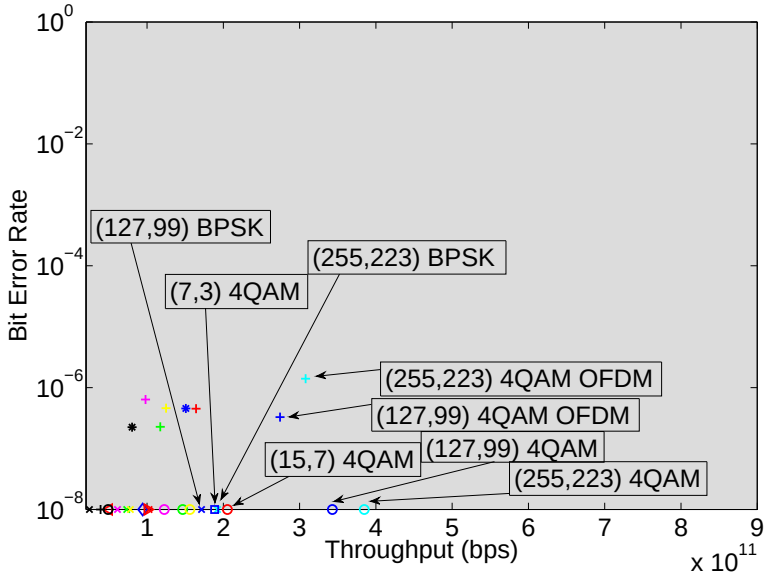

Figure 4.12: Throughput vs. BER, 44 transmitters and 352 receivers using two-ray model.

4.5 Higher M-ary Modulation

4.5.1 Throughput. Section 4.3.2 showed that BPSK and 4QAM modulation were not able to obtain a 1 Tbps throughput, and a higher modulation type, or bits per symbol, was desired. Tables 4.14 - 4.17 show the throughput for higher M-ary modulations which include 8PSK, 16QAM, 32QAM, and 64QAM modulation for the three antenna configurations. Similar to previous observations, RS(255,223) and RS(127,99) had the highest throughput because their coding rates remained the same while the bits per symbol increased which resulted in a higher throughput. For visual clarity, all throughputs > 1 Tbps were highlighted. It can also be seen that one 8PSK, three 16QAM, four 32QAM, and eight 64QAM RS codes were able to achieve the 1 Tbps throughput. The highest throughput was 2.1 Tbps, which was obtained by the RS(255,223) 64QAM code using 80 T and 160 R.

Table 4.14: 8PSK Throughput (bps).

(n, k)	**80 T, 160 R**	**62 T, 248 R**	**44 T, 352 R**
(7,3)	5.13e11	3.99e11	2.83e11
(15,5)	3.99e11	3.09e11	2.20e11
(15,7)	5.61e11	4.35e11	3.09e11
(31,11)	4.26e11	3.30e11	2.34e11
(63,7)	1.33e11	1.03e11	7.32e10
(127,29)	2.74e11	2.12e11	1.51e11
(127,99)	9.36e11	7.26e11	5.16e11
(255,71)	3.33e11	2.59e11	1.84e11
(255,223)	1.05e12	8.13e11	5.76e11

4.5.2 Higher M-ary Modulation BER. Sections 4.3.2 and 4.3.3 showed that BPSK and 4QAM BER performances were zero and were difficult to discriminate. In Chapter III, this research indicated that if identical BER performance was seen for BPSK, 4QAM, or 4QAM OFDM modulation it would investigate higher M-ary modulation types. The purpose of these results was to examine what was the highest modulation type that could be used that had fixed transmit power and bandwidth, and a SNR of 4.77 dB. This research continued by examining 8PSK, 16QAM, 32QAM, and 64QAM modulation and looked to see if any of these modulation types would hit

Table 4.15: 16QAM Throughput (bps).

(n, k)	80 T, 160 R	62 T, 248 R	44 T, 352 R
(7,3)	6.84e11	5.32e11	3.77e11
(15,5)	5.32e11	4.12e11	2.93e11
(15,7)	7.48e11	5.80e11	4.12e11
(31,11)	5.68e11	4.40e11	3.12e11
(63,7)	1.78e11	1.38e11	9.76e10
(127,29)	3.66e11	2.83e11	2.01e11
(127,99)	1.25e12	9.68e11	6.88e11
(255,71)	4.44e11	3.45e11	2.45e11
(255,223)	1.40e12	1.08e12	7.68e11

Table 4.16: 32QAM Throughput (bps).

(n, k)	80 T, 160 R	62 T, 248 R	44 T, 352 R
(7,3)	8.55e11	6.65e11	4.72e11
(15,5)	6.65e11	5.15e11	3.67e11
(15,7)	9.35e11	7.25e11	5.15e11
(31,11)	7.10e11	5.50e11	3.91e11
(63,7)	2.22e11	1.72e11	1.22e11
(127,29)	4.57e11	3.54e11	2.51e11
(127,99)	1.56e12	1.21e12	8.60e11
(255,71)	5.55e11	4.32e11	3.07e11
(255,223)	1.75e12	1.36e12	9.60e11

BER saturation where implementing RS FEC would no longer serve any benefit. As was stated in Chapter II, these higher forms of modulation increase the number of bits per symbol, which increases the throughput for a given type of modulation. A major objective of this thesis was to find a set of RS codes that had the lowest BER while maintaining the highest throughput. Since a desired BER or throughput were not given, these results are made available.

4.5.2.1 BER with Two-Ray Multipath Model with Higher M-ary Modulation. The 8PSK, 16QAM, 32QAM, and 64QAM FEC BER results are listed in Tables 4.18 - 4.20. Based on material discussed in Chapter II, higher M-ary forms of modulation result in a higher BER due to denser symbol constellations. These results show that multipath helps discriminate which antenna configuration is better than

Table 4.17: 64QAM Throughput (bps).

(n, k)	80 T, 160 R	62 T, 248 R	44 T, 352 R
(7,3)	1.03e12	7.98e11	5.66e11
(15,5)	7.98e11	6.18e11	4.40e11
(15,7)	1.12e12	8.70e11	6.18e11
(31,11)	8.52e11	6.60e11	4.69e11
(63,7)	2.66e11	2.06e11	1.46e11
(127,29)	5.48e11	4.25e11	3.01e11
(127,99)	1.87e12	1.45e12	1.03e12
(255,71)	6.66e11	5.18e11	3.68e11
(255,223)	2.10e12	1.63e12	1.15e12

the others. The 1 transmitter to 2 receiver ratio has the lowest diversity setup of the three remaining antenna configurations in terms of BER. The best BER performance is the RS(63,7) using 8PSK modulation and resulted in a BER of 0.4% which is not too reliable. It can also be seen from this antenna configuration that all performances for a fixed modulation type for all higher modulation types investigated had similar results. From this configuration, it is clear that a 1 W transmit power creates BER saturation for these higher types of modulation. Table 4.19 reveals that RS(63,7) and RS(255,71) using 8PSK modulation were able to correct all errors. Unlike the previous antenna configuration, this antenna's configuration has BER saturation that occurs when using 32QAM modulation. Finally, Table 4.20 shows that this antenna configuration had the best performance. Not only did it have the best performance, but it had BER saturation using 64QAM modulation. One anomaly that can be noted from this table is the performance of the RS(127,29) code. From the table, BER improved from 8PSK to 16QAM modulation while in theory it should get worse. One possible explanation for this anomaly is severe attenuation in some of the simulated channels when testing the 8PSK modulation.

4.5.2.2 BER with Five-Ray Multipath Model using Higher M-ary Modulation. The BER results for 8PSK, 16QAM, 32QAM, and 64QAM modulation are listed in Tables 4.23 - 4.23. Again, these results are similar to those mentioned in

Table 4.18: 80 Transmitters, 160 Receivers Two-Ray Model Higher M-ary BER.

(n, k)	8PSK	16QAM	32QAM	64QAM
(7,3)	2.51e-2	7.93e-2	8.24e-2	8.35e-2
(15,7)	3.05e-2	1.01e-1	1.04e-1	1.05e-1
(15,5)	1.56e-2	8.19e-2	8.51e-2	8.59e-2
(31,11)	2.67e-2	1.08e-1	1.11e-1	1.12e-1
(63,7)	4.71e-3	1.05e-1	1.08e-1	1.09e-1
(127,29)	6.66e-2	1.13e-1	1.17e-1	1.18e-1
(127,99)	9.25e-2	1.13e-1	1.17e-1	1.18e-1
(255,223)	6.58e-2	1.13e-1	1.17e-1	1.17e-1
(255,71)	6.52e-2	1.13e-1	1.17e-1	1.17e-1

Table 4.19: 62 Transmitters, 248 Receivers Two-Ray Model Higher M-ary BER.

(n, k)	8PSK	16QAM	32QAM	64QAM
(7,3)	1.14e-3	1.20e-2	1.32e-2	1.42e-2
(15,7)	4.14e-4	1.14e-2	1.29e-2	1.40e-2
(15,5)	6.61e-5	4.32e-3	5.37e-3	6.65e-3
(31,11)	6.52e-6	4.79e-3	6.47e-3	7.61e-3
(63,7)	<1.00e-8	3.84e-5	1.36e-3	2.88e-3
(127,29)	3.07e-2	6.18e-4	3.11e-3	3.90e-3
(127,99)	4.68e-2	4.74e-2	4.99e-2	5.07e-2
(255,223)	2.05e-2	4.73e-2	4.93e-2	5.01e-2
(255,71)	<1.00e-8	6.69e-3	8.72e-3	9.52e-3

Section 4.5.2.1 and are presented for completeness. The BER vs. throughput plots for the five-ray model are shown in Appendix C.

4.5.3 Higher M-ary Modulation Throughput vs. BER Graphs for Two-Ray Multipath Model. This section displays the BER vs. throughput figures using the two-ray model multipath for higher forms of modulation that were tested. In each figure, only the best performers were marked. Figure 4.13 shows that none of these codes are attractive to use because all have unreliable BERs ($> 10^{-3}$). The two best were the RS(63,7) and RS(15,5) with 8PSK modulation but again neither of those two codes would be ideal candidates to use in a communications system due to their low coding rate. Figure 4.14 shows improvement in the BER and RS(31,11), RS(63,7) and RS(255,71) all have BERs that were $< 10^{-5}$. None of these three RS

Table 4.20: 44 Transmitters, 352 Receivers Two-Ray Model Higher M-ary BER.

(n, k)	8PSK	16QAM	32QAM	64QAM
(7,3)	2.28e-6	1.92e-3	2.11e-3	2.67e-3
(15,7)	<1.00e-8	1.60e-5	1.45e-4	1.12e-3
(15,5)	<1.00e-8	9.09e-7	4.09e-4	6.20e-3
(31,11)	<1.00e-8	<1.00e-8	2.71e-5	1.21e-3
(63,7)	<1.00e-8	<1.00e-8	1.95e-4	7.82e-4
(127,29)	3.05e-2	<1.00e-8	6.04e-4	2.17e-3
(127,99)	3.06e-2	5.93e-4	2.00e-3	2.80e-3
(255,223)	<1.00e-8	8.72e-3	9.56e-3	1.04e-2
(255,71)	<1.00e-8	<1.00e-8	1.60e-6	1.69e-3

Table 4.21: 80 Transmitters, 160 Receivers Five-Ray Model Higher M-ary BER.

(n, k)	8PSK	16QAM	32QAM	64QAM
(7,3)	2.52e-2	7.93e-2	8.24e-2	8.35e-2
(15,7)	3.05e-3	1.01e-1	1.04e-1	1.05e-1
(15,5)	1.56e-2	8.19e-2	8.51e-2	8.59e-2
(31,11)	2.67e-2	1.08e-1	1.11e-1	1.12e-1
(63,7)	4.71e-3	1.05e-1	1.08e-1	1.09e-1
(127,29)	6.67e-2	1.13e-1	1.17e-1	1.18e-1
(127,99)	9.25e-2	1.13e-1	1.17e-1	1.18e-1
(255,223)	6.57e-2	1.13e-1	1.17e-1	1.17e-1
(255,71)	6.51e-2	1.13e-1	1.17e-1	1.17e-1

codes have high coding rates which causes their throughputs to be low. With only three of the RS codes having a BER $< 10^{-5}$, this is still not the ideal set-up. Finally examining the highest ratio of transmitters to receivers in Figure 4.15 reveals 12 codes that have BERs $< 10^{-5}$. This configuration would be ideal because it allows the most flexibility in terms of selecting which RS code to use. Similar to the BPSK and 4QAM modulation BERs, the RS(255,223) code was the best in terms of BER performance and throughput. The overall conclusion from these plots is that using the 1 transmitter to 2 receiver ratio, all codes that had a throughput greater than 1 Tbps had BER of 10%. Looking at the 1 transmitter to 4 receiver ratio, all RS codes that had a throughput greater than 1 Tbps had BER improvement; however the BER is still at an unacceptable rate. Using the 1 transmitter to 8 receiver ratio shows that

Table 4.22: 62 Transmitters, 248 Receivers Five-Ray Model Higher M-ary BER.

(n, k)	**8PSK**	**16QAM**	**32QAM**	**64QAM**
(7,3)	1.14e-3	1.20e-2	1.32e-2	1.42e-2
(15,7)	4.14e-4	1.14e-2	1.29e-2	1.40e-2
(15,5)	6.61e-5	4.32e-3	5.37e-3	6.65e-3
(31,11)	6.51e-6	4.79e-3	6.47e-3	7.61e-3
(63,7)	<1.00e-8	3.84e-5	1.36e-3	2.88e-3
(127,29)	3.06e-2	6.18e-4	3.12e-3	3.89e-3
(127,99)	4.69e-2	4.74e-2	4.99e-2	5.07e-2
(255,223)	2.05e-2	4.73e-2	4.94e-2	5.02e-2
(255,71)	<1.00e-8	6.69e-3	8.72e-3	9.52e-3

Table 4.23: 44 Transmitters, 352 Receivers Five-Ray Model Higher M-ary BER.

(n, k)	**8PSK**	**16QAM**	**32QAM**	**64QAM**
(7,3)	2.28e-6	1.92e-3	2.11e-3	2.67e-3
(15,7)	<1.00e-8	1.60e-5	1.45e-4	1.12e-3
(15,5)	<1.00e-8	9.09e-7	4.09e-5	6.20e-4
(31,11)	<1.00e-8	<1.00e-8	2.71e-5	1.21e-3
(63,7)	<1.00e-8	<1.00e-8	1.95e-4	7.82e-4
(127,29)	3.05e-2	<1.00e-8	6.04e-4	2.17e-3
(127,99)	3.05e-2	5.93e-4	2.00e-3	2.80e-3
(255,223)	<1.00e-8	8.72e-3	9.56e-3	1.04e-2
(255,71)	<1.00e-8	<1.00e-8	1.60e-6	1.69e-3

two RS codes were above the 1 Tbps throughput, but a BER of .05% was present. All three of the antenna configurations had BERs that were at unacceptable levels.

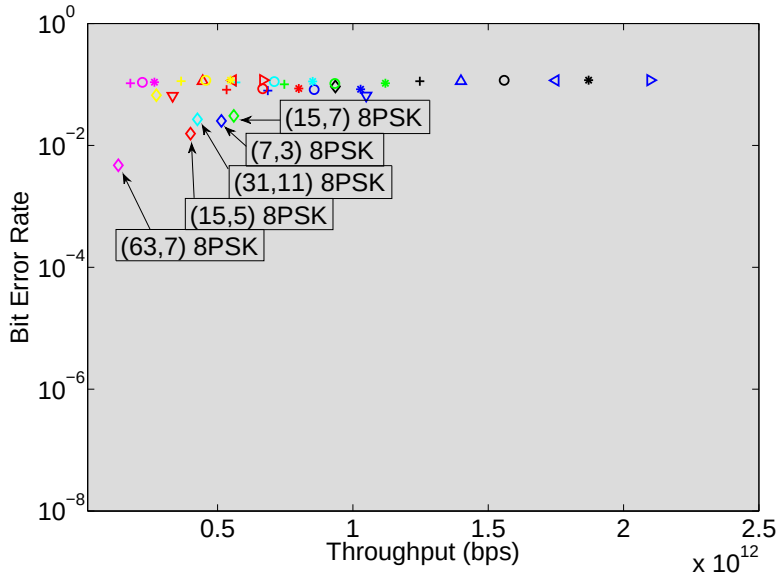

Figure 4.13: Throughput vs. BER for high M-ary Modulation, 80 transmitters and 160 receivers for two-ray model.

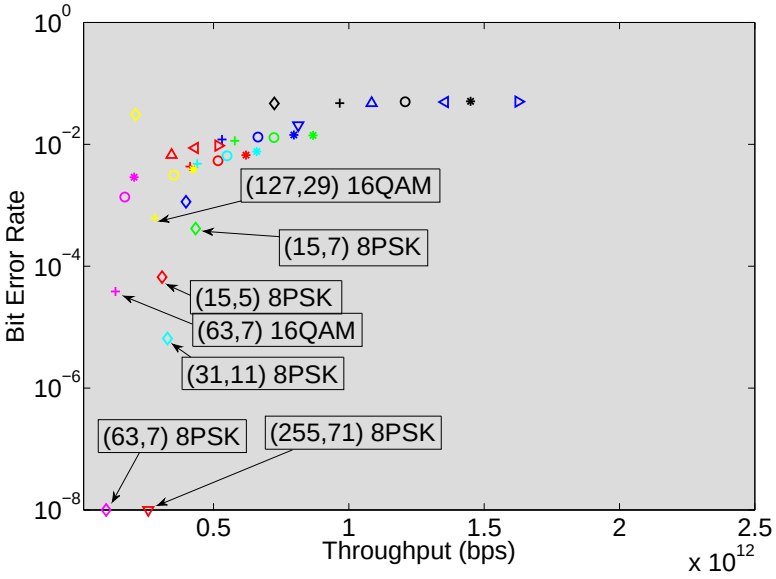

Figure 4.14: Throughput vs. BER for high M-ary Modulation, 62 transmitters and 248 receivers for two-ray model.

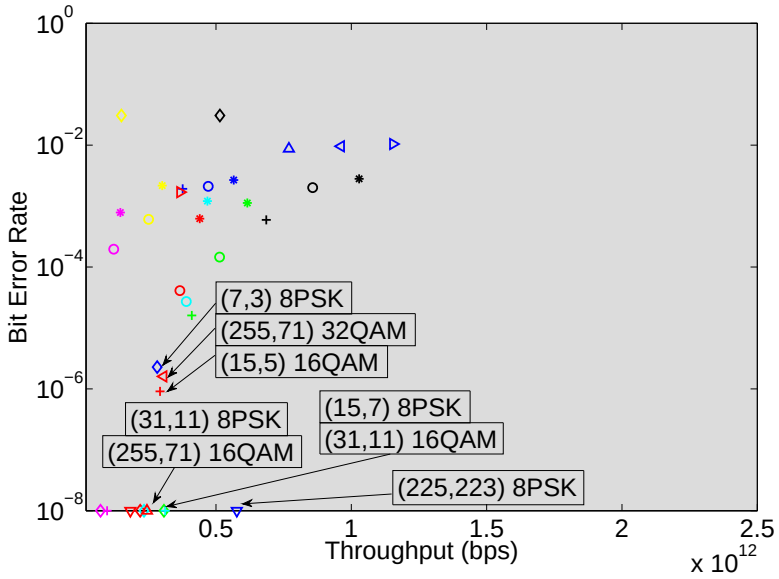

Figure 4.15: Throughput vs. BER for high M-ary Modulation, 44 transmitters and 352 receivers for two-ray model.

4.6 Best Results Plotted

Section 4.5.2 showed that the largest modulation size before BER saturation was dependent on the size of the antenna ratios. The higher the antenna ratio, the higher the type of modulation that could be used before BER saturation occurred. This section of the research takes three antenna configuration ratios and plots all BERs that were $< 10^{-5}$ for all types of modulation using the two-ray multipath model. A BER of 10^{-5} was an acceptable BER by the author and was chosen for BER criteria. This section shows the best system performers from this research. Figures 4.16 - 4.18 display the BER vs throughput for all codes in that antenna configuration which met the criteria. It can be noted that none of the RS codes in this section were able to achieve the 1 Tbps throughput. Table 4.24 lists the top four RS codes in terms of lowest BER and highest throughput for each figure. From Table 4.24, RS(255,223) appeared in half of the top listed positions. From the RS(255,223) codes listed, it is clear that the overall best code and modulation was the RS(255,223) 4QAM which appeared as the overall best performer for both the 1 to 2 ratio as well as the 1 to 4 ratio. The RS(255,233) code was the second best performer in the 1 to 8 ratio, only to finish after the RS(255,223) 8PSK because of its higher throughput capability. The RS(255,223) BPSK appeared as a top RS code candidate in the 1 to 2 and 1 to 4 ratio charts, but failed to make the top four in the 1 to 8 ratio because of it's low throughput value. The second best code was the RS(127,99) which appeared in each of the three antenna ratios. RS(31,11) appeared twice in the listings while RS(15,7) 4QAM appeared once. Although it is not clear what the desired BER is required, the more information provided allows more flexibility. In that case, it is best to select an antenna configuration that had the most codes that were able to exceed the chosen BER of 10^{-5}. Table 4.25 lists the number of RS codes with all studied forms of researched modulations that were able to reach a BER of 10^{-5} for each of the three antenna configurations. In terms of flexibility, it is clear that the 44 transmitter to 352 receiver antenna configuration had the highest number of RS codes that exceeded the BER of 10^{-5}. Hence, this thesis recommends the use of the 44 transmitter to

352 receiver antenna configuration. With this configuration, the RS codes that are recommended in order are listed in the right column of Table 4.24.

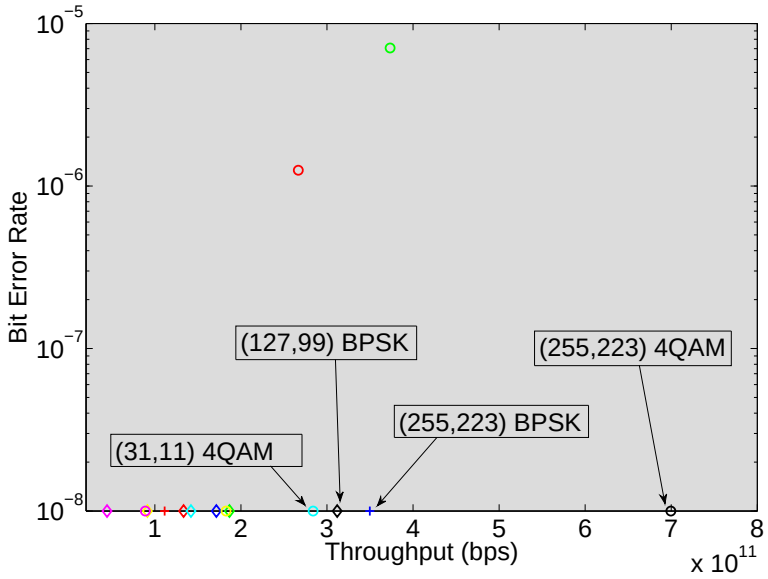

Figure 4.16: Throughput vs. BER $< 10^{-5}$ for all modulations, 80 transmitters and 160 receivers for two-ray model.

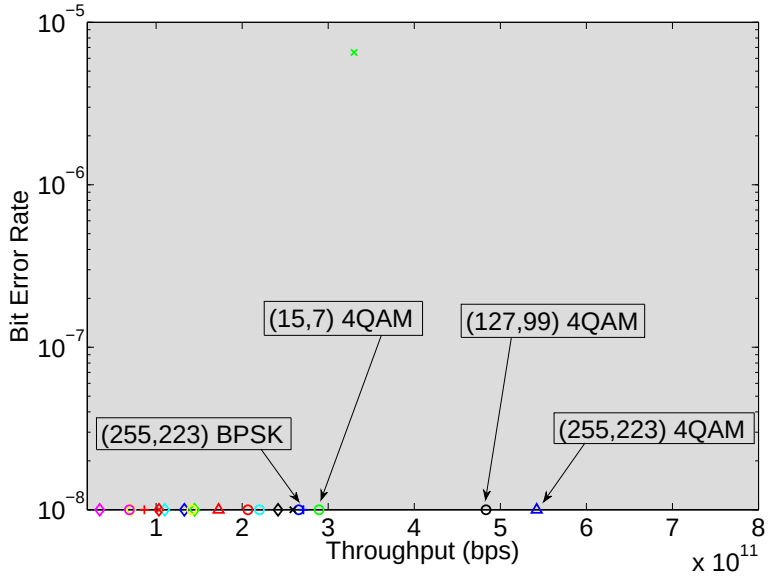

Figure 4.17: Throughput vs. BER $< 10^{-5}$ for all modulations, 62 transmitters and 248 receivers for two-ray model.

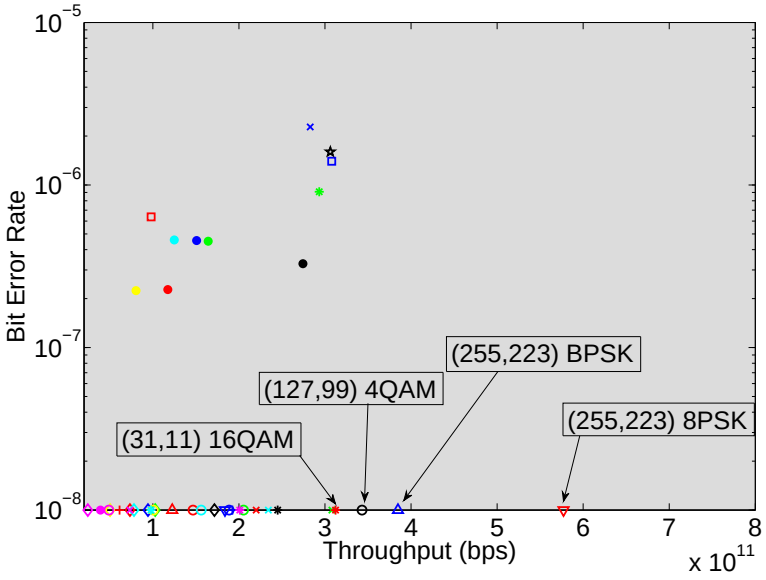

Figure 4.18: Throughput vs. BER $< 10^{-5}$ for all modulations, 44 transmitters and 352 receivers for two-ray model.

Table 4.24: Top RS Code Performers per Antenna Configuration.

Ranking	**80 T, 160 R**	**62 T, 248 R**	**44 T, 352 R**
First	RS(255,223) 4QAM	RS(255,223) 4QAM	RS(255,223) 8PSK
Second	RS(255,223) BPSK	RS(127,99) 4QAM	RS(255,223) 4QAM
Third	RS(127,99) BPSK	RS(15,7) 4QAM	RS(127,99) 4QAM
Fourth	RS(31,11) 4QAM	RS(255,223) BPSK	RS(31,11) 16QAM

Table 4.25: Number of RS FEC Codes with Different Modulations Capable of BER $< 10^{-5}$.

T	**R**	**Number of Codes with BER** $< 10^{-5}$
80	160	16
62	248	23
44	352	45

4.7 Conclusion

Chapter IV presented the results that were obtained in this research. These results included:

- transmit and receive antenna configurations to achieve 1 Tbps,
- beam forming,
- water filling,
- different types of modulation,
- uncoded signaling scheme,
- RS FEC,
- throughput, and
- multipath effects.

For performance metrics, this research was interested in a RS coding scheme that had a high throughput and a low BER. None of the BPSK, 4QAM, or 4QAM OFDM RS codes were able to achieve a 1 Tbps throughput. One 8PSK, three 16QAM, four 32QAM, and eight 64QAM RS codes were able to achieve the 1 Tbps threshold;

however, none of the codes that were able to achieve 1 Tbps had a BER lower than 1%. It was determined that a higher ratio of receivers to transmitters was desired due to their improvement in BER performance. The effects of multipath were researched by applying the two-ray and five-ray models. When examining BER performance, the two-ray and five-ray models had similar BER performances. The 44 transmitter and 352 receiver configuration was recommended, because it allowed the highest number of RS codes to exceed the BER performance of 10^{-5}. Although the 80 transmitter to 160 receiver configuration had a higher throughput, it was determined that future flexibility was needed.

V. Conclusions and Recommendations

5.1 Overview

This chapter summarizes the results found in this thesis pertaining to trade-offs of a 1 Tbps capacity communication system between an airship and an array of ground receivers using a bandwidth of 5 GHz.

5.2 Summary and Recommendations

5.2.1 Antenna Configurations. This research began by looking at different numbers of transmit and receive antennas needed to achieve 1 Tbps that operated in the Ku-Band. The algorithm investigated arrays from 2 to 150 antennas and ratios of 1:1, 1:2, 1:4, and 1:8 for both transmitters-to-receivers and receivers-to-transmitters. The research first investigated a constant amplitude, phase varying channel to obtain an estimate of the number of transmitters and receivers. *With the criteria that fewer antennas on the airship would be ideal due to resource restrictions, an antenna configuration of more receivers than transmitters that exceeded the 1 Tbps threshold had better capacity improvement as the ratio increased.* Next, this research investigated the same problem using a Rician distributed channel which simulated a LOS between the airship transmitters and ground receivers. The research observed similar capacities for both the phase varying channel as well as the Rician faded channel. While the ratio of transmitters to receivers was higher, improvement in capacity was observed but the improvement was minimal. *There was a higher improvement in the capacity when there was a higher ratio of receivers to transmitters.* Not only was there better improvement with a higher ratio of receivers to transmitters, but fewer transmitting antennas would be needed on the airship. Since the resources on the airship are limited compared to the ground, it is more advantageous to have a higher ratio of antennas on the ground. A higher ratio of ground receivers to transmitters is recommended for the airship.

5.2.2 Water Filling. A major goal of this research was to find the fewest number of antennas needed to achieve the objective capacity of 1 Tbps. One attempted way to increase the capacity was by implementing water filling power allocation. *Using (2.21), water filling was shown to significantly decrease overall system capacity for this particular system.* This was a result of the airship being power limited. Water filling power allocation was discovered to be dependent on the amount of power per channel. As the size of the transmitter array increased, the amount of power per channel decreased, which decreased the overall capacity. Unless the power allocated per channel remains constant, which is not in the case given the requirements of this system, water filling is not advantageous. With the water filling results that were obtained in this research, water filling is not recommended.

5.2.3 Beam Forming. A second way to decrease the number of antennas needed to reach the desired capacity was implementing beam forming. *This research showed that the capacity using beam forming was directly proportional to the square of the largest singular value of the channel and the SNR per channel.* As the MIMO array increased in size, the largest singular value increased; however due to power constraints, the SNR per channel decreased causing an overall neutralization of the two components. Similar to water filling, beam forming would be advantageous if the power per channel remained fixed regardless of the size of the transmitter array. Since the power requirements for this research showed that total power is fixed, beam forming is not advisable in this system.

5.2.4 Throughput. Throughput was investigated in this research for nine different RS coding schemes for BPSK, 4QAM, and 4QAM OFDM. *The results showed that as a group, 4QAM had the highest throughput, 4QAM OFDM had the second highest, and BPSK had the lowest throughput. None of the BPSK, 4QAM, or 4QAM OFDM RS codes were able to achieve a 1 Tbps throughput.* Throughput values were found to be a function of the type of modulation selected, which resulted in different bits/symbol, as well as the coding rate of the RS code; the higher the coding rate,

the higher the throughput was found to be. Throughput is one of the metrics that was used in determining which signaling scheme would be used.

5.2.5 Uncoded vs Coded Performance with no Multipath. Appendices A and B show the uncoded and coded BER for nine RS codes. From the figures, three conclusions were made: *The BER remained constant for any number of antennas within a fixed ratio.* The constant BER meant that there was no BER advantage in selecting a different number of antennas other than the number required to surpass the 1 Tbps capacity because the BER performance was the same. The BER performance also encourages the fewest number of antennas. The second observation was that *all coded performance was better than uncoded performance which indicated that the SNR of 4.77 dB was greater than the cross-over point of the coded versus uncoded performance.* The third observation was that *as the ratio of receivers to transmitters increased, the BER performance improved.* If BER performance is important, a higher receiver to transmitter ratio is advantageous. The results recommend that at least a 2 to 1 receiver to transmitter ratio be used for the design to take advantage of the BER improvement caused by diversity.

5.2.6 Two-Ray BER Results. Multipath has advantages and disadvantages associated with it. One advantage is that the received signal power is slightly higher due to the reflected multipath. The two-ray model includes the LOS Rician distributed link and a Rayleigh distributed multipath. The multipath time arrival, K, is a function of the sampling frequency and was calculated to have a delay factor of 5 sampling periods. *The research examined the minimum number of antennas needed to exceed the 1 Tbps capacity for the 1:2, 1:4, and 1:8 transmitter to receiver ratio which ended up being 80 to 160, 62 to 248, and 44 to 352 transmitter to receiver antennas respectively.* BPSK signaling had the best BER performance while 4QAM OFDM had the worse BER performance. The BER improved as the ratio of receivers to transmitters increased. One disadvantage of 4QAM and BPSK modulation is that most codes had a BER below 10^{-8} and being able to discriminate between the codes

was difficult to accomplish with a transmit power of 1 W. It was then concluded that other forms of modulation would be needed to help discriminate between the different RS codes.

5.2.7 Five-Ray BER Results. The five-ray model, which is an extension of the two-ray model except there were 4 multipath links instead of 1, was the most realistic simulated model that this research investigated. *The BER results were similar to the two-ray multipath model, and a reason to examine higher ray multipath models was deemed unnecessary* because of the similarities between the two-ray and five-ray models.

5.2.8 Throughput vs BER Results. All BER performances were plotted against throughput to assist in making a decision on which coding scheme was best. Since the two-ray and five-ray multipath models had very similar BER results, only the two-ray throughput vs BER plots were provided in Chapter IV. The five-ray model plots are provided in Appendix C. By examining the two-ray model results, it was shown that *the best was the RS(255,223) 4QAM followed by the RS(127,99) 4QAM. The 62 transmitter to 248 receiver RS(255,223) and RS(127,99) 4QAM had the same BER as they did for the 44 transmitter to 352 receiver ratio; however, the throughputs were nearly 40% higher for the 62 transmitter to 248 receiver array.* Not only was the throughput higher, but the total number of antennas required was lower.

5.2.9 Higher Modulation BER Results. A result that was noticed was the lack of distinction between the RS codes using BPSK and 4QAM modulation when using a fixed transmit power of 1 W. *When examining throughput, one 8PSK, three 16QAM, four 32QAM, and eight 64QAM RS codes were able to achieve the 1 Tbps throughput.* The highest obtained throughput was 2.1 Tbps, which was obtained using the RS(255,223) 64QAM using 80 R and 160 R. *A major drawback was that none of the 1 Tbps or greater throughput RS codes were able to obtain a BER less than* 1%. The research investigated higher forms of modulation to investigate which modula-

tion type had BER saturation. *BER saturation was where all the codes had similar performances and no distinction between them could be made.* From the results, it was shown that the 1 to 2 ratio had a BER saturation beginning with 16QAM modulation. The 1 to 4 ratio had a BER saturation with 32QAM modulation and the 1 to 8 ratio reached BER saturation with 64QAM modulation. The type of antenna ratio selected allowed the system designer to decide what types of modulations were acceptable. From these three configurations, the results showed that as the ratio of antennas increased, so did the size of the allowable modulation type. In the 1 to 2 antenna ratio, none of the RS codes were able to obtain a BER of zero while the 1 to 4 antenna configuration had two BERs of zero which included RS(63,7) and RS (255,71) with 8PSK modulation. The 1 to 8 ratio had ten RS codes, six were using 8PSK modulation and four were using 16QAM modulation, that had a BER of zero. If higher modulations are desired, then it is recommended that the 1 to 8 ratio be used because it had the best BER performance.

5.2.10 FEC Coding Recommendation. The last portion of this research took all BERs that were $< 10^{-5}$ for all modulations for the three antenna ratios and plotted them against throughput for comparison. *Since none of the RS codes were able to achieve 1 Tbps throughput and a BER* $< 10^{-5}$*, it was decided to recommend codes that were the closest to the 1 Tbps and low BER.* The best four codes for each antenna configuration were displayed in Table 4.24. It was shown that *the RS(255,223) appeared in six of the twelve spots with the RS(255,223) 4QAM appeared as the overall best in two of the three antenna ratios.* The RS(127,99) appeared in each of the three antenna ratio lists while RS(31,11) appeared twice and RS(15,7) 4QAM made the list once. This thesis showed that the 1 to 2 antenna ratio had 16 RS codes whose BER $< 10^{-5}$ while the 1 to 4 antenna ratio had 23 that had a BER $< 10^{-5}$. The antenna configuration with the most RS codes that had a BER of $< 10^{-5}$ was the 1 to 8 ratio, which had 45 RS codes. In terms of flexibility, *the highest antenna ratio or the 1 to 8 case was the best configuration because it had the*

highest number of codes that could be selected for optimal performance. The overall best performing RS code was the RS(255,223) with 8PSK modulation followed by the RS(255,223) with 4QAM modulation using the 1 to 8 ratio.

5.3 Future Research

This research was the first AFIT thesis to investigate a 1 Tbps MIMO communication system between an airship and ground station. The algorithms developed from this thesis lay the foundation down for future research. Since this was the first step in more research, there are many other areas that can be studied including

- moving airship,
- channel estimation,
- turbo coding,
- implementation of rake receivers,
- hardware implementation of a smaller MIMO array,
- link budgets, and
- adaptive antenna array.

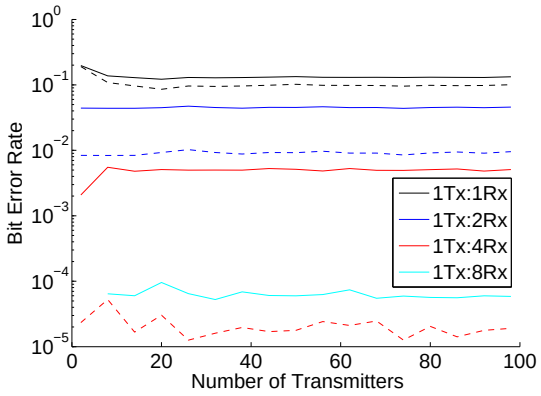

Figure A.1: RS(7,3) BPSK FEC, Rician Channel.

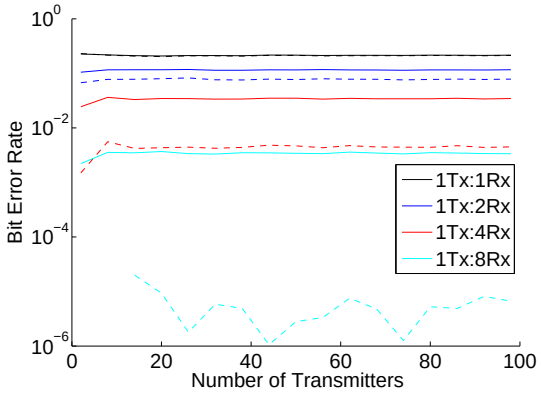

Figure A.2: RS(7,3) 4QAM FEC, Rician Channel.

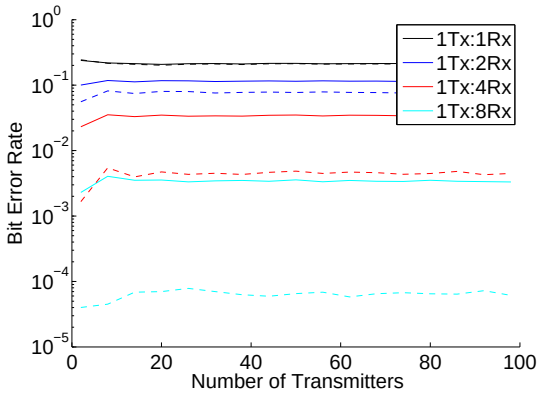

Figure A.3: RS(7,3) 4QAM OFDM FEC, Rician Channel.

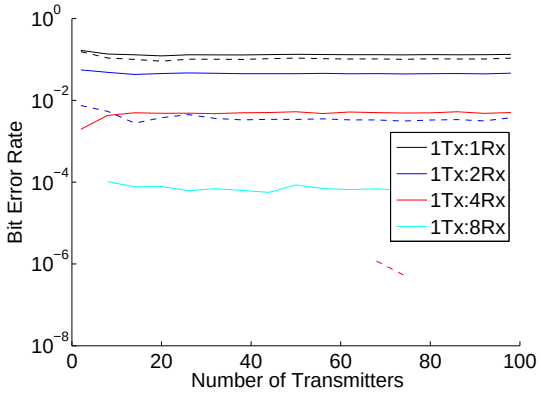

Figure A.4: RS(15,5) BPSK FEC, Rician Channel.

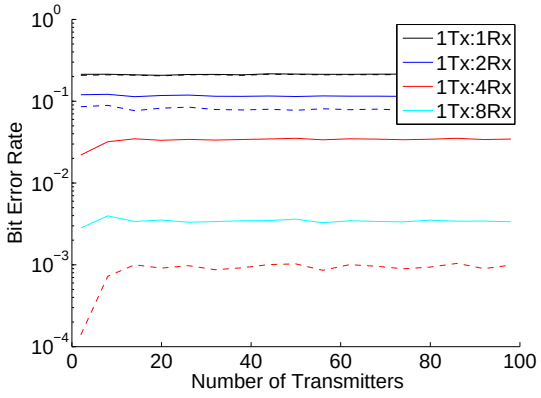

Figure A.5: RS(15,5) 4QAM FEC, Rician Channel.

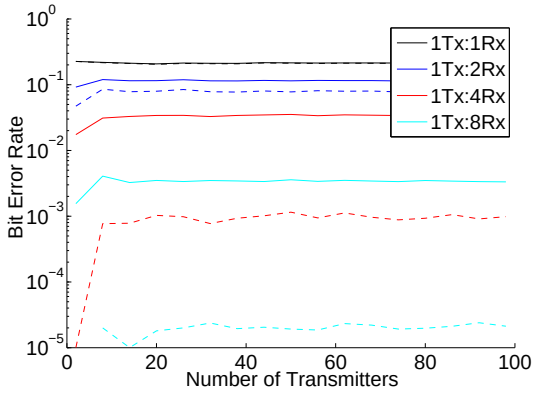

Figure A.6: RS(15,5) 4QAM OFDM FEC, Rician Channel.

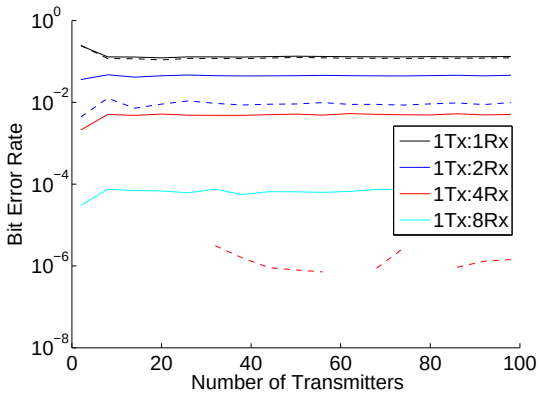

Figure A.7: RS(15,7) BPSK FEC, Rician Channel.

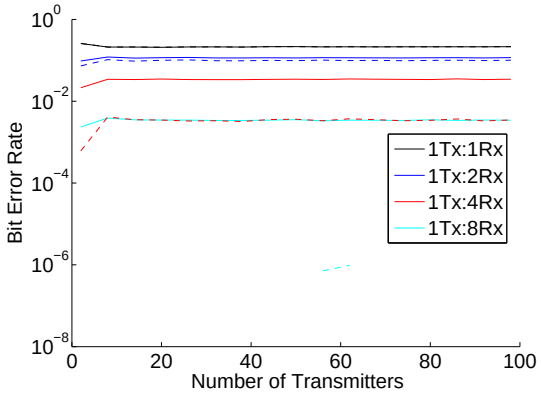

Figure A.8: RS(15,7) 4QAM FEC, Rician Channel.

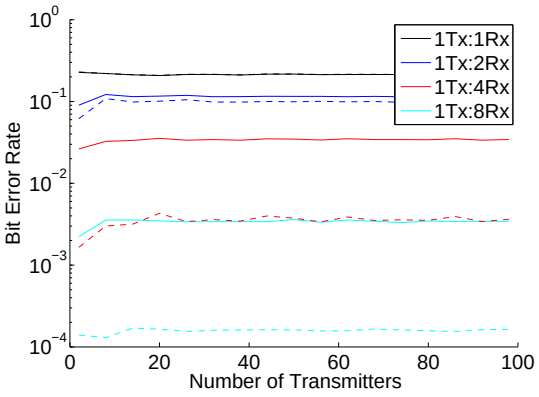

Figure A.9: RS(15,7) 4QAM OFDM FEC, Rician Channel.

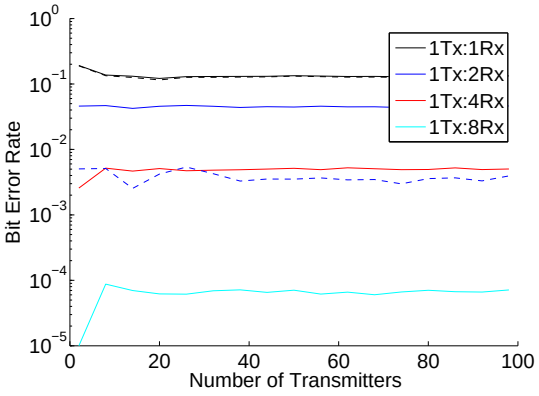

Figure A.10: RS(31,11) BPSK FEC, Rician Channel.

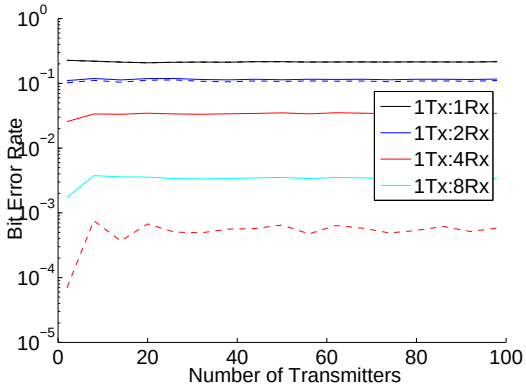

Figure A.11: RS(31,11) 4QAM FEC, Rician Channel.

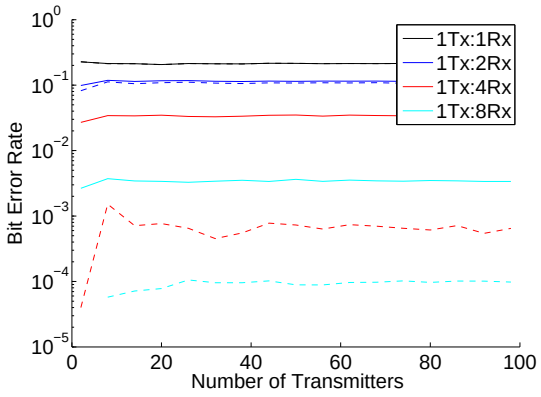

Figure A.12: RS(31,11) 4QAM OFDM FEC, Rician Channel.

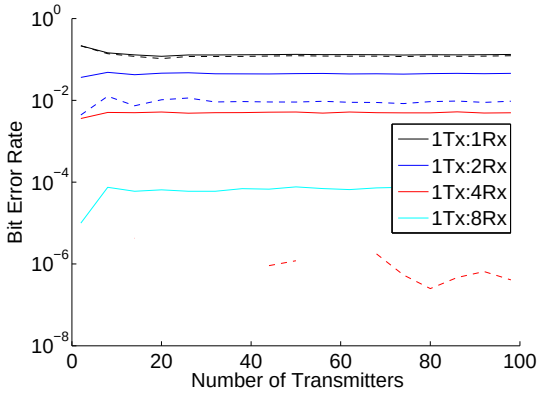

Figure A.13: RS(63,7) BPSK FEC, Rician Channel.

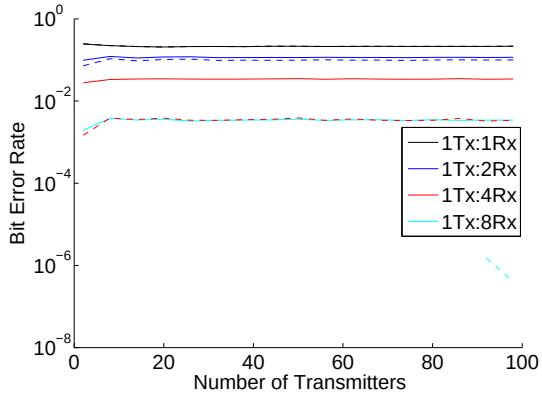

Figure A.14: RS(63,7) 4QAM FEC, Rician Channel.

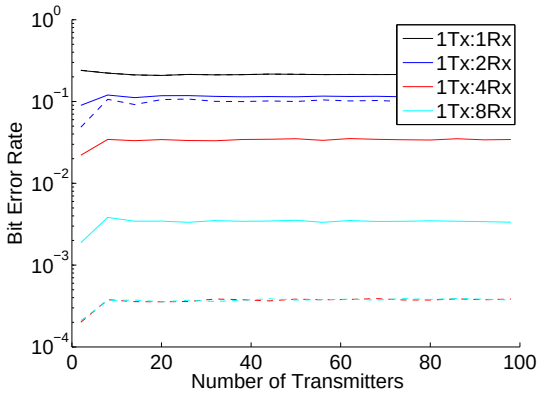

Figure A.15: RS(63,7) 4QAM OFDM FEC, Rician Channel.

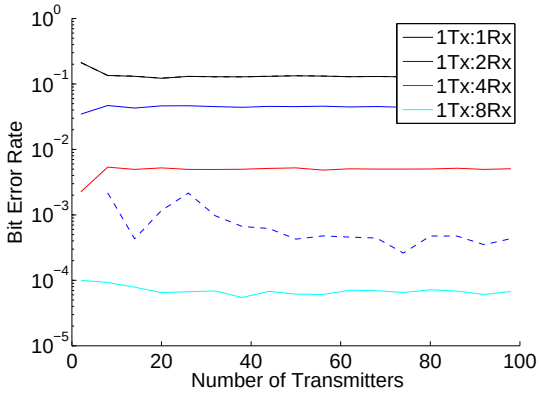

Figure A.16: RS(127,29) BPSK FEC, Rician Channel.

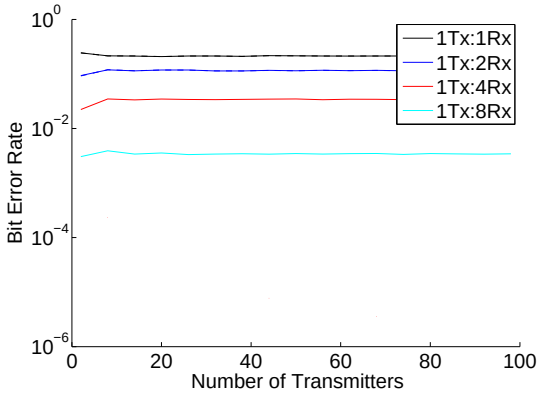

Figure A.17: RS(127,29) 4QAM FEC, Rician Channel.

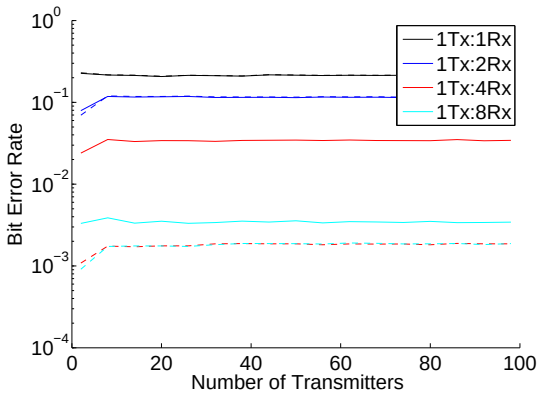

Figure A.18: RS(127,29) 4QAM OFDM FEC, Rician Channel.

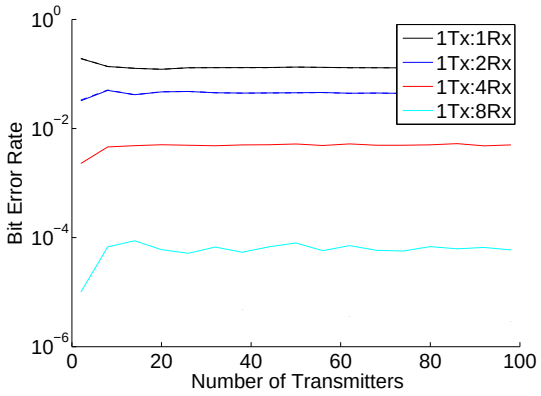

Figure B.1: RS(127,99) BPSK FEC, Rician Channel.

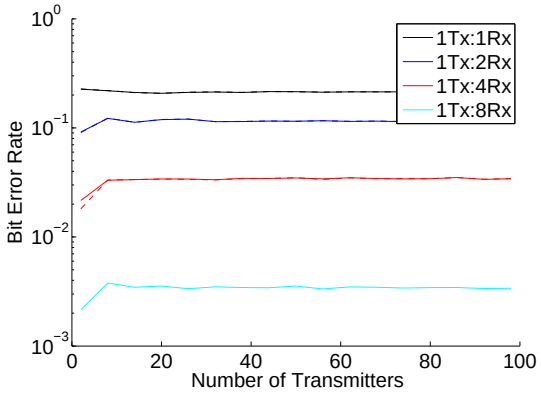

Figure B.2: RS(127,99) 4QAM FEC, Rician Channel.

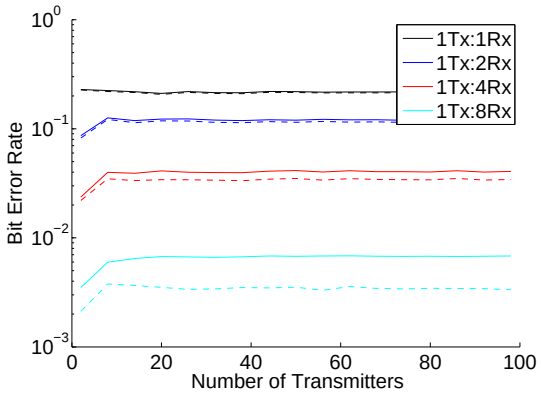

Figure B.3: RS(127,99) 4QAM OFDM FEC, Rician Channel.

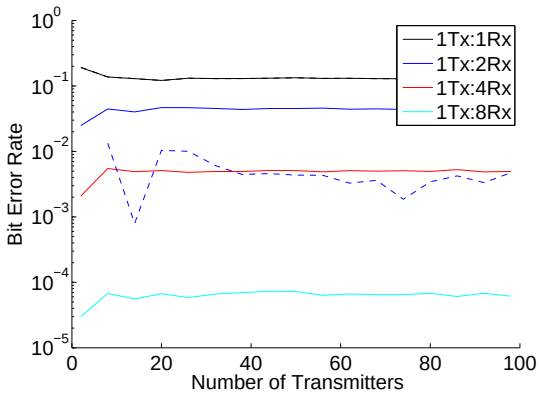

Figure B.4: RS(255,71) BPSK FEC, Rician Channel.

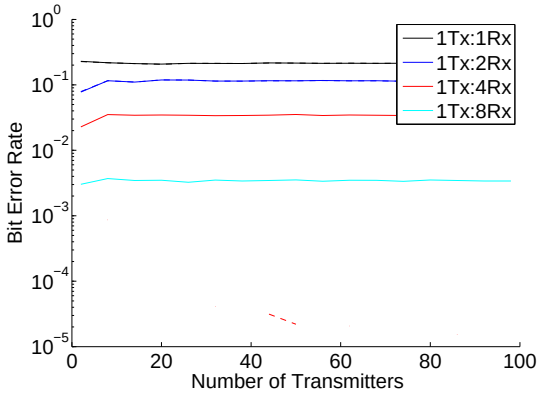

Figure B.5: RS(255,71) 4QAM FEC, Rician Channel.

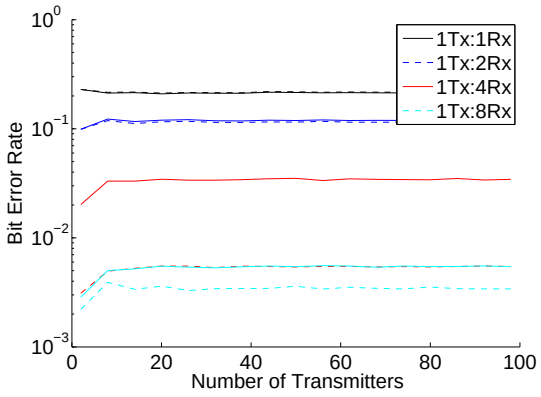

Figure B.6: RS(255,71) 4QAM OFDM FEC, Rician Channel.

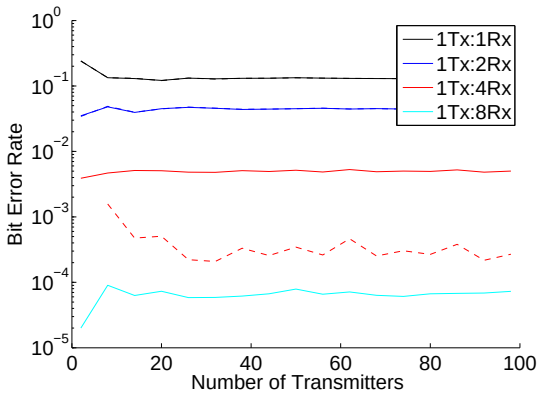

Figure B.7: RS(255,223) BPSK FEC, Rician Channel.

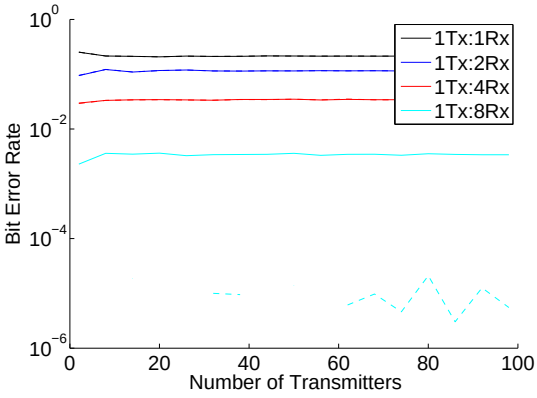

Figure B.8: RS(255,223) 4QAM FEC, Rician Channel.

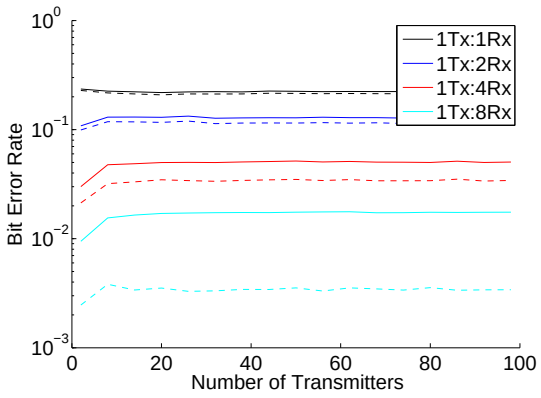

Figure B.9: RS(255,223) 4QAM OFDM FEC, Rician Channel.

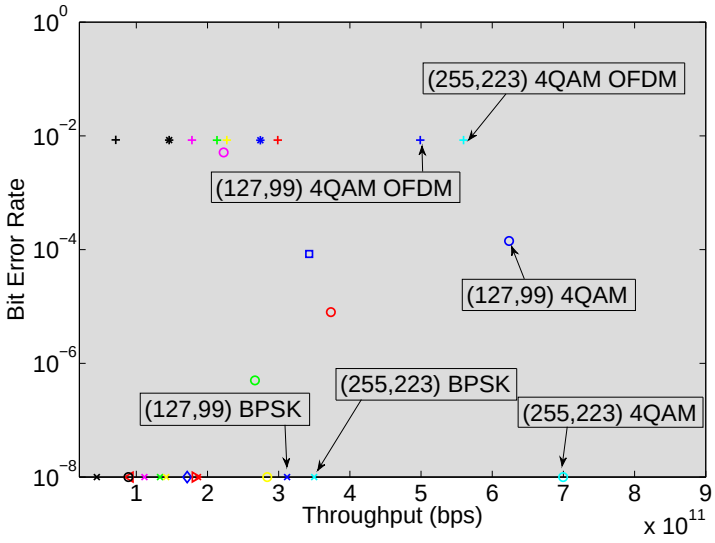

Figure C.1: 80 transmitters and 160 receivers five-ray model BER vs. throughput.

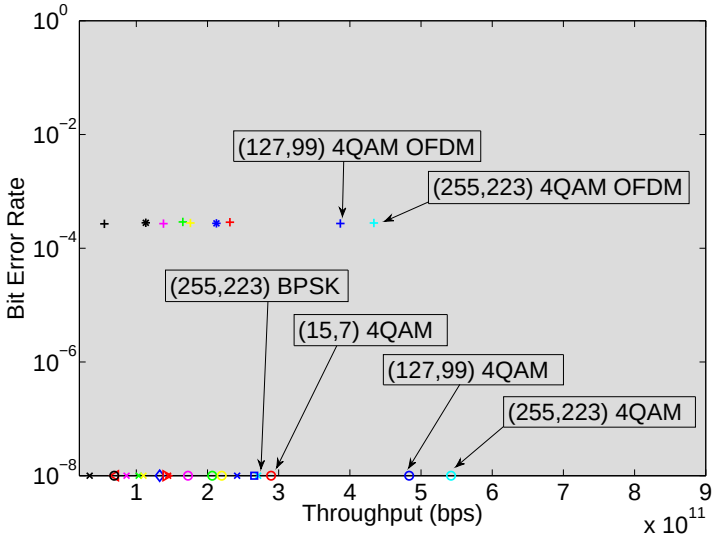

Figure C.2: 62 transmitters and 248 receivers five-ray model BER vs. throughput.

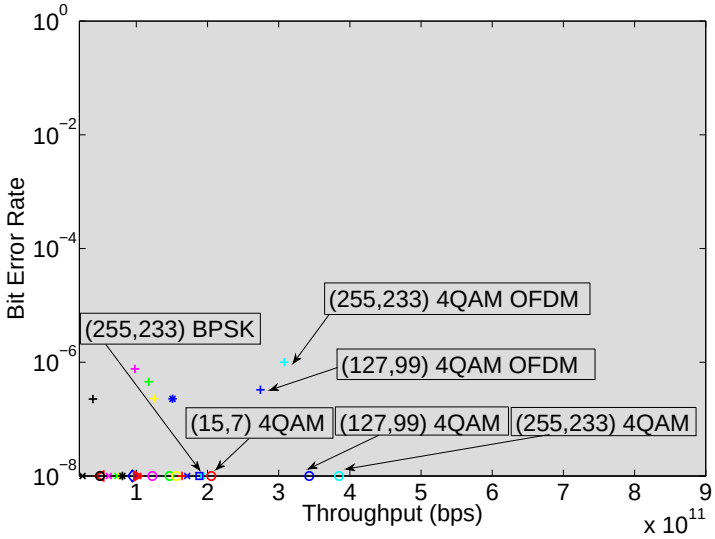

Figure C.3: 44 transmitters and 352 receivers five-ray model BER vs. throughput.

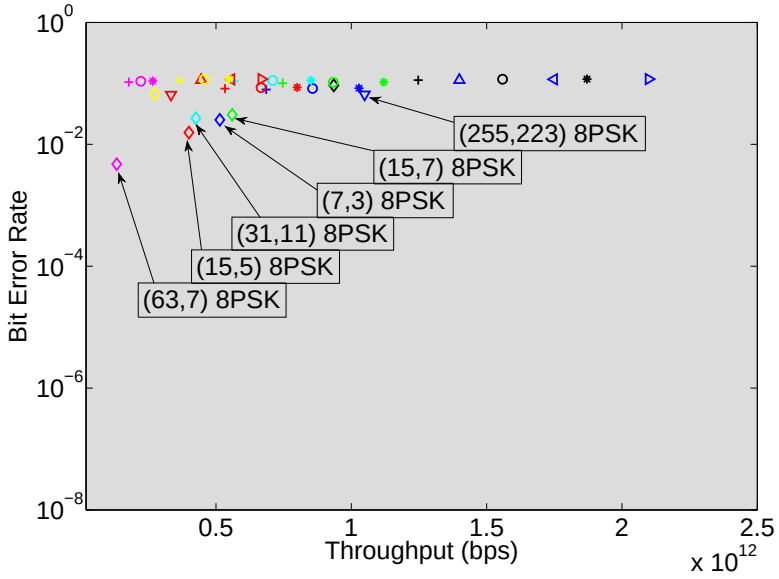

Figure C.4: 80 transmitters and 160 receivers five-ray model BER vs. throughput using higher modulation.

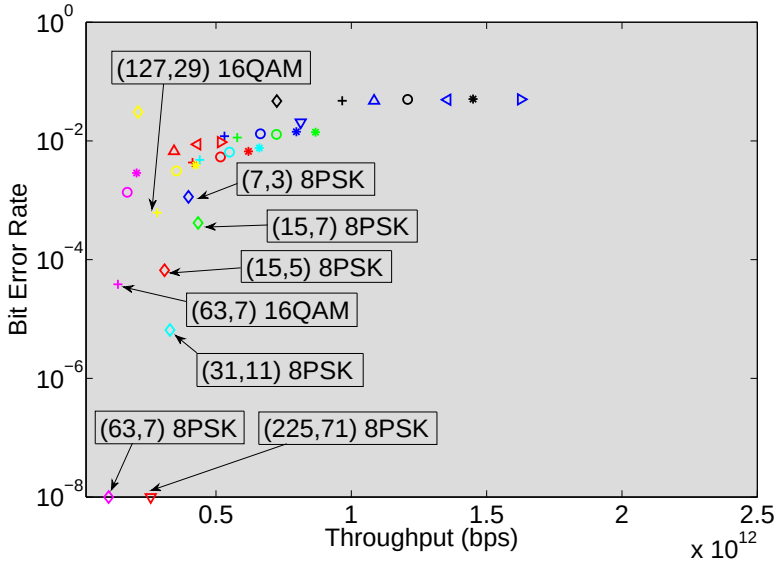

Figure C.5: 62 transmitters and 248 receivers five-ray model BER vs. throughput using higher modulation.

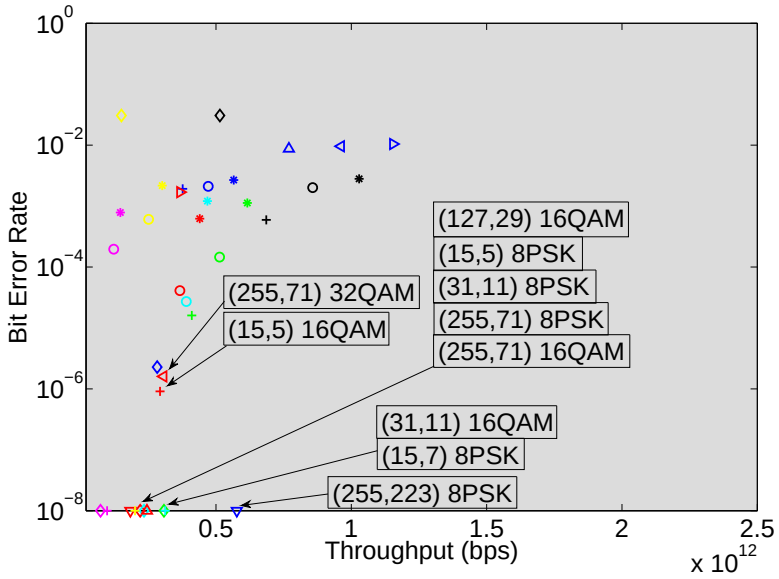

Figure C.6: 44 transmitters and 352 receivers five-ray model BER vs. throughput using higher modulation.

Bibliography

1. M. E. Dempsey, *Eyes of the Army - US Army Roadmap for Unmanned Aircraft Systems 2010-2035*, April 2010.
2. B. Sklar, *Digital Communications, 2nd Edition*, R. Kernan, Ed. Prentince Hall PTR, 2010.
3. T. S. Rappaport, *Wireless Communications, Principles and Practice*, C. Trentacoste, Ed. Prentince Hall PTR, 1996.
4. H. Yao, "Efficient signal, code, and receiver designs for mimo communication systems," Ph.D. dissertation, Massachusetts Institute of Technology, 2003.
5. J. G. Proakis, *Digital Communications, 3rd Edition*, G. T. Hoffman, Ed. McGraw Hill, 1995.
6. G. Durgin, *Space-Time Wireless Channels*, N. Radhuber, Ed. Prentice Hall PTR, 2003.
7. N. Costa and S. Haykin, *Multiple-Input Multiple-Output Channel Models Theory and Practice*, Wiley and Sons, Eds. John Wiley and Sons, Inc, 2010.
8. I. E. Telatar, "Capacity of multi-antenna gaussian channels," *Transactions on Emerging Telecommunications Technologies*, vol. 10, pp. 585–595, Dec 1999.
9. A. Goldsmith, *Wireless Communications*. Cambridge University Press, 2005.
10. S. M. Alamouti, "A simple transmit diversity technqiue for wireless communications," *IEEE Journal on Selected Areas in Communications*, vol. 16, pp. 1451–1457, Oct 1998.
11. W. C. Jakes, *Microwave Mobile Communications*. Wiley, 1974.
12. F. Espax and J. Boutros, "Capacity considerations for wireless mimo channels," *Multiaccess, Mobility, and Teletraffic in Wireless Communications*, vol. 4, pp. 286–292, 1999.
13. N. Blaunstein, *Radio Propagation and Adapative Antennas for Wireless Communication Links*, J. Wiley and Sons, Eds. Wiley Series, 2007.
14. H. Taub and D. Schilling, *Principles of Communication Systems*, S. Rao, Ed. McGraw Hill, 1991.
15. T. Cover and J. Thomas, *Elements of Information Theory*, D. Schilling, Ed. Wiley & Sons, Inc, 1991.
16. D. Roddy, *Satellite Communications, Fourth Edition*, S. S. Chapman, Ed. McGraw Hill, 2006.
17. M. A. Temple, "Digital Communications II Class Notes," PowerPoint Slides, April 2011.

REPORT DOCUMENTATION PAGE

Form Approved
OMB No. 0704–0188

1. REPORT DATE *(DD–MM–YYYY)*	2. REPORT TYPE	3. DATES COVERED *(From — To)*
22–03–2012	Master's Thesis	Sept 2010 — Mar 2012

4. TITLE AND SUBTITLE

Trade-offs in a 1 Tbps MIMO Communication System
Between an Airship and an Array of Ground Receive Antennas

5a. CONTRACT NUMBER

5b. GRANT NUMBER

5c. PROGRAM ELEMENT NUMBER

6. AUTHOR(S)

Adam R. Brueggen, Capt, USAF

5d. PROJECT NUMBER

5e. TASK NUMBER

5f. WORK UNIT NUMBER

7. PERFORMING ORGANIZATION NAME(S) AND ADDRESS(ES)

Air Force Institute of Technology
Graduate School of Engineering and Management (AFIT/EN)
2950 Hobson Way
WPAFB OH 45433-7765

8. PERFORMING ORGANIZATION REPORT NUMBER

AFIT/GE/ENG/12-04

9. SPONSORING / MONITORING AGENCY NAME(S) AND ADDRESS(ES)

Intentionally Left Blank

10. SPONSOR/MONITOR'S ACRONYM(S)

11. SPONSOR/MONITOR'S REPORT NUMBER(S)

12. DISTRIBUTION / AVAILABILITY STATEMENT

Approval for public release; distribution is unlimited.

13. SUPPLEMENTARY NOTES

14. ABSTRACT

As demand for higher data-rate wireless communications increases, so will the interest in multiple-input and multiple-output (MIMO) systems. In a single transmit- ter, single receiver communication system, there is a fundamental limit to the data- rate capacity of the system proportional to the systems bandwidth. Since increasing the bandwidth is expensive and limited, another option is increasing the systems ca- pacity by adding multiple antennas at the transmitter and receiver to create a MIMO communication system. With a T transmitter, R receiver MIMO communication system, TR channels are created which allow extremely high data-rates. MIMO systems are attractive because they are extremely robust as they are able to operate when encountering channels with severe attenuation also known as deep fades. MIMO sys- tems are known for their ability to achieve extremely high data-rates created by the multiple channels while improving bit error rate (BER) through diversity.

15. SUBJECT TERMS

Multiple-Input and Multiple-Output, Bit Error Rate, Terabit per Second, Reed Solomon, Forward Error Correction

16. SECURITY CLASSIFICATION OF:			17. LIMITATION OF ABSTRACT	18. NUMBER OF PAGES	19a. NAME OF RESPONSIBLE PERSON
a. REPORT	b. ABSTRACT	c. THIS PAGE			Dr. Richard K. Martin
U	U	U	UU	128	19b. TELEPHONE NUMBER *(include area code)* (937) 785-3636, ext 4625; richard.martin afit.edu